„Characterization of tumor-antigen-specific T cells – insights into WT1- and HPV16-specific T cell repertoires"

Inaugural Dissertation

zur

Erlangung des Doktorgrades

Dr. nat. med.

der Medizinischen Fakultät

und

der Mathematisch-Naturwissenschaftlichen Fakultät

der Universität zu Köln

vorgelegt von

Sabine Schmied, MSc. Biol.

aus Waldshut

November 2014

Eidesstattliche Erklärung

Ich versichere, dass ich die von mir vorgelegte Dissertation selbstständig angefertigt, die benutzen Quellen und Hilfsmittel vollständig angegeben und die Stellen der Arbeit – einschließlich Tabellen, Karten und Abbildungen -, die anderen Werken im Wortlaut oder dem Sinn nach entnommen sind, in jedem Einzelfall als Entlehnung kenntlich gemacht habe; dass diese Dissertation noch keiner anderen Fakultät oder Universität zur Prüfung vorgelegen hat; dass sie – abgesehen von unten genannten Teilpublikationen – noch nicht veröffentlicht worden ist sowie, dass ich eine solche Veröffentlichung vor Abschluss des Promotionsverfahrens nicht vornehmen werde. Die Bestimmungen dieser Promotionsordnung sind mir bekannt. Die von mir vorgelegt Dissertation ist von Prof. Dr. Hinrich Abken, PD Dr. Thomas Wunderlich, Dr. Mario Assenmacher und Dr. Anne Richter betreut worden.

Übersicht der Publikationen:

Schmied S., Gostick E., Price D., Abken H., Assenmacher M., Richter A. Analysis of the functional WT1-specific T cell repertoire in healthy donors reveals a discrepancy between $CD4^+$ and $CD8^+$ memory formation. Submitted to *Immunology*.

Schmied S., Preuss SF., Wolber P., Huebbers CU., Abken H., Assenmacher M., Richter A. Functional HPV16-reactive T cells in periphery and tumor tissue of $HPV16^{pos}$ HNSCC patients. Submitted to *The International Journal of Cancer*.

Ich versichere, dass ich alle Angaben wahrheitsgemäß nach bestem Wissen und Gewissen gemacht habe und verpflichte mich, jedmögliche, die obigen Angaben betreffenden Veränderungen, dem Promotionsausschuss unverzüglich mitzuteilen.

Köln, den 05. März 2015 _____

Unterschrift

Abstract

This thesis provides characterization of rare tumor-associated antigen (TAA)-specific T cells concerning their *in vivo* prevalence, functionality, and phenotype in healthy and diseased individuals. Such knowledge on the existing *in vivo* repertoire is crucial for the understanding of T cell immunity towards tumors and furthermore for the utilization of TAA-specific T cells in immunotherapeutic approaches. Thus far, low frequencies of such TAA-specific T cells in blood and tissues hindered an in-depth characterization, even in tumor patients. Here, we establish and implemented highly sensitive methods, based on magnetic enrichment of TAA-specific T cells in combination with a multiparameter flow cytometry analysis to overcome existing sensitivity hurdles and allow *ex vivo* description of the T cells. Two different activation markers were implemented, CD154 (CD40L) for *ex vivo* enumeration and characterization of blood CD4$^+$ T cells, and CD137 (4-1BB) for subsequent characterization of rare antigen-specific CD4$^+$ and CD8$^+$ T cell subsets from blood and tumor tissue after a short-term *in vitro* expansion.

On the one hand, T cells specific for the self-antigen WT1 and, on the other hand, T cells specific for the viral antigens HPV16 E6 and E7 were investigated.

The Wilms' tumor 1 (WT1) protein is a transcription factor expressed at high levels in several hematological malignancies and some solid tumors and is considered a prime target for cancer immunotherapy. Remarkably, in this study, WT1-specific CD4$^+$ and CD8$^+$ T cell populations were detected in the vast majority of healthy individuals. Memory responses specific for WT1 were commonly present in the CD4$^+$ T cell compartment, whereas WT1-specific CD8$^+$ T cells almost universally displayed a naïve phenotype. Moreover, WT1-specific memory CD4$^+$ and naïve CD8$^+$ T cells were found to co-exist in healthy individuals. Collectively, these findings suggest a natural discrepancy between the CD4$^+$ and CD8$^+$ T cell lineages responsive to self-antigens with respect to memory formation. Nonetheless, WT1-specific T cells from both lineages were readily activated *ex vivo* and expanded *in vitro*, supporting the general use of strategies to exploit this expansive reservoir of self-reactive T cells for immunotherapeutic purposes.

Furthermore, characteristics of HPV16-specific T cells were investigated in head and neck squamous cell carcinoma (HNSCC) patients, as HNSCC is frequently induced by HPV16 infection. This study revealed that HPV16-specific T cells in the blood of HPV16^{pos} HNSCC patients exhibit profound differences in prevalence, functionality, and phenotype between individuals. While all patients harbored HPV-specific T cells in peripheral blood, we identified a subgroup of patients with significantly elevated frequencies of functional effector memory HPV16-specific CD4$^+$ T cells compared to other patients. Moreover, these high responder patients had a more active anti-tumor immunity in comparison to low responders. Despite

these variations, HPV16-specific T cells with functional capacities could be isolated and propagated both from blood and tumor tissue of all HPV16^{pos} HNSCC patients. Furthermore, this data supports the notion that HPV16-reactive tumor infiltrating lymphocytes were suppressed by intratumoral T$_{reg}$ cells, the depletion of which restored T cell effector functions and facilitated expansion of reactive T cells for therapeutic use.

In summary, the techniques established in this study permit detection of rare antigen-specific T cells and therefore are superior to common immune monitoring methods in terms of sensitivity and determination of T cell properties. In particular, these techniques were implemented to provide novel insights into the naturally occurring repertoire of WT1- and HPV16-directed T cells. These findings support the use of WT1- and HPV16-specific T cells in immunotherapy and provide knowledge crucial for the optimal design of WT1- and HPV16-directed immunotherapeutic interventions.

Zusammenfassung

Diese Arbeit umfasst eine Charakterisierung in Bezug auf Prävalenz, Funktionalität und Phänotyp von den sehr seltenen T-Zellen, die spezifisch für Tumor-assoziierte Antigene (TAA) sind. Wissen über das *in vivo* existierende T-Zellrepertoire ist für das Verständnis der Immunität gegenüber dem Tumor und darüber hinaus für die Entwicklung von immuntherapeutischen Ansätzen notwendig. Eine solche detaillierte Charakterisierung war bislang nicht möglich, da TAA-spezifische T-Zellen im Blut und im Tumor nur in sehr geringer Frequenz vorliegen. In dieser Arbeit werden hoch sensitive Methoden etabliert, basierend auf magnetischer Anreicherung von TAA-spezifischen T-Zellen in Kombination mit einer Analyse mittels Multiparameter-Durchflußzytometrie, die die bisher bestehenden Sensitivitätsgrenzen überwinden und damit die *ex vivo* Charakterisierung der T-Zellen zulassen. Zwei Aktivierungsmarker kamen für die Zellanreicherung zum Einsatz; zum einen wurde CD154 (CD40L) zur *ex vivo* Enumeration und Charakterisierung von CD4$^+$ T-Zellen aus dem Blut benutzt und zum anderen wurde CD137 (4-1BB) für die Charakterisierung von antigen-spezifischen CD4$^+$ und CD8$^+$ T-Zellpopulationen aus Blut und Tumorgewebe nach einer kurzen *in vitro* Expansion eingesetzt.

Im Speziellen wurden T Zellen untersucht, die spezifisch für das Selbstantigen WT1 sind, und T Zellen, die spezifisch für das E6 und E7 Antigen des humanen Papillomavirus Typ 16 (HPV16) sind.

Das Wilms' Tumor 1 (WT1) Protein ist ein Transkriptionfaktor, der im hohen Maße in hämatologischen Tumoren und einigen soliden Tumoren exprimiert wird. WT1 gilt als geeignetes Zielantigen für die Immuntherapie. Erstaunlicherweise konnten in dieser Studie WT1-spezifische CD4$^+$ und CD8$^+$ T-Zellen im Blut von der Mehrheit der gesunden Spender detektiert werden. Eine Gedächtnisantwort, die spezifisch gegen WT1 gerichtet ist, war häufig im CD4$^+$ T-Zellkompartiment zu finden, während WT1-spezifische CD8$^+$ T-Zellen fast ausschließlich einen naiven Phänotyp zeigten. Darüber hinaus wurde die Koexistenz von WT1-spezifischen Gedächtnis CD4$^+$ und naïve CD8$^+$ T-Zellen in einem Individuum nachgewiesen. Zusammenfassend implizieren die Resultate, dass eine Diskrepanz in der Entwicklung von Gedächtnisantworten zwischen den CD4$^+$ and CD8$^+$ T-Zellkompartimenten, die auf Selbstantigen reagieren, vorliegt. Dennoch ließen sich WT1-spezifische T-Zellen aus beiden Kompartimenten *in vitro* aktivieren und expandieren. Dieses spricht für die Umsetzung von Strategien, die das Repertoire von Selbstantigen-spezifischen T-Zellen für immuntherapeutische Ansätze nutzen.

Des Weiteren wurden HPV16-spezifische T-Zellen in Patienten mit Kopf-Hals-Tumor (head and neck squamous cell carcinoma, HNSCC) untersucht, da HNSCC häufig durch HPV16 Infektion induziert wird. Die vorliegende Arbeit zeigt auf, dass die Häufigkeit, die

Funktionalität und der Phänotyp von HPV16-spezifischen T-Zellen im Blut sich deutlich zwischen den HPV16^{pos} HNSCC Patienten unterscheiden. Während in allen Patienten spezifische T-Zellen nachweisbar sind, konnte ein Gruppe von HPV16^{pos} HNSCC Patienten identifiziert werden, die eine auffällig hohe Frequenz an HPV16-spezifischen Effektor-Gedächtnis-CD4^{+} T-Zellen mit hoher Funktionalität aufweist. In diesen ,high responder' Patienten war darüber hinaus eine aktivere Anti-Tumorimmunität im Tumorgewebe zu finden als in den ,low responder' Patienten. Trotz dieser Unterschiede konnten HPV16-spezifische T-Zellen sowohl aus Blut als auch aus Tumorgewebe von HPV16^{pos} HNSCC Patienten gewonnen werden. Dennoch verdeutlichen die Daten, dass T$_{reg}$ im Tumorgewebe die Aktivität der HPV16-spezifischen Tumor-infiltrierender Lymphozyten abschwächen, denn das Eliminieren von T$_{reg}$ aus den *in vitro* gewonnenen tumor-infiltrierenden Lymphozyten führte zur einer deutlich verstärkten Effektorfunktion und Expansion von HPV16-spezifischen T-Zellen.

Die in dieser Arbeit etablierten Methoden ermöglichen eine detaillierte Charakterisierung von sehr seltenen tumor-spezifischen T-Zellen und sind damit bislang üblichen Methoden des Immunmonitoring an Sensitivität und Informationsgehalt überlegen. Insbesondere wurden mittels der etablierten Methoden neue, tiefreichende Erkenntnisse über die T-Zell-Immunität gegenüber WT1 und HPV16 gewonnen. Die erzielten Daten sprechen für die immuntherapeutische Nutzung von WT1- und HPV16-spezifischen T Zellen und stellen wichtige Erkenntnisse für die optimale Gestaltung von WT1- und HPV16-basierten Immuntherapien bereit.

Content

Abbreviations

Ab	antibody / antibodies
APC	antigen presenting cells
CD	cluster of differentiation
CMV	cytomegalovirus
cTEC	cortical thymic epithelial cells
CTL	cytotoxic T cell
DC	dendritic cell
DLI	Donor lymphocyte infusion
E6	early protein 6
E7	early protein 7
EBV	Epstein-Barr virus
EC_{50}	half maximal effective concentration
FSC	forward scatter
GvHD	Graft-versus-host disease
GvL	Graft-versus-leukemia
Gy	gray
HLA	human leukocyte antigen
HNSCC	Head and neck squamous cell carcinoma
HPV	human papilloma virus
HSCT	hematopoietic stem cell transplantation
IE-1	immediate early protein 1
IFN-γ	interferon-gamma
IL	interleukin
L1	late protein 1
MART-1	melanoma antigen recognized by T cells 1
MB	MicroBeads
MHC	major histocompability complex
MNC	mononuclear cells
mTEC	medullar thymic epithelial cells
NK	natural killer
PBMC	peripheral blood mononuclear cells
PI	propidium iodid
pp65	phosphoprotein 65
TAA	tumor-associated antigen
T_{CM}	central memory T cells
T_{eff}	Effector T cells
T_{EM}	effector memory T cells
T_{EM-RA}	end-differentiated effector memory T cells
T_H	helper T cells
TIL	tumor-infiltrating lymphocytes
TNF-α	Tumor necrosis factor alpha
T_{reg}	regulatory T cells
WT1	Wilms tumor 1

1   Introduction

The human immune system fights invading pathogens. Furthermore, the immune system is able to eliminate aberrant, genetically altered, mutated, autologous cells which are potential precursors of tumor cells. Human immunity is built on two major pillars, innate immunity and adaptive immunity. The innate immunity, including neutrophilic, eosinophilic and basophilc granulocytes, monocytes, macrophages, dendritic cells, and natural killer cells provides a general first defense against invading pathogens. A more delicate defense is generated by the adaptive immunity, built by B- and T-lymphocytes. B- and T-lymphocytes are capable of specific recognition of foreign antigens, brought in by pathogens, with the help of highly specific antigen receptors. The vast repertoire of antigen receptors allows for elimination of pathogens that evade or overwhelm the innate immunity. Furthermore, adaptive immunity provides an immunological memory to protect the body from reinfection.

The human immune system plays a major role in preventing the development of cancer. Especially T lymphocytes, which are essential for elimination of aberrant cells of the body. In case of cancer formation, however, the anti-tumor immune response is insufficient.

1.1   T lymphocytes

T lymphocytes, or T cells, originate from lymphoid progenitor cells in the bone marrow and mature in the thymus; the "T" in T cell stands for thymus. After maturation T cells circulate in the blood, lymph, and secondary lymphoid tissues, such as the lymph nodes, the spleen, and the mucosal lymphoid tissues, where they scan for the emergence of foreign peptides.

Main functions of T cells are direct killing of target cells, i.e. infected or tumor cells, and activation of other immune cells via cell surface molecules or by the secretion of soluble mediators like cytokines upon antigen encounter.

1.1.1   Target antigen recognition by T cells

T cells recognize their targets via their T cell receptor (TCR). A minor population of T cells carries a TCR consisting of γ:δ chains, however, the majority of T cells express an α:β chain TCR. Each TCR chain is composed of a constant region and a variable region, the latter forming the antigen binding-site (Fig. 1.1). The α:β TCR binds to peptide loaded major histocompatibility (MHC) complexes on professional antigen-presenting cells (APC) or other cells of the body. Classically T cells fall into two major categories, which are CD4$^+$ T helper

cells and CD8⁺ cytotoxic T cells, defined by the expression of the co-receptors CD4 and CD8, which are engaged in TCR-MHC binding. CD4⁺ T cells recognize peptides presented on MHC class II molecules and CD8⁺ T cells recognize peptides presented on MHC class I molecules. Distinct pathways of antigen processing are responsible for loading of MHC class I and MHC class II molecules. Specifically, antigens taken up from the extracellular fluid by endocytosis are digested in the endosome and loaded onto MHC class II molecules. In contrast, peptides loaded onto MHC class I molecules are typically derived from intracellular proteins introduced by viral or bacterial infection of the cell. Cytosolic proteins are degraded via the proteasome and transported to the ER where they are loaded onto MHC class I molecules (Neefjes, Jongsma et al. 2011). An exception to this rule is exerted by DC, as they are able to process antigens from the extracellular space via the ER onto MHC class I molecules. This process is called cross-presentation (Joffre, Segura et al. 2012). Additionally, peptides loaded onto MHC class I and MHC class II differ in length. MHC class I molecules have a distinctly defined binding pocket, which binds peptides of 8 to 10 amino acids in length. Peptide binding is stabilized by specific anchor residues at the end of the peptide. In contrast, the binding groove of MHC class II molecules is more flexible as it can bind peptides of 13 to 17 amino acids in length. The ends of these peptides are not bound, but instead overlap the groove, and anchor residues for MHC class II are less defined. MHC class I molecules are constitutively expressed on all cells of the body, whereas MHC class II expression is restricted to professional APC of the immune system, such as DCs, macrophages, and B cells. Presence of IFN-γ can trigger the expression and upregulation of MHC class I and MHC class II molecules.
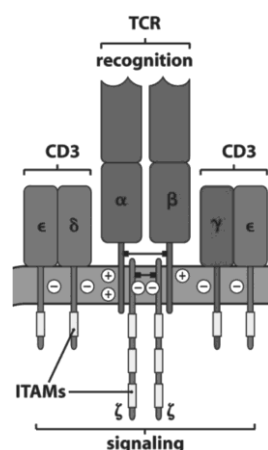
Figure 1.1 Structure of the T cell receptor complex. The T cell receptor itself is a heterodimer, each chain consisting of a constant and variable section. The variable section includes the CDR3 binding region, which accounts for the huge diversity in antigen-specificity of TCRs. The TCR co-localizes with CD3γ, CD3δ, and CD3ε molecules and the ζ chains, which carry immunoreceptor tyrosine-based activation motifs (ITAM) intracellularly. Through phosphorylation of these ITAMs the TCR signal is transmitted to the cell (Figure taken from (Murphy 2011).

1.1.2 Development of T cells

During maturation of the T cell in the thymus TCR rearrangement takes place. Here, different variable (V), joining (J), and diversity (D) segments are combined in a stochastic manner in both the α chain and β chain locus. This rearrangement and the combination of α and β chains creates the diversity of TCR binding specificities, which is estimated to comprise $>10^{11}$ possible specificities (Robins, Srivastava et al. 2010). Positive selection in the thymus ensures that only T cells carrying a TCR, that is able to bind self-peptide:self-MHC complexes, survive. This applies only to about 10% of T cells Positively selected T cells recognizing self-MHC complexes on cortical thymic epithelial cells (cTEC) do become single positive for either CD8 or CD4 depending on whether they recognize MHC class I or MHC class II complexes, respectively. 'Single positive' cells migrate from the thymic cortex to the medulla. In the thymic medulla negative selection takes place, which deletes the T cells bearing a strong affinity against self-peptide:self-MHC complexes to protect the body from strong autoimmunity (Fig. 1.2).
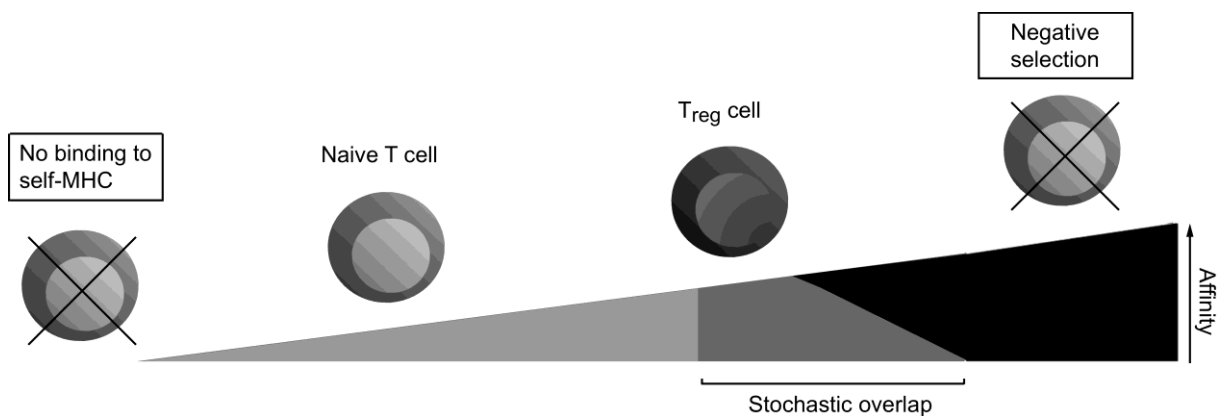
Figure 1.2 Affinity model of T cell selection. The strength of interaction of the TCR with peptide:self-MHC during development within the thymus determines the fate of the T cell. No binding leads to elimination during positive selection, likewise very strong binding also leads to elimination in the course of negative selection. Strong recognition can also lead to the development of regulatory T cells (T$_{reg}$). Recent studies provide evidence that there is a stochastic overlap in affinity, which can either lead to the development of a T$_{reg}$ or deletion of the T cell. Likewise, similar affinities can exist in the T$_{reg}$ and naïve T cell compartment (Bains, van Santen et al. 2013) (Figure adapted from (Klein, Kyewski et al. 2014)).

To enable negative selection against the full repertoire of self-antigens of the body, medullar thymic epithelial cells (mTEC) are able to express antigens normally only expressed on specific tissues or during embryonic development. This feature of mTEC is called promiscuous gene expression. However, there have been reports that the negative selection is incomplete for certain antigens. Reasons for this insufficient negative selection can be very low expression of the antigen in mTEC (Gotter, Brors et al. 2004, Lv, Havari et al. 2011),

differential splicing of mRNA (Klein, Klugmann et al. 2000, Pinto, Sommermeyer et al. 2014), or missing post-translational modifications of proteins in mTEC (Scally, Petersen et al. 2013, Van Lummel, Duinkerken et al. 2014). Strong recognition of self-antigens cannot just lead to deletion of T cells, but also to development of these CD4$^+$ T cells into T cells with regulatory functions (T$_{reg}$) (Hsieh, Lee et al. 2012). Only 2 - 4% of all thymocytes will leave the thymus as functional naïve T cells.

1.1.3 Primary activation of T cells

After leaving the thymus the naïve lymphocyte will circulate via lymph and blood between lymphoid organs until encountering its respective antigen. Naïve T cells express the lymph node homing receptor CD62L and the chemokine receptor CD197 (CCR7), which enable them to migrate to the secondary lymphoid tissues such as lymph nodes, spleen, and mucosal lymphoid tissues. Professional APC take up antigen at sites of infection or aberrant tissue formation and get activated following inflammation as part of innate immunity. This activation triggers the migration of APC to the secondary lymphoid organs. The T cell becomes activated when it meets such an activated professional APC, including DC, but also activated macrophages and B cells, presenting the respective antigen within the T cell zone of a lymphoid organ. This process is called T cell priming. The primed T cell starts to proliferate and differentiate into an effector T cell. For a successful priming of a naïve T cell, co-stimulatory signals mediated by molecules on the professional APC and the T cell are needed, in addition to TCR signaling through peptide:MHC binding. One crucial co-stimulatory signal is the interaction of B7 molecules (CD80, CD86) with CD28 on the T cell. Primed T cells leave the secondary lymphoid organs to migrate to the site of infection.

T cells specific for self-antigens, which were not negatively selected during their development in the thymus, are usually not activated in the periphery, as peripheral tissues do not express co-stimulatory molecules. Similarly, professional APC express very few co-stimulatory molecules in the absence of inflammatory signals. This peripheral self-tolerance provides a further safety mechanism to prevent autoimmunity. When pro-inflammatory signals such as pro-inflammatory cytokines produced by innate immune cells and/or co-stimulatory molecules on APC are missing, T cells can be anergized or converted into T$_{reg}$.
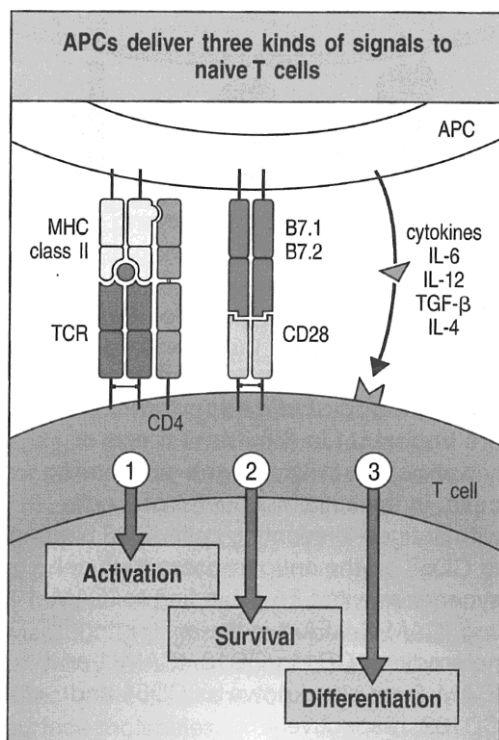
Figure 1.3 Priming of naïve T cells. Professional APC need to deliver three different signals to a naïve T cell to activate and therefore prime it. First, the TCR of the T cell needs to specifically bind the peptide:MHC complex. In addition, the co-receptor CD4 or CD8 bind to MHC. Second, the co-stimulatory B7 molecules need to be expressed on the APC and bind to CD28 expressed on the T cell. Also other co-stimulatory molecules, like members of the TNF receptor family, can provide such a signal. Third, the APC provides cytokines to trigger the differentiation of the primed T cells. In a non-inflammatory setting APC lack co-stimulatory molecules and T cell contact leads to anergizing of the T cell (Figure taken from (Murphy 2011)).

1.1.4 Differentiation of T cells

Cytokine signals released by the professional APC determine the fate of the primed T cell. Especially for CD4$^+$ T cells several subclasses are known, differing in the cytokines needed for differentiation and also in cytokines secreted by those CD4 T cells (Fig. 1.4). Different CD4$^+$ T cell subsets exert different effector functions.

CD8 T cells: peptide + MHC class I		CD4 T cells: peptide + MHC class II							
Cytotoxic (killer) T cells		T_H1 cells		T_H2 cells		T_H17 cells		T_{reg} cells	
Cytotoxic effector molecules	Others	Macrophage-activating effector molecules	Others	Barrier immunity activating effector molecules	Others	Neutrophil recruitment	Others	Suppressive cytokines	Others
Perforin Granzymes Granulysin Fas ligand	IFN-γ LT-α TNF-α	IFN-γ GM-CSF TNF-α CD40 ligand Fas ligand	IL-3 LT-α CXCL2 (GROβ)	IL-4 IL-5 IL-13 CD40 ligand	IL-3 GM-CSF IL-10 TGF-β CCL11 (eotaxin) CCL17 (TARC)	IL-17A IL-17F IL-6	TNF CXCL1 (GROα)	IL-10 TGF-β	GM-CSF

Figure 1.4 Major T cell subsets and their effector functions.
The main function of CD8$^+$ T cells is the killing of target cells presenting the respective peptide on MHC class I molecules by the release of cytolytic granules into the immunological synapse. CD4$^+$ T cells bear diverse functions. Main subclasses of CD4$^+$ T cells include T_H1, T_H1, T_H17, and T cells bearing regulatory functions (T_{reg}) (Figure taken from (Murphy 2011)).

T_H1 cells are specialized to stimulate innate immune responses, they activate macrophages and are also able to kill infected macrophages. Main effector cytokines of the T_H1 subset are IFN-γ and TNF-α. T_H1 cells are especially important for anti-tumor immunity as they can exert anti-tumor functions, both by direct tumor cell killing or by activation of other immune cells by secretion of pro-inflammatory cytokines (Haabeth, Tveita et al. 2014). T_H2 cells promote the immune response to extracellular pathogens mainly by activating B cells. Effector cytokines of T_H2 cells include IL-4, IL-5, and IL-13 (Wan and Flavell 2009). In addition to T_H1, T_H2, and T_{reg} cells also T_H9, T_H17, T_H22, and T follicular helper cells (T_{FH}) exist. Recent studies have discovered even more distinct subsets and have also shown the plasticity of T_H cells, adding to the complexity of human adaptive immunity (Lee, Turner et al. 2009, Wei, Wei et al. 2009). In an activated state, T_H cells express CD40 ligand (CD154) on their surface, which is important for activation of professional APC and CD8 T cell priming.

CD4$^+$ T cells with regulatory functions can evolve from the thymus (natural T_{reg} = nT_{reg}) and be induced in the periphery (induced T_{reg} = iT_{reg}). Both T_{reg} subsets are characterized by the constitutive expression of the transcription factor FoxP3 and the cell surface molecule IL-2R α-chain (CD25). T_{reg} cells are able to suppress effector T cell function through contact-dependent inhibition of T cell activation as well as inhibition of proliferation owing to release of soluble factors such as IL-10 and TGFβ (Corthay 2009) or competition for IL-2 (de la Rosa, Rutz et al. 2004).

Priming of CD8 T cells requires CD4 T cell help to APC, especially when inflammatory signals are lacking to activate the APC sufficiently. CD40 ligand (CD154) on activated CD4$^+$ T_H cells binding to CD40 on DC results in enhanced co-stimulatory signals to the naïve CD8$^+$ T cell. An activated CD8$^+$ effector T cell can kill antigen-presenting target cells specifically via release of cytolytic granules. Perforin-containing granules form holes in the targeted cells and allow for granzyme-containing granules to enter the target cells and trigger apoptosis (de Saint Basile, Menasche et al. 2010). As MHC class I molecules are present on virtually all cells of the body, CD8$^+$ T cells can kill autologous cells, which present non-self-peptides, as in the case of virus infected cells. However, the clear functional distinction between CD4$^+$ helper T cells and CD8$^+$ cytotoxic T cells is not as strict as previously thought, as cytolytic CD4$^+$ T cells and CD8-expressing T cells with helper cell functions have also been identified in recent years (Paludan, Bickham et al. 2002, Frentsch, Stark et al. 2013).

Once a T cell has differentiated into an effector cell, the T cell exerts its effector functions upon antigen encounter without the need for a professional APC providing co-stimulatory signals. Additionally, the T cell's homing behavior drastically changes, as it now needs to leave the lymphoid tissue and enter the sites of infection. Effector cells loose the expression of CCR7 and CD62L, which mediate homing to the secondary lymphoid organs. CCR7 and

CD62L are therefore markers, which can be used to distinguish naïve from effector T cells. Furthermore, the protein tyrosine phosphatase CD45, involved in TCR signaling, is expressed in different isoforms during differentiation. Naïve T cells expressing the long CD45RA isoform and memory T cells expressing the shorter CD45RO isoform. According to the expression patterns of these molecules, the differentiation status of the T cell can be phenotypically determined. Naïve T cells being CD45RO$^-$ CCR7$^+$, central memory T cells CD45RO$^+$ CCR7$^+$, effector memory T cells CD45RO$^+$ CCR7$^-$, and exhausted T cells being CD45RO$^-$ CCR7$^-$. After clearance of the infection or prolonged antigen-stimulation, an effector T cell eventually progresses to an exhausted state, its effector functions decrease and the T cell eventually dies. But central memory T cells exist also which retain the expression of CD62L and CCR7 (Sallusto, Geginat et al. 2004). Initial models of T cell differentiation suggested a unidirectional progression from naïve to effector T cells to exhausted effector T cell to apoptosis in which central memory T cells are cells arrested at intermediate stages of differentiation preceding effector T cells. Newer models suggest the existence of a memory T cell population bearing stem cell-like properties. This stem T cell population is marked, amongst other, by the expression of the IL-7 receptor α-chain (CD127) in humans. CD127 is also expressed on naïve T cells but normally rapidly lost upon activation (Gattinoni, Lugli et al. 2011). These putative stem T cells are able to self-renew and give rise to central memory and effector memory T cells (Bondanza, Hambach et al. 2011, Mackall, Fry et al. 2011).

1.2 Anti-tumor immunity

The adaptive immunity is able to conduct a directed immune response against cancerous cells. It is believed that many aberrant cells, which are potential precursors of tumor cells, are cleared by these immunological defense mechanisms, a process called immunosurveillance (Corthay 2014). In case of tumor formation these immunological defense mechanisms are impaired or not sufficient. Then the tumor is able to overcome immunosurveillance. The hypothesis of immunoediting states that the immunosurveillance alters the composition of tumors towards more aggressive forms, which are able to circumvent recognition by the immune defense mechanism or actively suppress it (Kim, Emi et al. 2007). It is clear that many tumor entities exhibit such tumor escape features. Tumor escape mechanisms include, on the one hand, defects in antigen processing or presentation components and therefore loss of antigen presentation; on the other hand, formation of a immunosuppressive microenvironment by attraction of suppressive cell types, such as T_{reg}, myeloid suppressor cells, or release of suppressive cytokines (Kim, Emi et al. 2007). However, in the last decade it has been clearly shown that tumor escape can be overcome by immunotherapeutic

interventions even in quite aggressive forms of cancer by different strategies, e.g. increasing the number of anti-tumor T cells or modulating immunosuppressive features of the tumor.

1.2.1 Tumor-associated antigens

Tumor cells have an aberrant protein expression profile compared to normal cells of the body, which can result in presentation of distinct antigens. This feature renders them sensitive to recognition by cells of the adaptive immune system. Antigens especially expressed on tumor cells are referred to as tumor-associated antigens (TAA). T cells specific for TAA can mediate such an anti-tumor response. TAA fall into different classes and can be of self, "altered-self", or foreign origin: (1) Foreign antigens derived from viral oncogenes such as the human papilloma virus (HPV) E6 and E7 protein and (2) "altered-self" antigens, e.g. mutated antigens such as Bcl-Abl expressed in some forms of myeloid leukemia. On the other hand, TAA can also be classical self-antigens as in the case of: (3) Oncofetal antigens normally only expressed during embryonic and fetal development or in germ-line tissues (NY-ESO-1, MAGE-A3), (4) tissue differentiation antigens (MART-1, gp100) or (5) antigens overexpressed in tumor cells, such as WT1, overexpressed in myeloid leukemia and many solid tumors.

1.2.2 Implementation of anti-tumor T cell immunity

Several treatment approaches have proven the potential of naturally existing immunity, especially T cells, for the treatment of cancer.

Firstly, prophylactic vaccination has been successfully implemented for the protection against tumor formation in the case of HPV16 (and HPV18)-induced cervix carcinoma. Therapeutic vaccination has not been clinically established thus far; however, numerous studies have shown that an anti-tumor immunity can be triggered against multiple cancer entities, including HPV16-induced vulvar neoplasias (Kenter, Welters et al. 2009, Daayana, Elkord et al. 2010) and WT1-expressing tumors (Van Driessche, Berneman et al. 2012).

Secondly, so called checkpoint inhibitors have been used to re-activate existent immunity against tumors. Successfully used in the clinic is a CTLA-4 inhibitor (ipilimumab) used for treatment of melanoma, which blocks the inhibitory CTLA-4:B7 interaction and leads to enhanced general activation of T cells (Hodi, O'Day et al. 2010, Ott, Hodi et al. 2013). The clinical effect of re-activation of intratumoral T cells underlines that naturally occurring T cells have a good anti-cancer potential.

Thirdly, adoptive transfer of naturally derived TAA-specific T cells has directly demonstrated their therapeutic potential. The feasibility and efficacy of adoptive T cell transfer was successfully proven in melanoma where tumor-infiltrating lymphocytes are expanded *in vitro* with the use of IL-2 and administered to lympho-depleted patients. This therapy has led to shrinkage and also clearance of major tumor lesions in metastatic melanoma patients (Rosenberg, Yannelli et al. 1994). Additionally to naturally derived TAA-specific T cells, genetically engineered T cells specific for a TAA or T cells transduced with a chimeric antigen receptor specific for a surface protein of the tumor cell are successfully used in the clinic (Porter, Levine et al. 2011, Kershaw, Westwood et al. 2013).

For adoptive T cell therapy, several studies have highlighted that the quality of the administered T cells is crucial for clinical success (reviewed in (Riddell 2007) and (Klebanoff, Gattinoni et al. 2012). Therefore, attempts were made to design the best *in vitro* expansion protocol to achieve a good *in vivo* performance and persistence of T cells. Firstly, extensive *in vitro* cultivation leads to an exhausted state of T cells, characterized by loss of expression of co-stimulatory markers and expression of exhaustion markers such as CD57. Exhausted T cells were shown to have decreased effector functions compared to non-exhausted T cells *in vivo* and to have a short *in vivo* persistence and hence are not preferred for adoptive transfer (Powell, Dudley et al. 2005, Hinrichs, Borman et al. 2009). The recently identified stem T cell population (see section 1.1.4) is favored for the use in adoptive T cell therapy, as this population is characterized by good *in vivo* persistence (Zhang, Joe et al. 2005). Cytokines used for expansion are a critical factor. Use of IL-7 and IL-15 has been reported to preserve a non-exhausted phenotype of *in vitro* expanded T cell cultures, which harbor superior *in vivo* antitumor functions compared to cells expanded with IL-2 (Cieri, Camisa et al. 2013, Xu, Zhang et al. 2014). Secondly, polyfunctionality of the applied T cells has been shown to provide enhanced protection, as they combine a broader repertoire of effector functions, i.e. the ability of one individual T cell to secrete more than one different cytokine (Seder, Darrah et al. 2008). Thirdly, early adoptive transfer studies used mostly CTL clones, but within the last decade it became clear that CD4^{+} T cells are also important for anti-tumor efficacy of a cell product, both due to cytolytic functions of the CD4^{+} T cells themselves (Quezada, Simpson et al. 2010), help for anti-tumor CD8^{+} T cells (Wong, Bos et al. 2008), and recruitment of other cells with anti-tumor functions (Perez-Diez, Joncker et al. 2007). Therefore, a CD4^{+} and CD8^{+} mixed TAA-specific T cell product might have the best efficacy.

A combined phenotypic and functional analysis of the T cell product can give important insights into whether a T cell population is effective in therapy. To date, the knowledge regarding the effective tumor-specific T cell response is incomplete. However, such knowledge is crucial in order to, on the one side, develop immunotherapies such as adoptive

T cell transfer or vaccination and, on the other side, monitor and predict clinical outcome of such an intervention.

1.3 Detection of antigen-specific T cells

Antigen-specific T cells can be detected with various techniques. The most common tool for direct detection of antigen-specific T cells are pHLAI multimers, where multimerized, peptide loaded MHC class I molecules are conjugated to a fluorophore, which enables detection of peptide-specific CD8$^+$ T cells via flow cytometry. Recently, pHLAII multimers have also been successfully introduced for detection of peptide-specific CD4$^+$ T cells (Moon, Chu et al. 2007, Obar, Khanna et al. 2008). Owing to the facts that only a limited amount of cells can be measured by flow cytometry and that multimers can produce unspecific background staining, which increases with increased numbers of measured cells, pHLA multimers have an approximate detection limit of 10^{-5} within PBMC.

Another commonly used method is the enzyme-linked immuno spot assay (ELISPOT), which allows for detection of a released cytokine upon antigen stimulus with an estimated detection limit of 10^{-5} within PBMC (reviewed in (Schmittel, Keilholz et al. 1997)). The ELISPOT is an indirect method, it is therefore only semi-quantitative and does not allow for a further characterization of single T cells. Cytokine-producing T cells after stimulation can also be detected in a direct method via intracellular staining and flow cytometric analysis. However, only a subset of activated T cells produce a certain cytokine upon stimulation, therefore enumeration of the entire pool of antigen-specific T cells is not feasible.

More recently, surface molecules upregulated after antigenic stimulation (activation markers) have been successfully used for visualization of antigen-specific T cells. For example, CD154 (CD40L) is expressed within a few hours after antigen-specific stimulation of CD4$^+$ T cells. CD137 (4-1BB) is upregulated on both CD4$^+$ and CD8$^+$ T cells after longer stimulation times (>24 h). Both marker have been shown to be expressed both on activated naïve and memory T cells and thus enable detection of antigen-specific T cells independent of their differentiation status. Furthermore, when peptide pools are used for T cell stimulation a previous knowledge of epitope specificities and HLA status is not needed. Thus, activation markers, in principle, provide a compelling opportunity to detected the full repertoire of antigen-specific T cells.

T cells specific for one particular antigen are commonly present in very low frequencies, as the human T cell repertoire comprises approximately 10^6 - 10^7 different antigen specificities (Arstila, Casrouge et al. 1999). Therefore, self-antigen-specific and tumor-associated-antigen (TAA)-specific T cells in healthy individuals cannot be detected with commonly used

technologies such as ELISPOT and pHLAI multimer staining, as they are not sensitive enough. An exception are T cells specific for the melanoma-associated self-antigen MelanA/MART-1, where rather high frequencies of specific T cells (up to 10^{-3} within $CD8^+$ T cells), exhibiting a naïve phenotype, in healthy individuals were reported (Pittet, Valmori et al. 1999, Zippelius, Pittet et al. 2002). Apart from this exception normally only T cells specific for immune-dominant recall antigens can be readily detected, as for example CMV pp65-specific T cells in CMV-infected donors, where frequencies of up to 5% pp65-specific T cells within the $CD8^+$ T cell compartment can occur.

To circumvent detection limitations for rare antigen-specific T cells, enrichment strategies can be employed. Here, cells of interest are magnetically labeled and applied to a column placed in a magnetic field where they are retained. Non-labeled cells are washed away, and the enriched, magnetically labeled cells are eluted (Miltenyi, Muller et al. 1990). Magnetic enrichment of pHLA multimer$^+$ T cells was successfully used to detect $CD4^+$ and $CD8^+$ antigen-specific at very low frequencies from the memory and naïve repertoire (Barnes, Ward et al. 2004, Obar, Khanna et al. 2008, Chu, Moon et al. 2009, Alanio, Lemaitre et al. 2010, Kwok, Tan et al. 2012). Recently, an elegant magnetic enrichment technique based on CD154-expression after antigen stimulation was established, which allows a simultaneous enumeration and functional characterization of antigen-specific T cells directly *ex vivo*, this method was named antigen-reactive T cell enrichment (ARTE) (Bacher, Schink et al. 2013). CD137 was also used to enrich antigen-specific T cells (Wolfl, Kuball et al. 2007). However, stimulation periods >24 h, which are needed for the expression of CD137 on naïve T cells, render CD137 only limited suitable for *ex vivo* characterization, as prolonged stimulation can alter the expression of phenotypic markers on activated T cells.

With the help of these magnetic enrichment techniques rare TAA-specific T cells were detected and characterized. Two model antigens of current clinical interest were chosen, the self-antigen WT1 and the viral antigens HPV16 E6 and E7. Apart from providing crucial information on the TAA-specific T cell repertoire for each TAA separately, investigation on T cells specific for these two distinct TAA antigens could unravel potential principle differences in the T cell repertoire for self- and virus-specific T cells, due to divergent negative selection mechanisms during T cell development (introduced in 1.1.2).

1.4 WT1

The Wilms' tumor 1 (WT1) protein is a transcription factor, which is expressed at high levels in several types of hematological malignancies as well as in some solid-tumors. WT1 expression in adult humans is restricted to early hematopoietic precursor cells (Baird and Simmons 1997) and is rapidly lost upon differentiation of these precursors (Maurer, Brieger

et al. 1997). WT1 was ranked top in a list of potential tumor antigens to be used in anti-cancer immunotherapy because of its oncogenic potential and presumptive immunogenicity (Cheever, Allison et al. 2009). Indeed, spontaneous T cell responses towards WT1 are induced in leukemia patients after allogeneic stem cell transplantation (SCT) or donor lymphocyte infusions (Rezvani, Yong et al. 2007, Kapp, Stevanovic et al. 2009, Tyler, Jungbluth et al. 2013) and are associated with disease regression ((Tyler, Jungbluth et al. 2013). In order to design WT1-directed immunotherapies, knowledge about the *in vivo* existence of WT1-specific T cells is a prerequisite. However, until now, such detailed insight into the naturally occurring WT1-specific T cell repertoire is vastly limited. This is due to the fact that *ex vivo* detection and hence also the characterization of WT1-specific T cells so far is hindered owing to their exceedingly low frequencies, especially in blood of healthy donors.

WT1-specific CD8$^+$ T cells have been detected *ex vivo* in myeloid leukemia patients via WT1$_{126}$-HLAI multimers (Sloand, Melenhorst et al. 2011) and via qPCR of IFN-γ mRNA after stimulation, with raised prevalence after SCT (Rezvani, Grube et al. 2003, Rezvani, Brenchley et al. 2005). Using highly sensitive IFN-γ mRNA detection Rezvani et al. also gave a first hint, that CD8$^+$ WT1-specific T cells indeed do exist in low frequencies even in healthy individuals, but an in depth characterization was not feasible with the used approach (Rezvani, Grube et al. 2003, Rezvani, Brenchley et al. 2005).

WT1 is under current investigation for the use in immunotherapeutic approaches. On the one side, several clinical WT1 vaccination trials have been done and showed promising results. Here, a clinical response was detectable in 45% of patients bearing solid tumors and even 63% in patients with hematopoietic tumors and also immunological responses could be detected in some cases (Van Driessche, Berneman et al. 2012). However, the design of vaccines was not ideal as HLA-restricted peptides have been used in some trials. Furthermore, the immunomonitoring was also limited as it was restricted to the detection of WT1-HLAI tetramer$^+$ CD8$^+$ T cells. Further knowledge about the characteristics of WT1-specific T cells, as provided in this study, will hopefully improve vaccine design to achieve optimal clinical efficiency. On the other side, usage of WT1-specific T cells for adoptive transfer after hematopoietic stem cell transplantation (HSCT) is currently under investigation. A first clinical trial has recently proven the safety of WT1$_{126}$-specific CD8$^+$ T cells in this setting (Chapuis, Ragnarsson et al. 2013).

1.5 HPV16 E6/E7

The human papilloma virus (HPV) is a DNA virus infecting the basal layer of epithelia by entering wounds or lesions of skin and mucosal tissues. Only after differentiation of the epithelial cells to cells of the squamous cell layer virus particles are assembled and released.

It is believed that more than 50% of people are infected by any type of HPV once during their life time. Certain high risk types of HPV, including HPV16 and HPV18, however, can induce lesions which can eventually progress to cancer if not cleared.

The E6 and E7 proteins of HPV16 are oncogenes, which induce cell-cycle progression. The E6 protein of high risk HPV acts as an E3 ligase for the p53 tumor suppressor protein and therefore triggers its degradation (Scheffner, Werness et al. 1990). The E7 protein binds and destabilizes the retinoblastoma (Rb) tumor suppressor protein and related proteins (Boyer, Wazer et al. 1996). The expression of E6 and E7 oncoproteins is mandatory for the uncontrolled growth of infected cells resulting in tumor formation. Therefore, these proteins are suggested to be ideal targets for immunotherapeutic approaches (Cheever, Allison et al. 2009).

The most prominent example for HPV-induced cancer is cervix carcinoma, which is induced by the high risk types HPV16 or HPV18 in about 70% of cases (Munoz, Bosch et al. 2004, Schiffman, Castle et al. 2007). Also head and neck squamous cell carcinoma (HNSCC) can be induced by HPV high risk types. A subgroup of HNSCC, the oropharynx carcinoma, is induced by high risk type HPV16 in more than 50% of cases (Ramqvist and Dalianis 2010, Jayaprakash, Reid et al. 2011). The incidence of HPV induced HNSCC is rising (Chaturvedi, Engels et al. 2011).

HNSCC patients bearing an HPV16^{pos} tumor have a better prognosis than HPV16^{neg} HNSCC patients. The reasons for better prognosis of HPV16^{pos} HNSCC patients are unknown so far. However, there is evidence that the better outcome results from the formation of an anti-tumor immunity. In general, the presence of CD3^{+} and CD8^{+} tumor-infiltrating lymphocytes (TIL) was found to be stronger in HPV16^{pos} HNSCC tumors (Jung, Guihard et al. 2013) and HPV16^{pos} tumors have a higher CD8^{+} to regulatory T cell (T$_{reg}$) ratio (Russell, Angell et al. 2013). Both findings were correlated with prolonged disease-specific survival. In specific, HPV16-specific T cells have also been detected in tumor tissue of HPV16-related HNSCC (Heusinkveld, Goedemans et al. 2012).

Furthermore, the peripheral HPV16-directed immunity was investigated. For HPV-related cervical carcinoma the systemic HPV-immunity was linked to the intratumoral HPV16-directed immunity and improved prognosis (Piersma, Jordanova et al. 2007). However, the overall functionality of peripheral HPV-specific T cells in cervical cancer seems to be impaired, either due to skewing to a T$_{H}$2 phenotype (Clerici, Merola et al. 1997, Bais, Beckmann et al. 2005, Sharma, Rajappa et al. 2007) or due to impaired functionality of the T$_{H}$ cells (de Jong, van Poelgeest et al. 2004). For HNSCC, a systemic HPV16-specific T cell immunity was also found in the periphery of HPV16^{pos} HNSCC patients. MHC class I tetramer analysis revealed higher frequencies of CD8^{+} HPV16-specific T cells in the blood of

HPV16^{pos} HNSCC patients compared to HPV16^{neg} patients and healthy individuals (Albers, Abe et al. 2005, Hoffmann, Arsov et al. 2006). Similar to cervix carcinoma, the peripheral HPV16-specific immunity in HNSCC patients revealed a partial functional impairment of T cells and the absence of a systemic HPV16-directed T cell immunity in some HPV16^{pos} HNSCC patients (Heusinkveld, Goedemans et al. 2012). A detailed characterization in terms of frequency, phenotype, and functionality of such systemic HPV16-specific T cell immunity in HNSCC patients, however, has been missing until now.

Two phase II clinical trials for therapeutic vaccination for patients with vulvar intraepithelial neoplasia, a pre-stage of cervix carcinoma, are ongoing. Both studies use a HPV16 vaccine, consisting of either HPV16 E6 and E7 peptides or an HPV16 E6E7L2 fusion protein, and showed promising results, as both achieved clinical response rates >60% (Kenter, Welters et al. 2009, Daayana, Elkord et al. 2010). For therapeutic HPV16 vaccination of HNSCC the first clinical phase I trials have been started (Center SKCC 2013 and Inovio Pharmaceuticals 2014, ClinicalTrials.gov). Adoptive transfer of HPV16-specific T cells is also under current investigation (Ramos, Narala et al. 2013), but has not been implemented in the clinic as of yet.

1.6 Objectives

In this study, unbiased and in-depth knowledge about rare tumor antigen-specific T cells is provided. This knowledge allows for conclusions on the feasibility and efficacy of immune-based anti-cancer therapies, such as vaccination and adoptive T cell transfer.

In the first part of this thesis the establishment of the highly-sensitive strategies, which were used to characterize the rare antigen-specific T cells, is outlined. Main objectives were: (i) Establishment of method(s) for *ex vivo* detection and characterization of rare antigen-specific T cells and (ii) establishment of an efficient method to generate antigen-specific T cell cultures starting from low frequent, presumably naïve T cells. The established techniques were then used to provide in-depth characterizations of TAA-specific T cells. Here, T cells specific for two distinct TAAs were investigated, the self-antigen WT1 and the viral antigens E6 and E7 derived from HPV16.

In the second part of this thesis the in-depth characterization of WT1-specific T cells is described. This second part aims at the investigation of quantity and quality of WT1-specific T cells in healthy donors to provide crucial knowledge for immunotherapeutic interventions in leukemia and other solid tumor entities.

In the third and final part of this thesis HPV16-specific T cells are characterized in HPV16^{pos} and, for comparison, in HPV16^{neg} patients and healthy individuals. Both blood and tumor derived HPV16-specific T cells of HNSCC patients were investigated to obtain so far missing knowledge on HPV16-directed peripheral and intratumoral immunity in those patients, which is valuable for the design of immunotherapeutic interventions in HPV16^{pos} HNSCC.

The approach used and the results obtained in this study are unique, as a characterization of these tumor-antigen specific T cells was so far not feasible due to their low frequencies. The established highly sensitive enrichment methods, for the first time, enable the detection and comprehensive functional and phenotypical characterization of these rare tumor-antigen specific T cells. Additionally, in contrast to other studies focusing on WT1- or HPV16-specific T cells this study provides a characterization of the full repertoire of antigen-specific T cells including both CD4^{+} and CD8^{+} T cells, naïve as well as memory T cells.

The consequences of the findings relating to the design of immunotherapeutic interventions will be discussed.

2 Materials and Methods

2.1 Reagents, media, supplements, and antigens

2.1.1 Staining antibodies

The following antibody reagents were used for staining and flow cytometric measurements: anti-CD3-VioGreen (BW264/56), anti-CD4-allophycocyanin-Vio770 (VIT4), anti-CD8-PE-Vio770 (BW135/80), anti-CD14-PerCP (TÜK4), anti-CD20-allophycocyanin, anti-CD20-PerCP (LT20), anti-CD27-FITC (M-T271), anti-CD28-FITC (15E8), anti-CD31-FITC (AC128), anti-CD44-allophycocyanin-Vio770 (DB105), anti-CD45-VioGreen (5B1); anti-CD45RA-VioBlue (T6D11), anti-CD45RO-FITC (UCHL1), anti-CD57-VioBlue (TB03), anti-CD62L-FITC (145/15), anti-CD107a-PE (1D4B), anti-CD127-FITC (MB15-18C9), anti-CD137-allophycocyanin, anti-CD137-biotin, anti-CD137-PE (4B4-1), anti-CD154-allophycocyanin, anti-CD154-VioBlue (5C8), anti-CD178-PE (NOK-1), anti-CD279-allophycocyanin (PD1.3.1.3), anti-CD197 (CCR7)-allophycocyanin, anti-CD197 (CCR7)-PE (150503), anti-CD324-allophycocyanin (67A4), anti-CD326-VioBlue (HEA-125), anti-FoxP3-PE (3G3), anti-HLA-ABC-PE (REA230), anti-IL-2-PE-Vio770 (N7.48A), anti-IL-4-PE (7A3-3), anti-IL-17-FITC (CZ8-23G1), anti-IFN-γ-FITC, anti-IFN-γ-PE-Vio770 (45-15), anti-TIM-3-allophycocyanin (F38-2E2), anti-TNF-α-PE, and anti-TNF-α-VioBlue (cA2) (all Miltenyi Biotec, Bergisch Gladbach, Germany).

2.1.2 MHC/peptide multimers

Soluble biotinylated pHLA-A*0201 molecules loaded with $WT1_{37-45}$ (VLDFAPPGA), $WT1_{126-134}$ (RMFPNAPYL), $WT1_{187-195}$ (SLGEQQYSV), $WT1_{235-243}$ (CMTWNQMNL), or cytomegalovirus (CMV) $pp65_{495-503}$ (NLVPMVATV) were produced as described previously (Price 2005 JExpMed). Tetramerization was done by incubating 2 nmol pHLA molecules with 0.5 nmol streptavidin-PE or streptavidin-allophycocyanin (both BioLegend, San Diego, USA) at 4°C, PBS supplemented with Protease Inhibitor (Roche, Basel, Switzerland) was used for dilution.

2.1.3 Antibodies for cell culture

Pure anti-CD28 (clone 15E8), anti-CD40 (clone HB14), and anti-MHC class I (clone W6/32) were obtained from Miltenyi Biotec.

2.1.4   Reagents for cell isolation

All antibody bead reagents, separation, and isolation kits used in this study were obtained from Miltenyi Biotec.

2.1.5   Media and supplements

RPMI1640 (Miltenyi Biotec) was supplemented with 2mM L-Glutamine (PAA Laboratories GmbH, Pasching, Austria) and 5% human AB-Serum (Lonza, Basel, Switzerland). X-Vivo15 (Lonza) was supplemented with 5% human AB-serum (Lonza).

2.1.6   Recombinant cytokines

Recombinant human IL-7, IL-15, IL-21 and IFN-γ were obtained from Miltenyi Biotec and recombinant human Proleukin S was obtained from Novartis Pharma, Basel, Switzerland.

2.1.7   Buffer

0.1 M phosphate-buffered saline containing 137 mM NaCl, 2.6 mM KCl, 8.1 mM Na_2HPO_4, and 1.4 mM KH_2PO_4 (all chemicals purchased from Sigma Aldrich, St. Louis, USA) was stored as 10x stock solution and freshly diluted. Sterile 0.1 M phosphate-buffered saline containing 2 mM EDTA was obtained from Miltenyi Biotec and optionally supplemented by sterile 0.5% human AB-Serum (PEB-buffer). Buffers for MACSPlex Cytokine 12 Kit and Tumor Dissociation Kit (both Miltenyi Biotec) was used as provided and indicated within kits. InsideFix solution and 10x InsidePerm solution are provided with the Rapid Cytokine Inspector Kit (Miltenyi Biotec).

2.1.8   Antigens

PepTivator CMV pp65, EBV EBNA-1, EBV LMP2a, HPV16 E6, HPV16 E7, and WT1 were obtained from Miltenyi Biotec. PepTivator peptide pools consist of 15-mer peptides overlapping by 11 amino acids and spanning the complete protein sequence. Peptides $WT1_{37-45}$, $WT1_{126-134}$, $WT1_{187-195}$, $WT1_{235-243}$ were synthesized by O. Braun and S. Kramer, Miltenyi Biotec.

2.1.9 Other

Propidium Iodide solution (PI) was obtained from Mitlenyi Biotec. CellTrace Violet was obtained from Invitrogen, Carlsbad, USA. Monensin was obtained from eBioscience, San Diego, USA. Mitomycin C and Brefeldin A and antibiotic antimycotic solution were obtained from Sigma-Aldrich.

2.2 Consumables, devices, and software

MACSQuant Analyzer 10	Miltenyi Biotec
Cell culture hood, Hera Safe KS	Thermo Fischer Scientific, Waltham, USA
CO2 Incubator, Hera Cell®	Thermo Fischer Scientific
Hematologic analyzer, Sysmex KX-21	Sysmex Corporation, Japan
Centrifuge, Eppendorf 5415D	Eppendorf, Hamburg, Germany
Centrifuge, Multifuge X3R	Heraeus Instruments, Hanau
Centrifuge, Multifuge 4KR	Heraeus Instruments
Centrifuge 4515R	Eppendorf
MACSmix Tube Rotator	Miltenyi Biotec
pH-Meter, pH-Meter 765 Calimatic	Elektronische Messgeräte GmbH, Berlin, Germany
Irradiator RS 2000	Rad Source Technologies, Inc., Suwanee, USA
MACS Separator (Mini, Midi, Octo, Quadro)	Miltenyi Biotec
MACS separation columns (MS, LS, LD)	Miltenyi Biotec
gentleMACS Dissociator	Miltenyi Biotec
gentleMACS C Tubes	Miltenyi Biotec
Microscope, Leica DM IL LED	Leica Microsystems, Wetzlar, Germany
Orbital shaker Titramax 100	Heidolph, Schwabach, Gemany
Conical bottom tubes, 50 ml, 15 ml	Falcon (BD Biosciences), New Jersey, USA
96/48/24/12-well flat bottom cell culture plates	Falcon (BD Biosciences)
75/175 cm^2 cell culture flasks	Falcon (BD Biosciences)
Cell Strainer 70 μm	Falcon (BD Biosciences)
96-well filter plate, 0.2 μm PVDF membrane	Corning, Corning, USA
Cell Scraper	MIDSCI, St. Louis, USA
Surgical Scalpell	Aesculap AG, Tuttlingen, Germany
NALGENE® Cryogenic vials	Nalge Nunc International, Rochester, USA
Dispenser Tips	Th. Geyer, Renningen, Germany
Microcentrifuge tubes	STARLAB, Hamburg, Germany
MACSQuantify, version 2.5	Miltenyi Biotec

Microsoft Office Professional 2010	Microsoft Coorporation, Redmond, USA
Graph Pad Prism 6.0	GraphPad Software, Inc., La Jolla, USA
TIGR MeV	Dana-Farber Cancer Institute, Boston, USA
Adobe Illustrator CS3 13.0	Adobe Systems, San Jose, USA

2.3 Cell separation and processing

2.3.1 Patients' characteristics

15 HNSCC patients were included in study at time of tumor resection and did not receive prior treatment. All six included HPV16^{pos} HNSCC patients had tonsillar tumors. Of the nine included HPV16^{neg} HNSCC patients five had tonsillar tumors, three tumors in the oral cavity and one in the hypopharynx. Primary tumor tissue and 50 ml of peripheral blood was obtained from patients during surgical intervention.

10 HNSCC patients were included in this study during a follow-up visit between 1 and 57 months after diagnosis. Six included HNSCC follow-up patients were HPV16^{pos}, five had oropharyngeal tumors (tonsil and base of tongue). Three included HNSCC follow-up patients were HPV16^{neg}, two patients had tonsillar tumors and one a tumor in the oral cavity. One follow-up patient was not included in the study as the status of HPV16 infection was not determined. HNSCC tumors were resected shortly after diagnosis and patients received radio- or chemotherapy or both. 50 ml of peripheral blood was obtained from these follow-up patients during a follow-up visit.

Patients characteristics are given in Table 2.1 and 2.2. This study was performed according to established ethical guidelines and all blood and tumor donors gave informed consent.

Table 2.1: Characteristics of HNSCC patients included at time of surgery. m: male, f: female, t.d.: technical difficulties, tumor were classified according to the TNM system accepted by the American Joint Committee on Cancer (AJCC): T: size and/or extent of the primary tumor, N: the amount of spread to nearby lymph nodes, M: presence of metastasis.

Patient	HPV16	Localisation of tumor	Age	Sex	Frequency CD4+ HPV-reactive T cells	Frequency CD8+ HPV-reactive T cells	T	N	M
1	neg	Oropharynx (tonsil)	69	m	none detected	none detected	3	3	1
2	neg	Hypopharynx (sinus piriformis)	73	m	7.3×10^{-6}	none detected	4	0	0
3	pos	Oropharynx (tonsil)	53	m	t. d.	-	2	3	0
4	neg	Oropharynx (tonsil)	69	f	t. d.	-	2-3	3	0
5	neg	Oral Cavity (tongue)	61	f	t. d.	-	1	0	0
6	neg	Oral Cavity (tongue)	58	f	t. d.	-	2	2b	0
7	neg	Oropharynx (tonsil)	69	m	3×10^{-6}	none detected	4	2b	0
8	pos	Oropharynx (tonsil)	46	m	5.7×10^{-5}	3.8×10^{-5}	1	2c	0
9	neg	Oropharynx (tonsil)	64	f	none detected	none detected	3	0	0
15	pos	Oropharynx (tonsil)	58	m	5×10^{-6}	4.9×10^{-7}	2	0	0
16	pos	Oropharynx (tonsil)	79	f	2.0×10^{-6}	1.0×10^{-6}	4	0	0
20	neg	Oropharynx (tonsil)	77	f	1×10^{-5}	none detected	3	0	0
23	pos	Oropharynx (tonsil)	62	m	5.6×10^{-5}	2.1×10^{-6}	1	2b	0
24	neg	Oral Cavity (tongue)	56	m	4×10^{-6}	4.3×10^{-7}	1	0	0
25	pos	Oropharynx (tonsil)	69	m	2.5×10^{-5}	none detected	1	1	0

Table 2.2: Characteristics of HNSCC patients included at follow-up. n.d.: not determined, m: male, f: female, n: no, y: yes, t.d.: technical difficulties, tumor were classified according to the TNM system accepted by the American Joint Committee on Cancer (AJCC): T: size and/or extent of the primary tumor, N: the amount of spread to nearby lymph nodes, M: presence of metastasis.

Patient	HPV16	Localisation of tumor	Age	Sex	Frequency CD4+ HPV-reactive T cells	Frequency CD8+ HPV-reactive T cells	Radio-therapy	Chemo-therapy	T	N	M	Time since diagnosis (months)
10	pos	Oropharynx (tonsil)	69	m	t. d.	-	y	y	2	2c	0	2
11	pos	Larynx (glottis)	75	m	t. d.	-	n	n	3	2b	0	1
12	neg	Oropharynx (tonsil)	51	f	1.7×10^{-6}	none detected	y	y	3	1	0	6
13	neg	Oral Cavity (tongue)	58	m	4.0×10^{-6}	none detected	n	n	1	0	0	4
14	n.d.	Oropharynx (tonsil)	65	f	not included	-	y	y	2	0	0	0
17	pos	Oropharynx (base of tongue)	64	m	8.0×10^{-5}	9.1×10^{-6}	y	y	3	2b	0	15
18	neg	Oropharynx (tonsil)	78	f	5.0×10^{-6}	none detected	y	n	2	2b	0	13
19	pos	Oropharynx (tonsil)	49	f	3.0×10^{-5}	none detected	y	y	2	1	0	31
21	pos	Oropharynx (base of tongue)	57	m	5.5×10^{-6}	5.6×10^{-7}	y	y	3	2b	0	57
22	pos	Oropharynx (base of tongue)	35	f	6.0×10^{-6}	none detected	y	y	2	0	0	36

2.3.2 PBMC preparation

Buffy coats or leukapheresis products from healthy donors were obtained from the university hospital in Dortmund and Cologne. This study was performed according to established ethical guidelines and all blood donors gave informed consent. PBMC were isolated under sterile conditions by Ficoll-Hypaque (GE Healthcare, Chalfont St. Giles) density gradient centrifugation.

2.3.3 Tumor dissociation

HNSCC tumors were surgically removed and stored in MACS Tissue Storage Solution (Miltenyi Biotec) at 4°C for a maximum of 6 h. Subsequently, tumors were cut into pieces of 2 mm size and dissociated according to the GentleMACS protocol for dissociation of tough tumors (Miltenyi Biotec), enzyme R was omitted. Erythrocytes were depleted using CD235a-MB, according to the provided protocol (Miltenyi Biotec).

2.3.4 Separation of T cell subsets

2.3.4.1 Isolation of Pan T cells

Freshly isolated PBMC from buffy coats were used for isolation of Pan T cells. Pan T cells were sorted at >99% purity using a human Pan-T Cell Isolation Kit (Miltenyi Biotec).

2.3.4.2 Isolation of naïve T cells

Freshly isolated PBMC from leukapharesis products were used for the isolation of naïve T cells. Naïve T cells were sorted at >99% purity using a human Naïve Pan-T Cell Isolation Kit (Miltenyi Biotec). $1x10^8$ sorted naïve T cells were supplemented with $1x10^7$ antigen-presenting cells (2.3.2.4) and peptide pool for stimulation.

2.3.4.3 Isolation of memory T cells

Freshly isolated PBMC from leukapharesis products were used for the isolation of memory T cells. Memory T cells were sorted using a human Pan-T Cell Isolation Kit (Miltenyi Biotec) and additionally depleted of CD45RA$^+$ cells using CD45RA-MicroBeads (Miltenyi Biotec), resulting in >99% purity of memory T cells. $1x10^8$ sorted memory T cells were supplemented with $1x10^7$ antigen-presenting cells (2.3.2.4) and peptide pool for stimulation.

2.3.4.4 Isolation of antigen-presenting cells

Freshly isolated PBMC from leukapheresis products were used for the isolation of antigen-presenting cells. Antigen-presenting cells were obtained by depletion of $CD3^+$ cells using CD3-MB according to the provided protocol (Miltenyi Biotec).

2.3.5 Stimulation of T cells

Stimulation of isolated PBMC or dissociated tumor was done in RPMI 1640 medium, supplemented with 5% human AB Serum (Lonza, Basel), 2 mM L-Glutamine (GE Healthcare) and 1 µg/ml CD28 functional grade pure Ab (Miltenyi Biotec). PBMC were stimulated at 1×10^7 cells/ml using PepTivator (Miltenyi Biotec), at a final concentration of 0.6 nmol/ml/peptide. Controls in the absence of exogenous peptide were included. Single cell suspensions obtained from tumor dissociation were stimulated under similar conditions, however due to low cell numbers cell density was sometimes lower than 1×10^7 cells/ml. Controls in the absence of exogenous peptide were included where possible. For generation of WT1-specific T cell cultures from healthy donors WT1 PepTivator and the optimal epitope $WT1_{126-134}$ (RMFPNAPYL) were used for stimulation. For generation of HPV16-specific T cell cultures from healthy donors and HNSCC patients HPV16 E6 PepTivator and HPV16 E7 PepTivator were used for stimulation.

2.3.6 Enrichment of antigen-specific T cells

2.3.6.1 Enrichment via CD154 for *ex vivo* characterization of antigen-specific T cells

For *ex vivo* characterization of antigen-specific T cells, PBMC were stimulated for 7 h in the presence of 1 µg/ml CD40 mAb at functional grade purity (Miltenyi Biotec). Brefeldin A (1 µg/ml; Sigma-Aldrich, St. Louis) was added 2 h before harvest. $CD154^+$ cells were isolated by indirect magnetic labeling using CD154-allophycocyanin and anti-allophycocyanin-MicroBeads (Miltenyi Biotec). Samples were loaded on MS Columns (Miltenyi Biotec) and intracellular staining was performed directly in the magnetic field using an Inside Stain Kit (Miltenyi Biotec). $CD154^+$ cells were eluted using 450 µl PEB-buffer and 400 µl were directly analyzed at the MACSQuant Analyzer. Frequencies of antigen-specific $CD4^+$ T cells were calculated by subtracting the mean number of $CD4^+CD154^+$ cells (triplicates) obtained after enrichment of non-stimulated PBMC from the mean number of $CD4^+ CD154^+$ cells (triplicates) obtained after enrichment of peptide-stimulated PBMC and dividing by the total number of $CD4^+$ T cells applied to the column. Frequencies of antigen-specific $CD8^+$ T cells were determined respectively. A positive antigen-specific response was recorded if the mean

CD4$^+$CD154$^+$ count after peptide pool stimulation exceeded the 95% confidence interval for the CD4$^+$CD154$^+$ count in the unstimulated sample (mean plus two times the standard error of the mean). For patient material only single or duplicate samples were done.

2.3.6.2 Enrichment via CD137 for *in vitro* expansion of antigen-specific T cells

For *in vitro* expansion of antigen-reactive CD4$^+$ and CD8$^+$ T cells, PBMC of healthy donors or patients or single cell suspensions obtained from dissociation of fresh HNSCC tumors were stimulated for 24-36 h in the presence of 1 µg/ml CD28 mAb at functional grade purity (Miltenyi Biotec). Cells were harvested on ice using a cell scraper to remove also adherent and semi-adherent cells. CD137$^+$ cells were isolated by indirect magnetic labeling using either CD137-PE and anti-PE-MB (Miltenyi Biotec) or CD137-allophycocyanin and anti-allophycocyanin-MB according to the protocol of the CD137 MicroBead Kit (Miltenyi Biotec). Samples were loaded on MS Columns (Miltenyi Biotec), flow-through (CD137$^-$) cells were collected for preparation of feeder cells. CD137$^+$ cells were eluted using 500 µl X-Vivo15, spin down and plated in 24-well plates according to 2.3.7.

2.3.6.3 Enrichment via pHLA tetramer

For antigen-specific T cell enrichment, 1x10^8 Pan-T cells were labeled with PE-conjugated WT1$_{37-45}$ tetramer (0.5 µg/ml) for 15 min at 37°C. Allophycocyanin-conjugated WT1$_{37-45}$ tetramer (1 µg/ml) and Abs were then added for 15 min at 4°C. After washing, cells were incubated with anti-PE-MB (Miltenyi Biotec) for 15 min at 4°C and washed again. Separation was performed using two subsequent MS columns according to the manufacturer's protocol (Miltenyi Biotec). The positive fraction was analyzed directly using a MACSQuant flow cytometer (Miltenyi Biotec). Cells were gated hierarchically as follows: lymphocytes, singlets, viable cells, CD14$^-$ and CD20$^-$, CD3$^+$ and CD8$^+$. Frequencies of WT1$_{37-45}$-specific CD8$^+$ T cells were determined by dividing the number of WT1$_{37-45}$ tetramer-PE/allophycocyanin double-positive CD8$^+$ T cells by the number of total CD8$^+$ cells applied to the column.

2.3.7 Expansion of antigen-specific T cells

Antigen-reactive CD4$^+$ and CD8$^+$ T cells were isolated after 24-36 h using a CD137 MicroBead Kit (Miltenyi Biotec) and expanded in X-Vivo15 (Lonza) supplemented with 5% human AB serum (Lonza). Autologous feeder cells were prepared by depletion of CD3$^+$ cells from the negative fraction of CD137 enrichment. To inhibit proliferation of feeder cells they were treated with 25 µg/ml mitomycin C (Sigma-Aldrich) or irradiated with 50 Gy in an X-ray

irradiator. Activated and enriched CD137$^+$ cells were co-cultivated with feeder cells at a ratio of 1:100 with a final density of 5x10^6 cells/ml in 24-well plates in medium supplemented with 15 ng/ml IL-21. From day 2 on medium supplemented with recombinant IL-7 (5 ng/ml), IL-15 (5 ng/ml), and IL-21 (10 ng/ml) was used added. Medium, including the recombinant cytokines, was replenished every second day. Cells were washed and counted at day 6 and then expanded for further 3 days. Before restimulation experiments were done T cells were cultured in X-Vivo-15 containing only 5% AB-Serum and no cytokines for at least two days.

2.3.8 Cultivation of primary tumor cells

Tumor fragments were cultivated in RPMI supplemented with 10% human AB serum (Lonza), antibiotic antimycotic solution (1x, Sigma Aldrich) and Thiazovivin (10 µM, Miltenyi Biotec).

2.3.9 Freezing and thawing of cells

T cells and autologous APC were frozen in cell concentration of maximum 2x10^7 cells/ml in X-Vivo15 supplemented with 20% AB-Serum (Cellgro, Mediatech Inc.) and 10% DMSO (Sigma Aldrich). The cells were taken up in pre-cooled X-Vivo15 and AB-Serum and transferred to pre-cooled cryovials, DMSO was added and mixed. Cryovials were rapidly wrapped with tissue paper and frozen at -70°C The cells were thawed by incubation in a 37°C water bath and transferred into pre-warmed RPMI 1640 or X-Vivo15 supplemented with 5% AB-Serum. After complete thawing the cells were centrifuged and resuspended in medium

2.4 Detection methods

2.4.1 Determination of HPV16 Status of HNSCC tumors

Determination of HPV16 status was performed by PCR of viral DNA as published previously (Klussmann, Weissenborn et al. 2001, Preuss, Weinell et al. 2008). In brief, DNA integrity was determined by β-globin gene PCR, and HPV-DNA was detected by use of a nested PCR protocol with degenerated primers A5/A10-A6/A8 followed by sequencing of positive HPV PCR products.

2.4.2 Cell Surface marker staining

For flow cytometric analysis of cell surface markers 0.1 - 1x10^6 cells were resuspended in 50 µl cold PEB. Cells were stained with fluorochrome-coupled antibodies in a titer of 1:11 for 10

min at 4°C. Cells were washed with 900 µl PEB and centrifuged at 300 g for 5 - 10 min, resuspended in PEB, and analyzed. Cell surface marker staining was accordingly performed in 96-well flat-bottom cell culture plates, but staining was directly done in medium and washing volume was reduced to 100 µl PEB.

2.4.3 pHLA tetramer staining

pHLA tetramer staining was done with 1 µg/ml WT1 tetramer-PE or CMV pp65$_{495-503}$ tetramer-PE for 45 min at 4°C. For the last 10 min other surface staining antibodies were added. Samples were washed once using PEB-buffer and directly analyzed.

2.4.4 Staining of intranuclear FoxP3

Staining of the transcription factor FoxP3 was done using Fixation/Permeabilization solution and 10x Permeabilization solution provided with the FoxP3 Staining buffer set (Miltenyi Biotec). Samples were handled on ice and pre-cooled solutions were used through-out the staining procedure. Samples resuspended in 50 µl PEB-buffer were stained with cell surface staining antibodies for 10 min at 4°C. Samples were washed with 1 ml of PEB-buffer, resuspended in 1 ml freshly prepared, cold Fixation/Permeabilization solution, mixed, and incubated for 30 min at 4°C. Samples were washed once using 1 ml PEB-buffer and once using freshly prepared, cold 1x Permeabilization solution. Cell pellet was resuspended in 90 µl 1x Permeabilization solution, 20 µl FcR blocking reagent (Miltenyi Biotec) was added and incubated for 5 min at 4°C. 10 µl anti-FoxP3-allophycocyanin or anti-FoxP3-PE antibody was used for staining for 30 min at 4°C. Samples were washed once using 1x Permeabilization solution, resuspended in 200 µl PEB-buffer, and directly analyzed.

2.4.5 Intracellular cytokine staining

Antigen-specific cytokine expression of expanded T cell cultures was determined by co-cultivation of 1 – 2.5x10^5 T cells with 5x10^4 antigen-loaded APC in 50 µl RPMI supplemented with 5% AB-Serum, 1 µg/ml CD28 mAb in a 96-well cell culture plate for 6 h. 1 µg/ml brefeldin A was added after 2 h of co-culture. Cells were stained intracellular directly in the 96-well cell culture plate. Staining antibodies for cell surface marker staining and cytokine staining were added at a titer of 1:11, mixed and incubated for 10 min at room temperature. 25 µl InsideFix solution (Miltenyi Biotec) was added, plate was mixed using an orbital shaker and incubated for 20 min at room temperature. 25 µl 10x InsidePerm solution (Miltenyi Biotec) was added, plate was mixed using an orbital shaker and incubated for 10 min at

room temperature. Samples were washed once using 100 ml PEB, centrifuged and resuspended in 200 µl PEB. Samples were directly analyzed at the MACSQuant Analyzer or stored at 4°C for maximum 12 h.

2.4.6 Detection of released cytokines by Multiplex

Cellculture supernatants were collected after 6 – 36 h stimulation of T cells or dissociated tumor material on ice, centrifuged for 10 min at 10000 g at 4°C, transferred to a new, cold microcentrifuge tube and stored at -70°C until further analysis. Assay was performed using the MACS Plex cytokine 12 Kit, human (Miltenyi Biotec) according to the provided protocol. Supernatants were diluted 1:2 and were measured in triplicates where possible. Analysis was done using the MAQSQuant Express Mode for MACSPlex.

2.4.7 Determination of CD107a expression

Antigen-specific cytotoxic potential of expanded T cell cultures was determined by co-cultivation of $1 – 2.5 \times 10^5$ T cells with 5×10^4 antigen-loaded APC in 50µl RPMI supplemented with 5% AB-Serum, 1 µg/ml CD28 mAb, 1 µg/ml monensin and 5µl of CD107a-PE in a 96-well cell culture plate for 6 h. Subsequently cells were transferred to microcentrifuge tubes, washed once, resuspended in 50 µl PEB. Staining antibodies for surface and intracellular staining were added at a titer of 1:11 and samples were mixed and incubated for 10 min at room temperature. Then cell were fixed by addition of 25 µl InsideFix solution (Miltenyi Biotec), mixing and incubation for 20 min at room temperature. Cells were then permeabilized by addition of 25 µl 10x InsidePerm solution (Miltenyi Biotec), mixing and incubation for 10 min at room temperature. Cells were washed once by addition of 500 µl PEB, centrifuged, resuspended in 200 µl PEB and analyzed.

2.4.8 Cytotoxicity assay

For measurement of direct cytotoxicity, T2 cells were either pulsed with peptide pools (specific: WT1; unrelated: HPV16 E7; Miltenyi Biotec) or left unpulsed overnight, labeled with different concentrations of CellTrace Violet (Invitrogen, Carlsbad) for 5 min at 37°C. Unloaded T2 cells were labeled with 1 µM, WT1 loaded T2 cells were labeled with 0.1 µM, and HPV16 E7-loaded T2 cells were labeled with 0.0125 µM CellTrace Violet. Cells were washed 3 times, and pooled subsequently. 0.25×10^4 labeled and pooled T2 cells were then co-cultured with 0.5×10^4, 2.5×10^4, 1.25×10^5, or 2.5×10^5 expanded T cells to achieve different effector to target (E:T) ratios in a 96-well flat-bottom cell culture plate for 4 h. For blocking

experiments, 1 µg/ml αMHC class I mAb (W6/32) was added to the co-culture. Subsequently, cells were stained by adding 2 µl anti-CD20-allophycocyanin, mixing and incubation for 10 min at 4°C to label T2 cells. 50 µl PEB-buffer was added and cells were analyzed directly at the MACSQuant Analyzer. PI (1 µg/ml) was added to each well directly prior to measurement. Antigen-specific killing was determined by flow cytometric measurement of T2 cell viability. Percentage killing was calculated by subtracting the ratio of living antigen-loaded T2 cells after co-culture in the presence or absence of T cells from unity. Percentage antigen-specific killing was calculated by subtracting killing determined for non-loaded T2 cells from killing determined for antigen-loaded T2 cells.

2.4.9 Determination of functional avidity

For determination of functional avidity, T2 cells were pulsed overnight with escalating doses of the optimal CMV pp65$_{495-503}$ (NLVPMVATV) peptide or WT1$_{37}$ peptide (VLDFAPPGA) and co-cultured with expanded T cells at a ratio of 1:5 for 6 h. CD107a expression was determined as described before (2.4.7). Cytokine expression was determined as described before (2.4.5).

2.5 Statistics

Descriptive statistics were done using Microsoft Excel 14.0, Graph Pad Prism 6.0 and TIGR Multi Experiment Viewer 4.9. Calculation of statistical significances and correlations was done with Graph Pad Prism 6.0. For all data sets showing a Gaussian distribution the parametric paired or unpaired two-tailed Student *t* test was used. Significance was defined as: * = p < 0.05, ** = p < 0.01, and *** = p ≤ 0.001.

3 Results

3.1 Establishment of enrichment strategies based on activation markers for the detection of rare antigen-specific T cells

T cells specific for TAA, such as WT1 and HPV16, are present in the blood of healthy and diseased individuals only in very low frequencies. Due to frequencies below 1×10^{-4} cells within PBMC these TAA-specific T cells cannot be detected *ex vivo* with commonly used detection methods for antigen-specific T cells, such as flow cytometric detection of pMHC multimer^{+} T cells or ELISPOT. However, implementation of an magnetic enrichment of antigen-specific T cells, as already demonstrated for magnetic enrichment of pMHC multimer^{+} T cells (Moon, Chu et al. 2007, Obar, Khanna et al. 2008, Kwok, Tan et al. 2012), cytokine secreting T cells (Goodyear, Pratt et al. 2008) and activation marker expressing cells (Bacher, Schink et al. 2013) can drastically enhance the sensitivity.

Therefore, it was investigated whether a combination of magnetic enrichment of activation marker expressing T cells with a subsequent multi parameter flow cytometric analysis is suitable for the detection and characterization of rare TAA-specific T cells. The methods were evaluated for T cells specific for the recall antigens such as CMV or EBV, which have been detected and enumerated *ex vivo* and comprise up to 10% (10^{-1}) of the CD4^{+} and CD8^{+} T cell compartment, respectively (Sylwester, Mitchell et al. 2005). In the next step the methods were transferred to rare TAA-specific T cells. To allow the detection of the complete repertoire of antigen-specific T cells, enrichment of activation marker expressing T cells after short-time stimulation using a pool of peptides spanning the amino acid sequence of the proteins, was evaluated. For *ex vivo* detection, enumeration, and characterization enrichment of CD154^{+} cells after antigen stimulation was implemented; for characterization following *in vitro* expansion enrichment of CD137^{+} cells after antigen stimulation was employed.

3.1.1 Enrichment of CD154^{+} T cells

CD154 (CD40L) is a member of the TNF-family of co-stimulatory molecules and has been introduced as a molecule specifically expressed on activated, not resting T_H cells after stimulation times of 4 h to 24 h (Chattopadhyay, Yu et al. 2005, Frentsch, Arbach et al. 2005). Enrichment of antigen-specific T cells using the T cell activation marker CD154 has recently been well characterized (Bacher, Schink et al. 2013). Antigen-reactive T cell enrichment (ARTE) facilitates direct *ex vivo* analysis of antigen-specific CD4^{+} T cells after a magnetic enrichment of antigen-activated, CD154-expressing cells. The short antigen stimulation times

needed for CD154 up-regulation allows for the complete antigen-reactive T_H cell compartment to be simultaneously enumerated and phenotyped according to the cytokine expression profile and expression of cell surface differentiation markers by multi-parametric flow cytometry.

First, *ex vivo* detection and characterization of T cells specific for recall antigens via CD154 enrichment and multi-parametric analysis by flow cytometry was established. To this end, $2.5x10^7$ PBMC obtained from CMV^{pos} healthy donors were stimulated *in vitro* for 7 h using a CMV pp65 peptide pool, CD154-expressing cells were enriched. The count of CD154^{+} T cells was determined by flow cytometry before and after enrichment in the positively selected cell population as well as in the flow-through fraction.
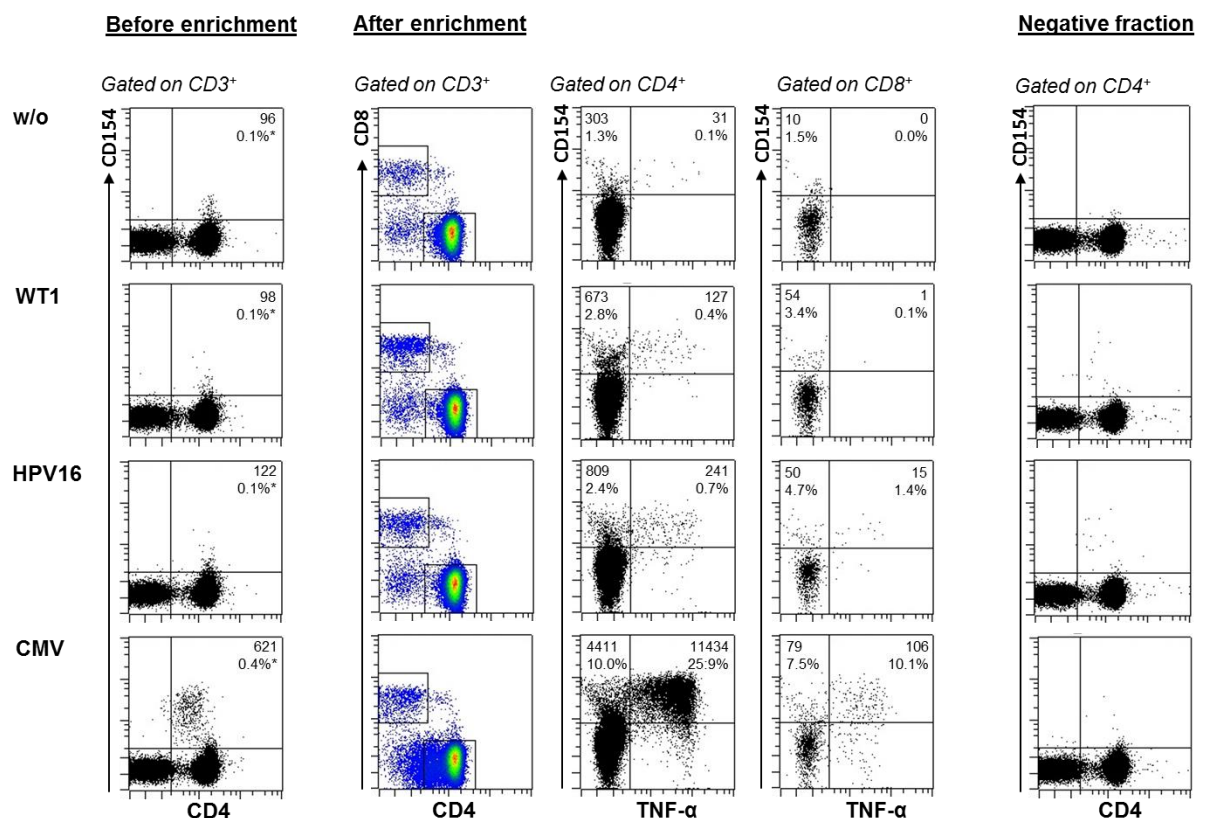
Figure 3.1: Enrichment of CD154^{+} cells allows detection of rare antigen-specific T cells. $2.5x10^7$ cells or $5.0x10^7$ PBMC of a CMV^{pos} healthy donor were stimulated using CMV peptide pool or TAA peptide pools (WT1 and HPV16), respectively, for 7 h. Dot plots of a representative CMV^{pos} healthy donor are shown. CD4^{+} CD154^{+} cells were assessed before (left) and after enrichment (middle). Cell count and percentage of CD4^{+} CD154^{+} and CD4^{+} CD154^{+} TNF-α^{+} cells within CD4^{+} T cells and of CD8^{+} CD154^{+} and CD8^{+} CD154^{+} TNF-α^{+} cells within CD8^{+} T cells is given. CD154 labeling of the flow-through of the separation is shown to prove efficiency of the enrichment procedure (right).

Antigen-specific CD154^{+} T cells were detected before enrichment in the CMV stimulated samples (0.4% within CD4^{+} T cells) (Fig. 3.1). After enrichment of CD154^{+} cells elevated numbers of CD154^{+} CD4^{+} T cells were detected in the stimulated sample compared to the

unstimulated control. Addition of a secretion inhibitor to the cultures 2 h before harvesting allowed for co-staining of effector cytokines by intracellular staining. More than 70% of CD154+ cells produced TNF-α. Furthermore, antigen-specific CD8+ CD154+ T cells, of which >55% produced TNF-α, were detected after enrichment (Fig. 3.1). Hardly any CD154+ expressing cells were detected in the negative fraction (flow-through) of the enrichment, demonstrating that the enrichment procedure was efficient.

The CD154 enrichment approach can be used to enumerate frequencies of antigen-specific T cells. CMV-specific CD4+ T cells can be detected before enrichment and therefore provide a good opportunity to validate the enumeration procedure (Table 3.1).

For CMV stimulation 2.5×10^7 cells have been used, of which 39% were CD4+ T cells. CD4+ cell count was determined before cells were applied to the column, as some cells get lost during staining and washing. The CD154+ CD4+ cell count detected after enrichment in the unstimulated sample was subtracted from the cell count detected in the stimulated sample. The absolute count needs to be extrapolated as not the whole sample can be measured, but only 4/5. By dividing the absolute count of antigen-specific CD4+ T cells by the number of CD4+ T cells applied on the column the frequency of antigen-specific CD4+ T cells was calculated. The calculated frequency (0.25%) lies in the same range as the frequency detected in the sample before enrichment (0.40%), but may in some cases underestimate the real frequency by factor of 1.5 up to 2 (Table 3.1).

Table 3.1: CD154+ cell enrichment allows enumeration of antigen-specific T cells. Example of enumeration of CMV-, WT1-, and HPV-specific T cells before and after enrichment of CD154+ cells. Cell counts and calculated frequencies within CD4+ T cells are given. Ag = antigen, n.d. = not detected.

	CMV	WT1	HPV
PBMC used for stimulation	2.5×10^7	5×10^7	5×10^7
CD4+ T cells applied on to the column	0.78×10^7	1.8×10^7	1.8×10^7
CD154+ CD4+ cells in stimulated sample	15845	800	1050
Ag-specific CD154+ CD4+ T cells	15678	466	716
Extrapolated count of Ag-specific CD154+ CD4+ cells	19597	582	895
Calculated frequency of Ag-specific CD154+ CD4+ cells within CD4+ (after enrichment)	2.5×10^{-3} (0.25%)	3.2×10^{-5}	4.9×10^{-5}
Measured frequency of Ag-specific CD154+ CD4+ cells within CD4+ (before enrichment)	4×10^{-3} (0.40%)	n.d.	n.d.

The same stimulation, enrichment, and analysis approach was done for the detection of WT1- and HPV16-specific T cells to prove feasibility for rare antigen-specific T cells. Before enrichment no elevated counts of CD154-expressing T cells were detected compared to the unstimulated control, in contrast to CMV-stimulated samples, clearly indicating that WT1- and HPV16-specific T cells are low frequent in healthy donors and cannot be detected without enrichment step (Fig. 3.1). After enrichment of CD154$^+$ cells elevated counts of CD4$^+$ CD154$^+$ cells were detected in both the WT1 and HPV16 stimulated samples compared to the unstimulated sample, showing that also low frequent TAA-specific T cells can be enriched and detected using this approach. The starting cell number for detection of rare antigen-specific T cells should be at least 1x10^7 PBMC to ensure detection of at least 10 to 100 specific events.

The CD154 enrichment approach also allows determination of the differentiation status and the functionality of antigen-specific T cells. To this end, cells were co-stained for differentiation markers CD45RO and CCR7 and for cytokines in samples of PBMC from an EBV^{pos} healthy donor stimulated with EBV antigens. These data show that both memory (CD45RO$^+$) and naïve (CD45RO$^-$ CCR7$^+$) T cells can be enriched via CD154 after antigen-specific stimulation (Fig. 3.2). TNF-α-producing T cells revealed a memory phenotype predominantly, but also naïve TNF-α$^+$ T cells were detected. IFN-γ-producing EBV-specific T$_H$ cells were memory T cells exclusively. Phenotyping is exemplarily shown for EBV-specific T cells, but similar patterns were observed for other antigen specificities.
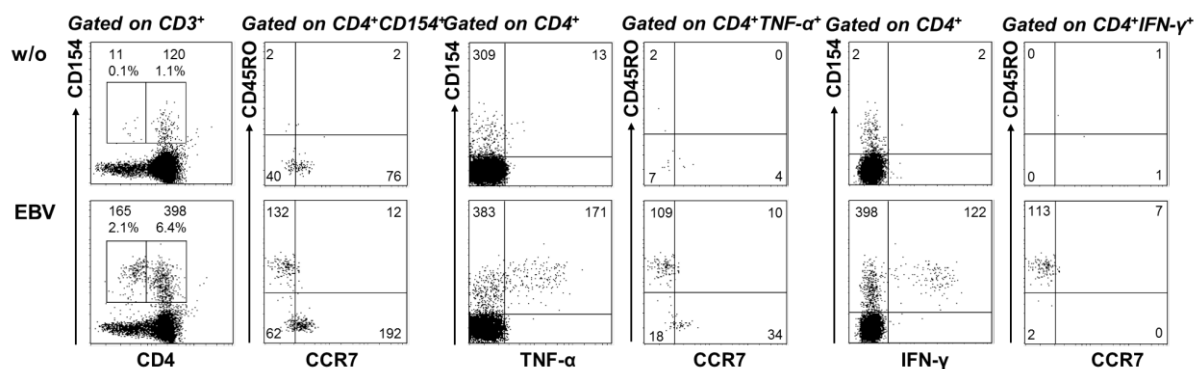
Figure 3.2: Enrichment of CD154$^+$ cells allows phenotyping of antigen-specific T cells. 5.0x10^7 PBMC were stimulated using EBV peptide pools EBNA-1 and LMP2a for 7 h and subsequently CD154$^+$ cells were enriched. Dot plots of a representative healthy donor are shown. CD4$^+$ CD154$^+$ cell counts and frequencies were assessed after enrichment.

Direct co-staining for several cytokines allows detection of poly-functionality of antigen-specific T cells. Apart from TNF-α and IFN-γ (Fig. 3.3A) also other cytokines were counterstained in an independent staining panel (Fig. 3.3B). IL-2 expression was commonly

co-detected in samples where TNF-α and IFN-γ production was detected. Some donors revealed a small proportion of IL-10-producing T cells among the CD154+ antigen-specific T_H cells. IL-17 production was not detected in EBV and CMV antigen-stimulated samples.
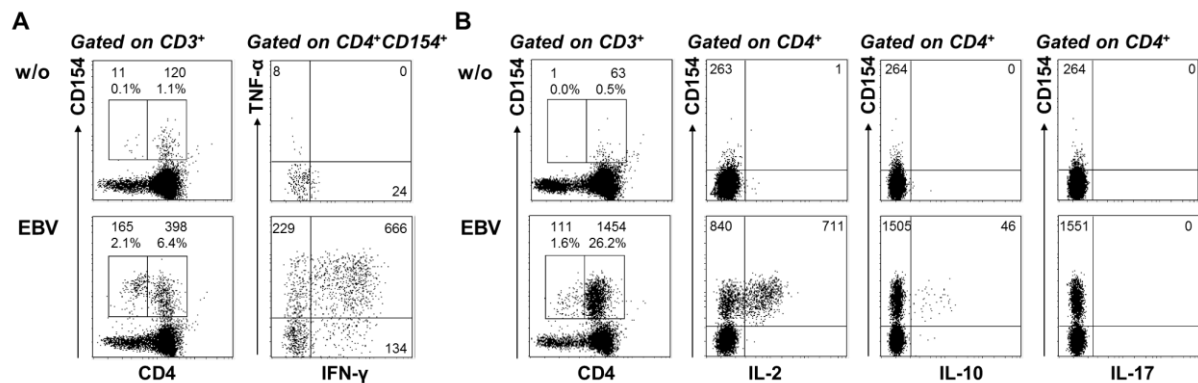
Figure 3.3: CD154 enrichment allows detection of poly-functional T_H cells. 5×10^7 PBMC were stimulated using EBV peptide pools EBNA-1 and LMP2a for 7 h and subsequently CD154+ cells were enriched. Dot plots of two representative healthy donors are shown. **(A)** Co-staining of TNF-α and IFN-γ on CD4+ CD154+ T cells. **(B)** Detection of IL-2, IL-10, and IL-17 among CD4+ CD154+ T cells.

Taken together, detection of CMV- and EBV-specific CD4+ and CD8+ T cells proves the suitability of characterization of antigen-specific T cells in terms of prevalence, differentiation status, and functionality using CD154+ cell enrichment. Enumeration of antigen-specific T cells is possible and reliable for the CD4+ T cell compartment. Furthermore, the feasibility for the detection and characterization of rare WT1- and HPV16-specific T cells was shown.

3.1.2 Enrichment of CD137+ T cells

CD137 (4-1BB) is a member of the TNF-family of co-stimulatory molecules and plays a major role in activation, survival, and proliferation of memory CD4+ and CD8+ T cells (Sabbagh, Snell et al. 2007). CD137 has been described as a marker to detect naïve and memory antigen-specific T cells after antigen stimulation and has also been used to sort antigen-specific T cells (Pollok, Kim et al. 1993, Wolfl, Kuball et al. 2007). In contrast to CD154, the kinetic of upregulation of CD137 is slower, as it is expressed on activated T cells 12 h up to 72 h after stimulation (Wolfl, Kuball et al. 2007, Wehler, Karg et al. 2008). A recent publication showed that CD137 expression is also found on activated T_{reg} cells already after 5 h of stimulation (Schoenbrunn, Frentsch et al. 2012). Therefore, CD137 marks both activated CD4+ and CD8+ effector T cells (T_{eff}), but also T_{reg}.

Similar to the CD154 protocol the CD137 protocol was tested for T cells specific for recall antigens and then transferred to the tumor-antigens of interest, WT1 and HPV16 E6 and E7, for which T cells are expected to be present in low frequencies in healthy donors.

3.1.2.1 CD137 is co-expressed with other T cell activation markers

To confirm that CD137 is upregulated specifically on antigen-specific T cells, co-expression with other T cell activation markers, such as CD154 and CD69, was analyzed. To this end, 5×10^7 PBMC obtained from a CMV^{pos} healthy donor were stimulated *in vitro* for 24 h using a CMV pp65 peptide pool and CD137^{+} cells were magnetically enriched. Expression of CD137, CD154, and CD69 was analyzed by flow cytometry before enrichment and after enrichment in the positively selected cells and in the flow-through. Before enrichment CD137^{+} were detected within CD4^{+} and CD8^{+} T cells, a subpopulation of CD4^{+} CD137^{+} cells expressing also the activation marker CD154 and all CD8^{+} CD137^{+} cells expressing the activation marker CD69 (Fig. 3.4A). After enrichment of CD137^{+} cells CD154 was co-expressed on the majority of CD4^{+} CD137^{+} T cells (Fig. 3.4B). However, a reasonable fraction of CD4^{+} CD137^{+} cells did not express CD154, this fraction most likely includes antigen-specific T[reg], which are known to not upregulate CD154 upon stimulation (Schoenbrunn, Frentsch et al. 2012), but also contains non-antigen-specific T cells (discussed in more detail in 3.1.2.3). CD4^{+} CD154^{+} CD69^{+} and thus activated CD4^{+} T cells were highly enriched in the positive fraction, clearly indicating that CD137 enrichment indeed selects antigen-activated CD4^{+} T cells. Likewise, CD8^{+} T cells that co-express CD137 and CD154 were detected after enrichment of CD137^{+} cells. Additionally, CD69 was highly co-expressed on CD137^{+} T cells, confirming their activated status following antigen-stimulation. The negative fraction of the enrichment contained hardly any CD137^{+} T cells, suggesting that CD137^{+} cells have been depleted efficiently and the majority of activated antigen-specific T cells was sorted into the positive fraction (Fig. 3.4C). These data show that CD137 is a suitable marker for the *ex vivo* enrichment of activated antigen-reactive CD4^{+} and CD8^{+} T cells after antigen stimulation.
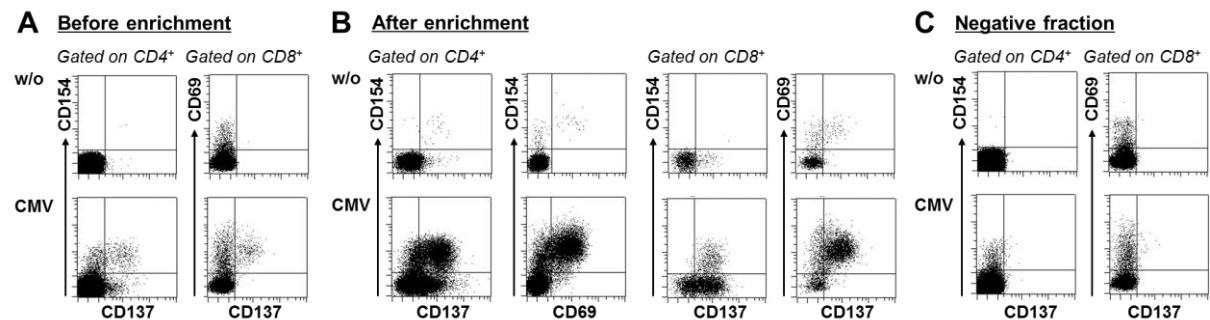
Figure 3.4: Feasibility test for enrichment of antigen-specific T cells via CD137. (A-C) Staining of activation markers CD137, CD154, and CD69 on CD4+ (left) and CD8+ (right) T cells after 24 h stimulation of 5x10^7 PBMC obtained from a CMVpos donor with CMV pp65 peptide pools. **(A)** Before enrichment, **(B)** on positive fraction after enrichment of CD137+ cells, and **(C)** on negative fraction after enrichment of CD137+ cells.

3.1.2.2 CD137+ cells are accurately detected after enrichment with anti-CD137-PE

In order to disclose differences in detection when different reagents are used for enrichment of antigen-specific CD137+ cells, labelling with anti-CD137-Biotin and anti-Biotin-MB was compared to labelling with anti-CD137-PE and anti-PE-MB. To this end, 1x10^7 PBMC from a CMVpos healthy donor were stimulated using CMV pp65 peptide pool for 18 h. Labelling with anti-CD137-PE results in comparable frequencies of detected CD137+ T cells both with and without additional labelling with anti-PE-MB (2.0 to 2.1% within CD4+ T cells and 4.0 to 4.3% within CD8+ T cells) (Fig. 3.5). Comparable frequencies of CD137+ T cells were detected when the staining was performed with anti-CD137-Biotin and anti-Biotin-PE (2.4% within CD4+ T cells and 4.5% within CD8+ T cells). However, when cells were additionally labeled with anti-Biotin-MB a decreased frequency of CD137+ T cells was found, independent of whether a subsequent staining was done with anti-CD137-PE or anti-Biotin-PE (0.6 to 0.7% within CD4+ T cells and 2.3 to 2.6% within CD8+ T cells). These results indicate that labeling with anti-Biotin-MB blocks in part the binding of anti-Biotin-PE, which results in underestimating the frequencies of CD137+ T cells.
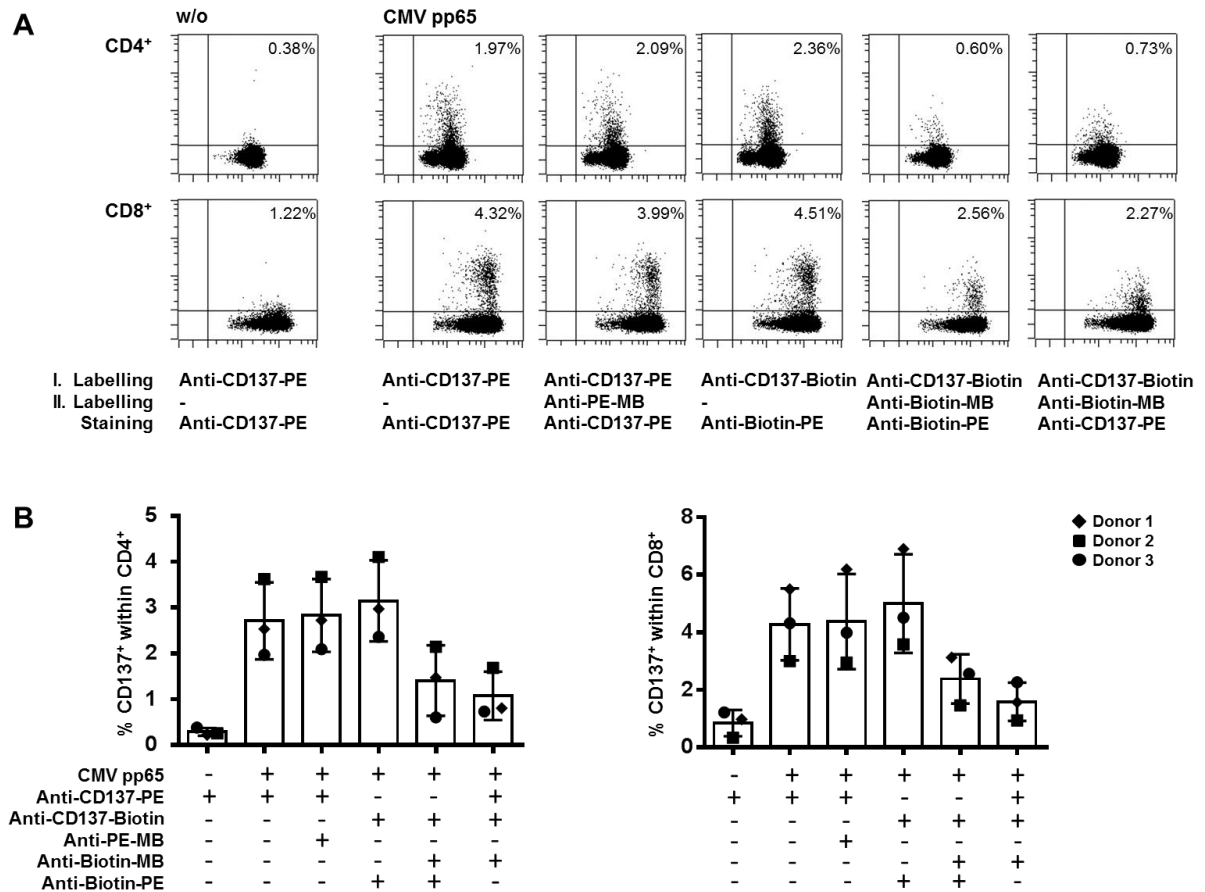
Figure 3.5: Anti-CD137-PE allows accurate determination of CD137$^+$ cells with and without MB-labelling. 1×10^7 PBMC from a CMV^{pos} healthy donor were stimulated using CMV pp65 peptide pool for 18 h and stained using either anti-CD137-PE or anti-CD137-Biotin as indicated, washed, and subsequently labelled with either anti-PE-MB, anti-Biotin-MB, or no MB as indicated. After washing cells were stained with either anti-CD137-PE or anti-Biotin-PE as indicated. **(A)** Dot plots of stimulated and stained PBMC. Percentage of CD137$^+$ cells within CD4$^+$ and CD8$^+$ T cells is given, respectively. **(B)** Frequency of CD137$^+$ cells within CD4$^+$ (left) and CD8$^+$ (right) T cells measured for the indicated labelling and staining conditions. Bars represent mean of 3 measurements, which have been done with PBMC of three donors, and standard deviation is given.

Using the PE-System an increased level of CD137$^+$ cells was discovered in the unstimulated sample (Fig. 3.6) compared to the Biotin-System. These CD137$^+$ cells are most likely pre-activated T cells that are not specific for the antigen used for stimulation. The higher background detected in the PE-System is due to the differences in detection efficiency, but number and quality of enriched cells in both the PE- and Biotin-System do not differ. The combination of CD137-PE and anti-PE-MB was chosen for the labeling in further analyses.
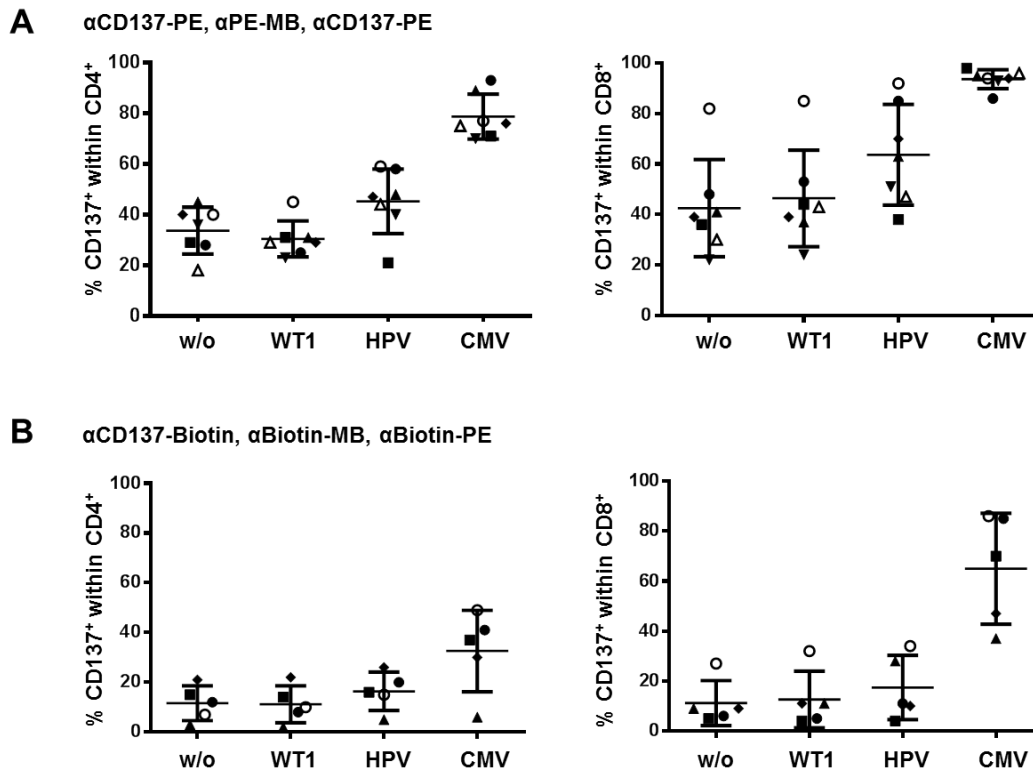
Figure 3.6: CD137-PE enrichment system detects higher frequencies of CD137⁺ cells after CD137 enrichment. PBMC from a CMV^{pos} healthy donor were stimulated using either no peptide (w/o), WT1 peptide pool, HPV16 and HPV18 peptide pools, or CMV pp65 peptide pool for 18 h and subsequent enrichment of CD137⁺ cells either via CD137-PE and PE-MB **(A)** or CD137-Biotin and biotin-MB **(B)**. Detection of CD137⁺ cells was done by staining with CD137-PE in all samples. Mean and standard deviation are given.

3.1.2.3 CD137⁺ effector and regulatory T cells are enriched via CD137

CD137 was shown to be also expressed on T_{reg} upon 5 h of antigen stimulation, whereas effector T cells need longer (>12 h) stimulation times (Schoenbrunn, Frentsch et al. 2012) for surface expression of CD137. Therefore it is expected that the CD137 enrichment approach also enriches antigen-specific, activated T_{reg}. To test whether activated T_{reg} are enriched with our approach we stimulated $5x10^7$ PBMC of an EBV^{pos} healthy donor using EBV EBNA-1 and LMP2a peptide pools for 34 h and enriched CD137⁺ cells. The transcription factor FoxP3 and the IL-2 receptor α-chain (CD25) are the most common markers to identify nT_{reg}. Accordingly, FoxP3 and CD25 were used to identify T_{reg}. However, both CD25 and also recently FoxP3 have been described to not exclusively be expressed on T_{reg}, but also transiently on activated effector T cells (Allan, Crome et al. 2007, Wang, Ioan-Facsinay et al. 2007). Indeed, high amounts of CD4⁺ FoxP3⁺ CD25⁺ cells were detected after enrichment when recall antigens with a high frequency of memory T cells, such as EBV antigens, were used for stimulation (Fig. 3.7A). These CD4⁺ FoxP3⁺ CD25⁺ showed a CD137^{dim} staining.
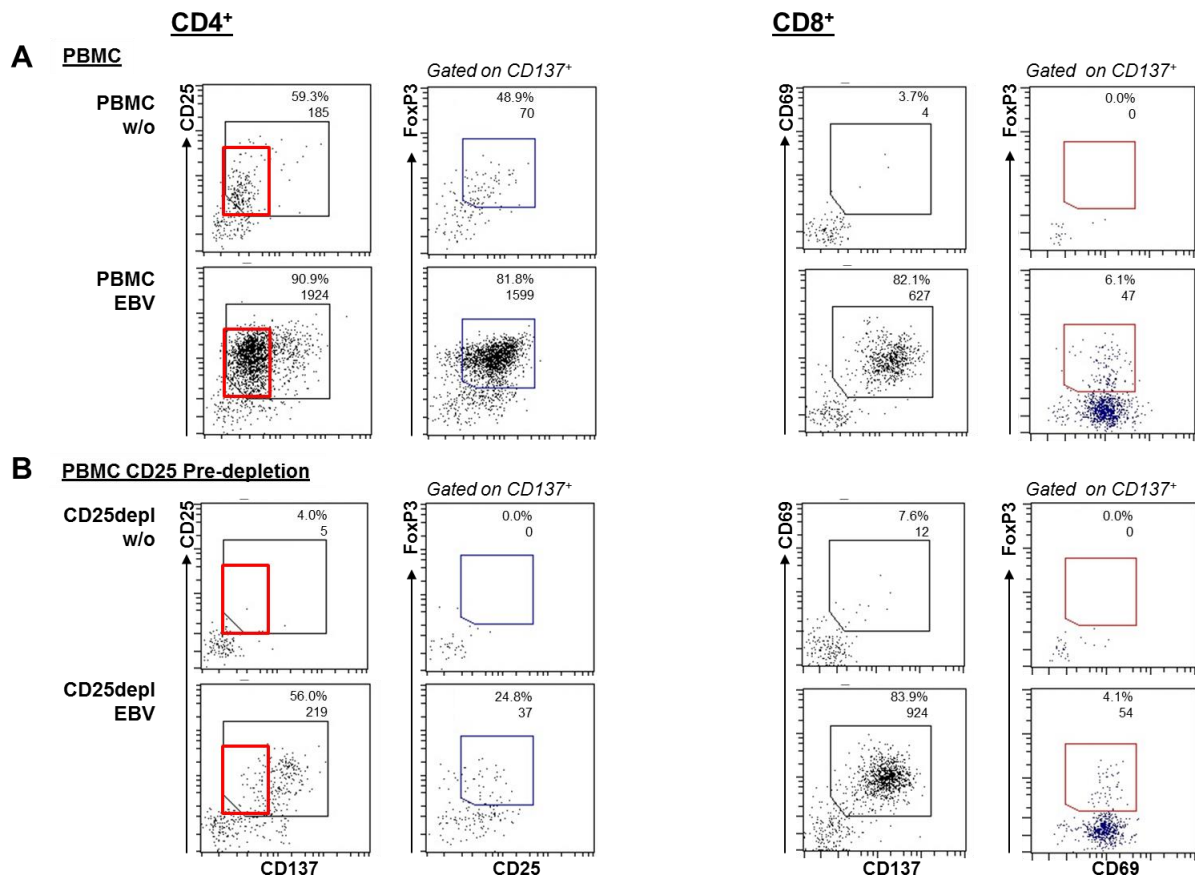
Figure 3.7: CD137^{dim} FoxP3$^+$ CD25$^+$ CD4$^+$ T cells are enriched via CD137 enrichment. PBMC of an EBV^{pos} healthy donor were stimulated with EBV EBNA-1 and LMP2a peptide pools (EBV) or left unstimulated (w/o) for 34 h. Subsequently CD137$^+$ cells were enriched via anti-CD137-PE and anti-PE-MB. Dot plots of a representative healthy donors are shown. Cells were gated on CD4$^+$ (left) and CD8$^+$ (right) T cells after enrichment of CD137$^+$ cells from **(A)** PBMC or **(B)** CD25-depleted PBMC. Cell count and percentage within gated cells are given. CD137^{dim} cells are encircled by a bold red line.

To further investigate whether these FoxP3$^+$ CD137^{dim} cells are nT$_{reg}$, experiments were performed where CD25$^+$ cells, which include all nT$_{reg}$ and also pre-activated T$_{eff}$, were depleted prior to antigen specific stimulation and CD137 enrichment (Fig. 3.7B). When CD25$^+$ cells were removed the enriched CD137$^+$ population in the unstimulated sample was diminished, indicating that a background of CD137$^+$ pre-activated T cells was depleted. Furthermore, the CD137^{dim} population is not detectable after CD137 enrichment in the stimulated sample, which indicates that this CD137^{dim} population indeed consists of activated nT$_{reg}$. However, the amount of CD137^{dim} CD25$^+$ FoxP3$^+$ T cells exceeded the number of antigen-specific CD137^{high} cells by several times (in the depicted example the ratio of CD137 expressing T$_{reg}$ to T$_{eff}$ was 5:1), which makes it unlikely that all CD137^{dim} cells were antigen-specific T$_{reg}$. Recently, ratios of fungi-specific T$_{reg}$ to T$_{eff}$ were determined, for *A. fumigatus* the number of T$_{reg}$ did indeed exceed the number of specific T$_{eff}$ in some donors, but only by 1.5-fold in the mean (Bacher, Kniemeyer et al. 2014). In our experiments, the distinct CD137^{dim} population was only detected in samples in which also a high T$_{eff}$ memory

response against the chosen antigen was induced, therefore we hypothesize that the CD137^{dim} population contained, additionally to antigen-specific nT$_{reg}$, also T$_{reg}$ that have been activated by bystander activation, most likely induced by soluble factors.
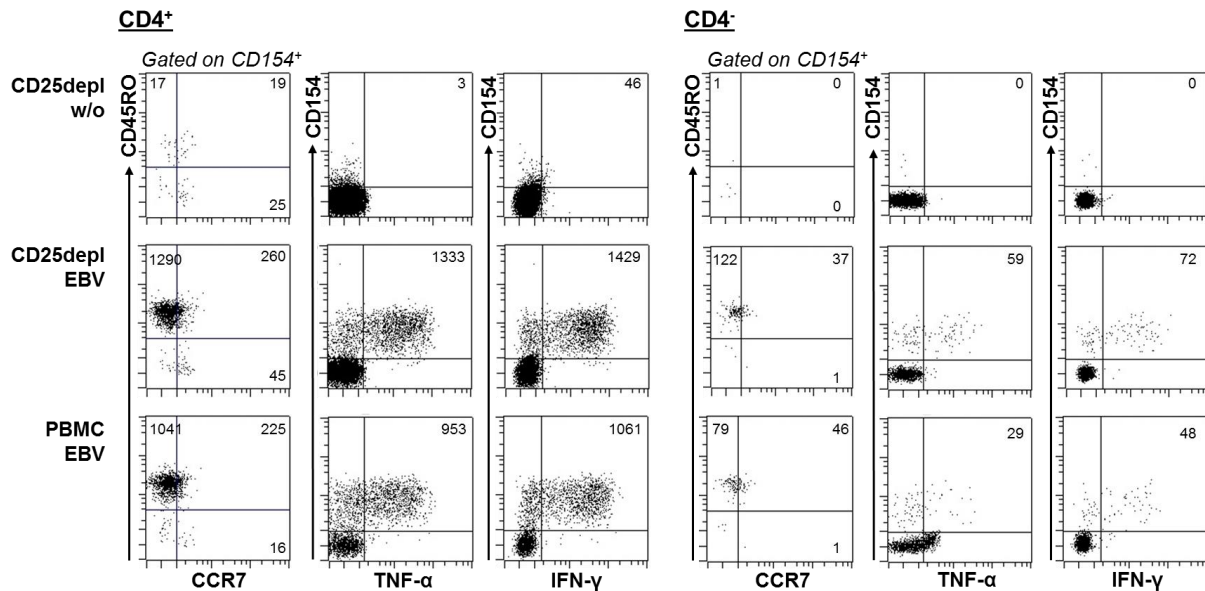
Figure 3.8: Depletion of CD25$^+$ cells can increase activation of antigen-specific T cells. PBMC or CD25-depleted PBMC were stimulated using EBV EBNA-1 and LMP2a peptide pools for 7 h and subsequently CD154$^+$ cells were enriched. Dot plots after enrichment of CD154$^+$ cells are shown for CD4$^+$ (left) and CD4$^-$ (right) T cells of one representative healthy donor. Cell counts are given.

Depletion of CD25$^+$ cells resulted in some cases in a detection of higher numbers of naïve and memory CD4$^+$ and CD8$^+$ antigen-specific effector T cells (Fig. 3.8). These data imply that the activation of antigen-specific effector T cells can be hampered by activated, antigen-specific T$_{reg}$.

3.1.2.4 Low frequent T cells can be enriched via CD137

The CD137 enrichment approach was transferred to the tumor-antigens of interest, WT1 and HPV16 E6 and E7. To this end, 1x10^8 PBMC were stimulated for 24 to 36 h and CD137$^+$ cells were enriched. CD137-expression was analyzed before and after enrichment. Frequencies of CD137$^+$ cells in the enriched fraction did only slightly increase when PBMC were stimulated with WT1 (30.4 to 86.0% and 13.2 to 64.1% within CD4$^+$ and CD8$^+$ cells, respectively) or HPV16 (47.3 to 86.3% and 10.6 to 74.7% within CD4$^+$ and CD8$^+$ cells, respectively), compared to the unstimulated control (16.6 to 80.0% and 7.9 to 38.0% within CD4$^+$ and CD8$^+$ cells, respectively), as the numbers of these specific T cells were very low, as already observed using the CD154 enrichment approach. When collecting data from

several samples of different healthy donors, however, a significant increase in frequencies of CD137+ T cells was detected in the stimulated samples compared to the unstimulated samples (Fig. 3.9). Thus, these results indicate that WT1- and HPV16-specific T cells have been enriched from healthy donors, however, suggest that a majority of enriched T cells in the samples were *in vivo* pre-activated and not induced by antigenic stimulation.
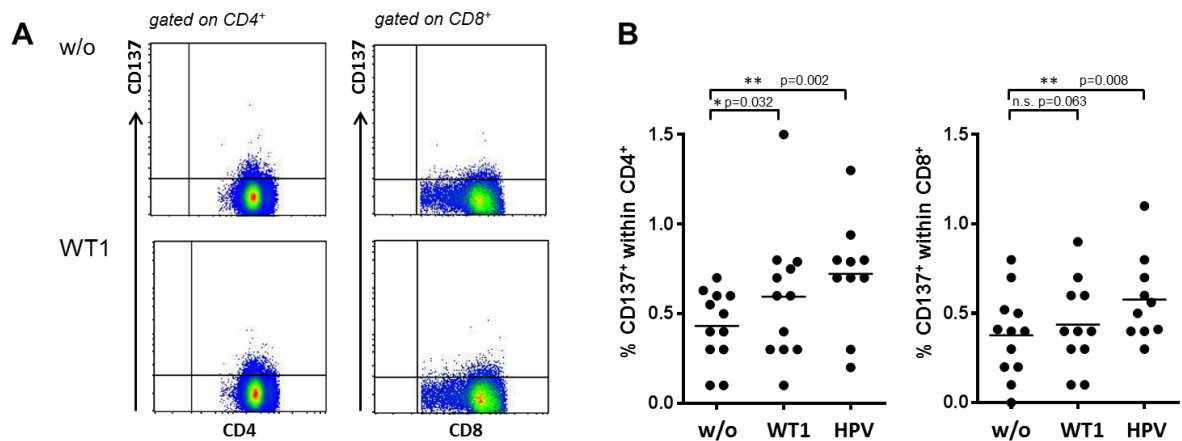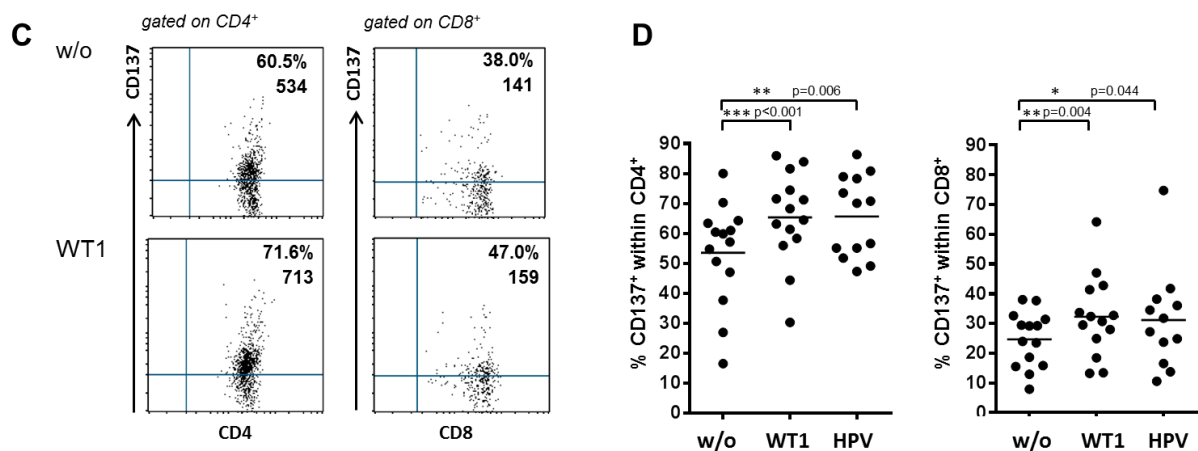
Figure 3.9: Enrichment of rare CD137-expressing antigen-specific T cells. 1×10^8 PBMC from healthy donors were stimulated with either WT1 peptide pool or HPV16 E6 and E7 and HPV18 E6 and E7 peptide pools as indicated or left unstimulated (w/o) for 24 - 36 h. CD137+ cells were enriched via anti-CD137-PE and anti-PE-MB. **(A and B)** Samples before enrichment. **(A)** Dot plots of a representative sample, unstimulated and stimulated with WT1 peptide pool, CD137 expression on CD4+ (left) and CD8+ (right) T cells is depicted. **(B)** Frequency of CD137+ T cells within CD4+ (left) and CD8+ (right) T cells is shown for 12 donors, 4 independent experiments were done. Mean is given. **(C and D)** Samples after enrichment of CD137+ cells. **(C)** Dot plots showing staining of an aliquot of a representative sample (same donor as depicted in (A)), unstimulated and stimulated with WT1 peptide pool, CD137 expression on CD4+ (left) and CD8+ (right) T cells is depicted. **(D)** Frequency of CD137+ T cells within CD4+ (left) and CD8+ (right) T cells is shown for the same 12 donors as depicted in (B). Mean is given.

3.1.2.5 Antigen-specific T cell lines can be generated after CD137 enrichment

To clearly demonstrate the presence of TAA-reactive T cells in the CD137$^+$ fraction and obtain sufficient cell numbers for further phenotypical and functional characterization, a protocol was established to generate WT1- and HPV-specific T cell lines (Fig. 3.10A). Therefore 1x10^8 PBMC were stimulated with the antigens for 24 – 36 h, CD137$^+$ cells were enriched, and subsequently co-cultured with CD3-depleted, irradiated autologous feeder cells (APC) derived from the negative fraction of the CD137 enrichment step for 11 to 12 days. IL-21 was added on day zero, from day two on cells were replenished with IL-21, IL-7, and IL-15 every second day. On day 9, cells were washed to remove the cytokines to start a resting phase before an antigenic restimulation for further analysis.

Flow cytometric analysis of the enriched cell fractions revealed significantly elevated numbers of CD4$^+$ CD137$^+$ and CD8$^+$ CD137$^+$ T cells in stimulated samples compared to unstimulated controls (Fig. 3.10B). Absolute cell numbers after enrichment ranged from 1.2x10^4 to 4.3x10^4 (mean 3.3x10^4) viable CD137$^+$ leukocytes in the WT1stimulated samples and 0.3x10^4 to 1.3x10^5 (mean 3.5x10^4) viable CD137$^+$ leukocytes in the HPV stimulated samples; compared to 0.9x10^4 to 3.2x10^4 (mean 2.5x10^4) in the control samples. During the 9-day culture period enriched T cells from either the stimulated as well as the unstimulated sample expanded about 100-fold (Fig. 3.10C).
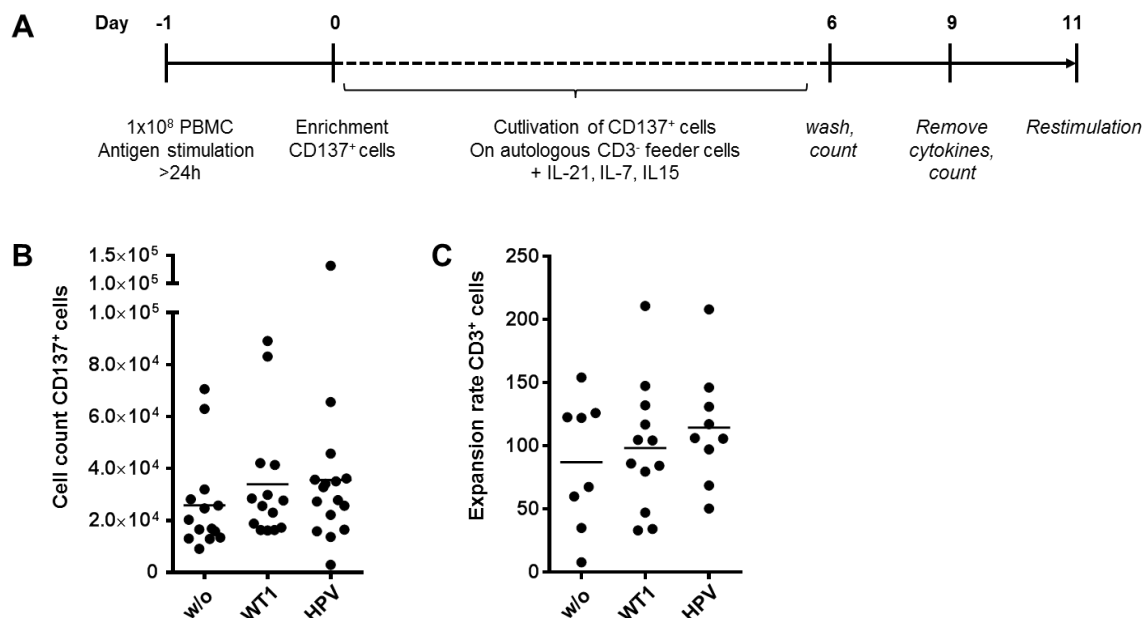
Figure 3.10: Generation of antigen-specific T cell lines via CD137 enrichment. (A) Scheme of enrichment and expansion protocol for the generation of antigen-specific T cell lines via CD137 enrichment. **(B)** Cell count of viable CD137$^+$ lymphocytes after enrichment of CD137$^+$ cells from 1x10^8 PBMC either without stimulation or stimulated with the indicated antigens, n = 17 healthy donors. Mean is given. **(C)** Expansion rate of CD3$^+$ cells within 9 days. Mean is given.

Antigen-specificity was confirmed after expansion by restimulation assays using antigen-loaded APC (Fig. 3.11). Only few T cells were activated when co-cultivated with unloaded, autologous APC. T cell cultures contained up to 54% and 15% WT1-specific CD4+ and CD8+ TNF-α-producing T cells, respectively; and 65% and 31% HPV-specific TNF-α-producing CD4+ and CD8+ T cells, respectively.
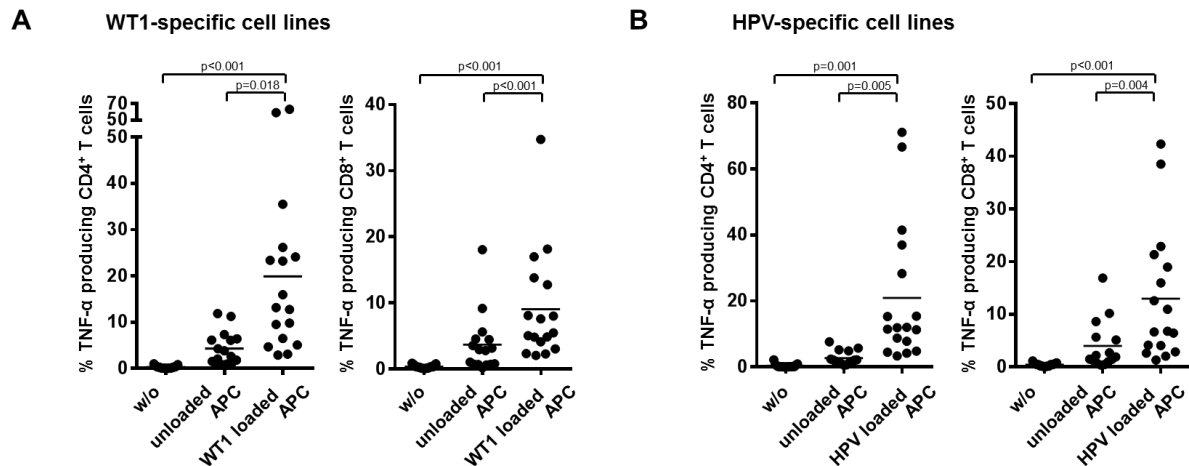
Figure 3.11: Restimulation of antigen-specific T cell lines. (A and B) TNF-α producing CD4+ (left) and CD8+ (right) T cells after restimulation of expanded T cells from 17 healthy donors with the indicated stimuli, no antigen, unloaded autologous APC, or autologous APC loaded with the respective peptide pool WT1 **(A)** and HPV16 E6, E7 and HPV18 E6, E7 **(B)**. Mean is given. Significance was determined using paired Student's *t*-test.

We further investigated the influence of T_{reg} on the generation of antigen-specific T cells via the CD137 enrichment approach. CD4+ FoxP3+ T cells get highly enriched through the CD137 enrichment step, due to the enrichment of T_{reg} and activated T_{eff} that transiently upregulate FoxP3 (see section 3.1.2.3). However, the levels of CD4+ FoxP3+ T cells were very low after the 9 day expansion phase (Fig 3.12A), as the chosen expansion conditions using IL-7, IL-15, and IL-21 did not favor the expansion of T_{reg}. Additionally, we checked whether pre-depletion of CD25+ cells alters the generation of antigen-specific T cell lines via CD137 enrichment (Fig. 3.12). The expansion rate of T cells after enrichment was comparable in both unsorted and CD25-depleted samples (Fig. 3.12B). Interestingly, significantly more CD8+ T cells were detected after the expansion of the CD25-depleted samples, most likely due to the fact that CD25-depletion removes most exclusively CD4+ T cells and thus skews the T cell composition towards CD8+ T cells (Fig. 3.12C). The quality and frequency of antigen-specific CD8+ and CD4+ T cells was not significantly different after expansion (Fig. 3.12D, E). In summary, the enrichment of CD137+ T_{reg} cells was not an issue for the enrichment and expansion of low frequent effector T cells, such as WT1- and HPV16-specific T cells, as the depletion of CD25+ cells did not alter the quality and expansion capacity of the enriched antigen-specific effector T cells. Therefore we did not deplete CD25+

cells before enrichment in further experiments. However, in some cases, for antigens that show high abundance of specific T_{reg} depletion of CD25$^+$ cells might be favorable to ensure an optimal expansion.
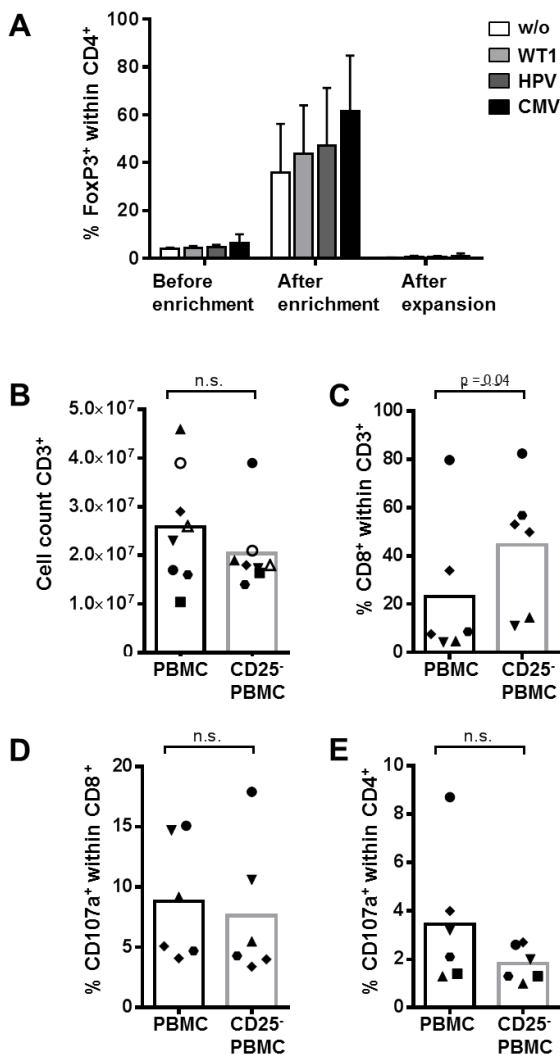
Figure 3.12: Influence of FoxP3$^+$ T cells on generation of antigen-specific T cell lines via CD137 enrichment. (A) Percentage of FoxP3$^+$ cells within CD4$^+$ T cells before and after enrichment of CD137$^+$ cells and after 9 day expansion of CD137$^+$ cells. Bars represents mean of 3 donors, standard deviation is given. **(B-E)** Characteristics of expanded T cells after 9 day expansion of WT1- or HPV-stimulated CD137$^+$ cells either preformed with unsorted or CD25-depleted PBMC. **(B)** Cell count of CD3$^+$ T cells (n = 8), **(C)** percentage of CD8$^+$ T cells within CD3$^+$ T cells (n = 6), and **(D and E)** percentage of antigen-specific CD107a-expressing CD8$^+$ **(D)** and CD4$^+$ **(E)** T cells upon restimulation (n = 6) is depicted. Bars represent mean. Significance was determined using paired Student's t-test.

In the next step, the established techniques based on antigen-specific stimulation with 15mer peptide pools and enrichment of activation marker-expressing T cells were used to characterize TAA-specific T cells.

3.2 Characterization of WT1-specific T cells in healthy individuals

The Wilms' tumor 1 (WT1) protein is a self-antigen, which is expressed at high levels in several types of hematological malignancies as well as in some solid-tumors. WT1 has been ranked as a top antigen for immunotherapy (Cheever 2009). This gave rise to multiple studies evaluating various WT1-based vaccination approaches and also adoptive transfer of WT1-specific T cells for cancer therapy. Until now, however, in-depth knowledge of the natural occurring T cell repertoire is vastly missing. Highly sensitive analysis methods, based on magnetic enrichment (introduced in 3.1), enabled *ex vivo* characterization and efficient *in vitro* propagation of WT1-specific T cells in healthy donors.

3.2.1 *Ex vivo* characterization of WT1-specific T cells

3.2.1.1 Majority of healthy donors have a pool of WT1-reactive CD4$^+$ memory T cells

For detailed enumeration and characterization of rare, preexisting CD4$^+$ WT1-specific T cells in healthy donors directly *ex vivo*, the Ag-reactive T cell enrichment (ARTE) protocol was utilized (introduced in 3.1.1). ARTE facilitates direct *ex vivo* analysis of antigen-specific CD4$^+$ T cells down to frequencies of 10^{-5}-10^{-6} specific T cells within 10^7-10^8 total PBMC after a magnetic enrichment of antigen-activated, CD154-expressing cells.

In order to detect and characterize WT1-specific CD4$^+$ T cells *ex vivo*, 5×10^7 PBMC of healthy donors were cultured either with or without addition of the WT1 peptide pool for 7 h and subsequently enriched CD154$^+$ expressing T cells. Significantly higher numbers of CD154$^+$ T cells can be detected in the positive enriched fraction of WT1-stimulated samples (50 to 555 cells, mean 190 cells) compared to the unstimulated control samples (27 to 198 cells, mean 87 cells) (Fig. 3.13A), only in 2 out of 24 samples no elevated CD154$^+$ cell count was detectable upon stimulation. On the basis of the detected count of WT1-specific CD154$^+$ cells and the overall number of CD4$^+$ T cells used in the particular experiment, the frequencies of WT1-reactive T cells were calculated to range between 1×10^{-6} and 2×10^{-5} within the CD4$^+$ T cell compartment (Fig. 3.13B).

As these results imply a considerable variation in the frequency of detectable WT1-reactive CD154$^+$ cells, a more comprehensive characterization of the WT1-reactive CD4$^+$ T cells regarding their differentiation status and cytokine profile was included. This analysis was done under identical conditions for 20 of the 24 donors, in which phenotypic markers CD45RO, CD45RA, and CCR7 and, in a separate sample, TNF-α, IFN-γ, and in some donors also IL-2, IL-4, IL-10, and IL-17 were stained in the positively selected cells. Determination of the phenotype of the positively selected cells revealed that in samples of some healthy donors WT1-reactive naïve and memory Th cells can be detected, whereas in

others only a few WT1-reactive Th cells, exhibiting a naïve phenotype, were detected. On the basis of this finding we divided the 20 donors in two groups. The first group of samples showing a memory and naïve response for WT1 was assigned "memory response" group (n = 13). The second group of samples showed solely a naïve response for WT1 and was therefore assigned "no memory response" group (n = 7).

In the "memory response" group all samples revealed a higher number of CD154$^+$ cells showing memory (CD45RO$^+$ CCR7$^{+/-}$) and naïve (CD45RO$^-$ CCR7$^+$) phenotype in the stimulated compared to the corresponding unstimulated samples (Fig. 3.13C). Furthermore, these 13 samples showed at least 1.5-fold higher numbers of CD154$^+$ cells after enrichment in the WT1 stimulated samples compared to background. Additionally, ten or more CD154$^+$ TNF-α$^+$ events above background could be detected in these samples and the frequency of TNF-α$^+$ cells within CD154$^+$ cells was generally higher than in the "no memory response" group (mean 29.6%, range 14.1 – 53.6%) (Fig. 3.13F).
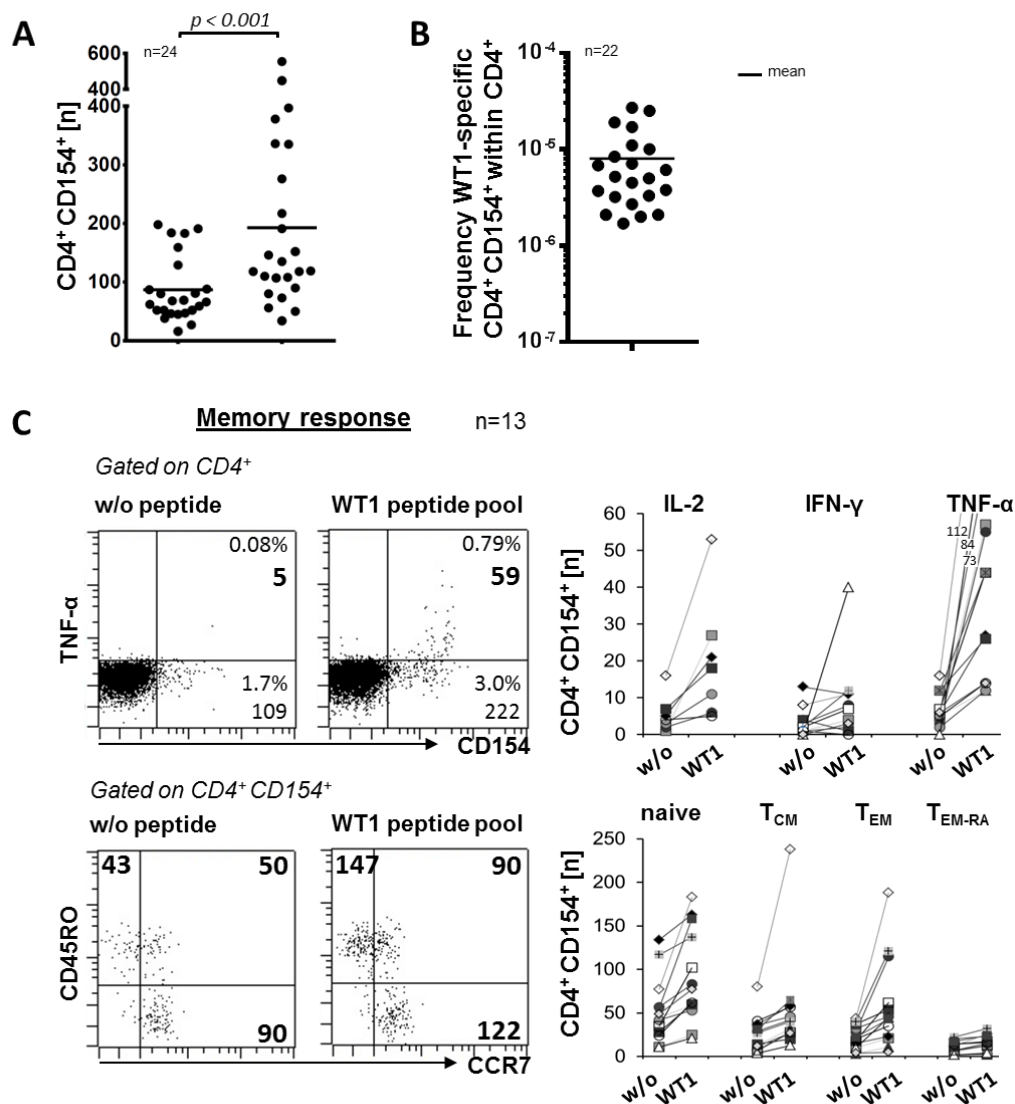
Figure 3.13 (A – C): For figure legend see next side.
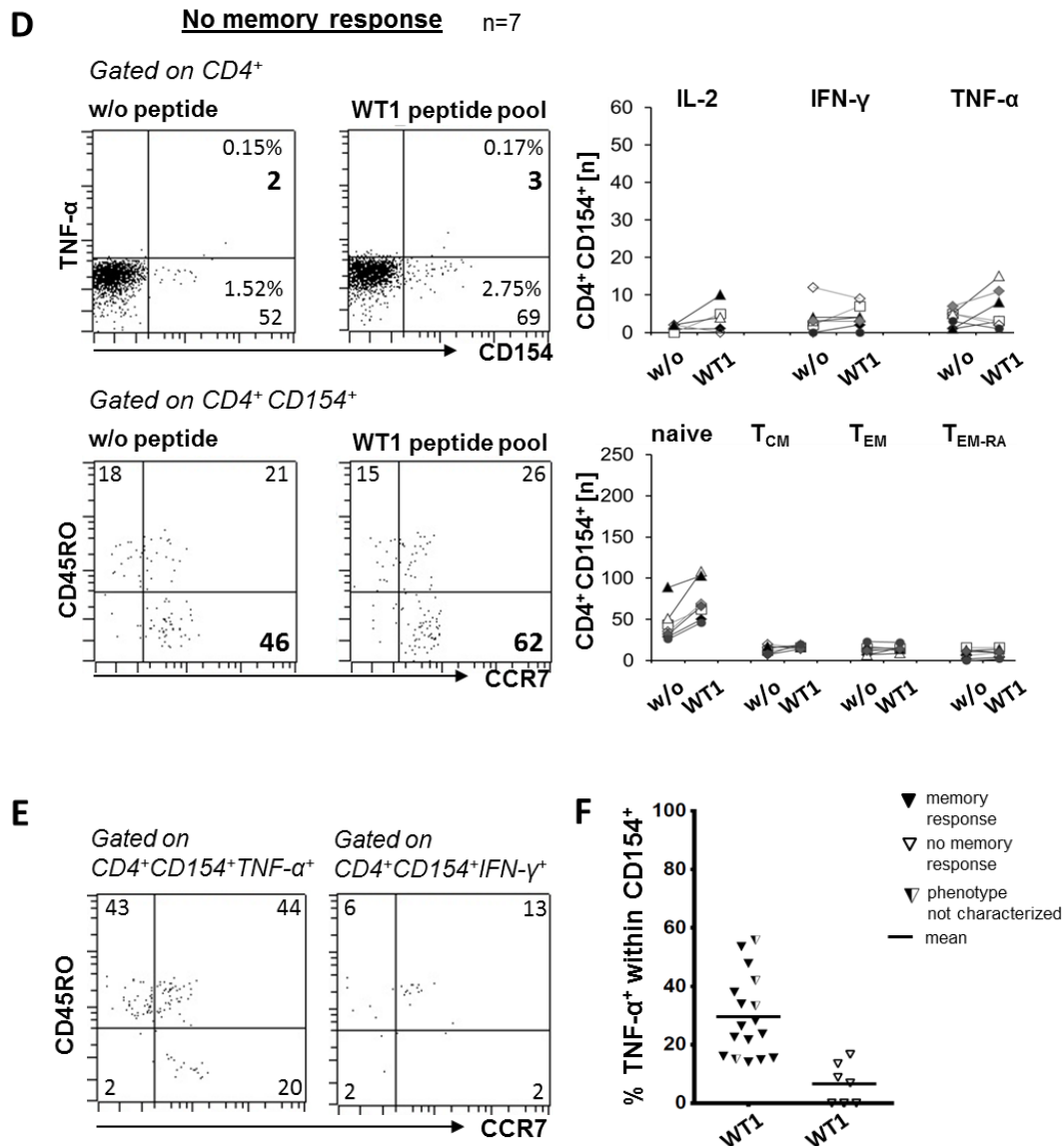
Figure 3.13: WT1-specific CD4+ memory T cells can be detected in the majority of donors. 5x10^{7} PBMC were stimulated using WT1 peptide pool or left unstimulated for 7 h and CD154+ cells were enriched subsequently. **(A)** Cell count (n) of CD4+ CD154+ cells after enrichment of CD154+ cells in unstimulated (w/o) and WT1 stimulated (WT1) samples (n = 24; means of at least 2 technical replicates are depicted, 12 independent experiments were performed, significance was determined using paired Student's t-test). **(B)** Calculated frequencies of CD4+ CD154+ cells within total CD4+ T cells (n = 22). **(C and D)** Dot plots (left) and enumeration (right) of flow cytometric analysis of TNF-α expression and phenotyping of CD4+ CD154+ cells. Dot plots show unstimulated and stimulated samples for two representative donors, one exhibiting a T_H memory response **(C)** and one exhibiting no memory response **(D)**. Enumeration of enriched CD4+ CD154+ cells, subdivided into naïve (CD45RO- CCR7+), central memory (T_{CM}, CD45RO+ CCR7+), effector memory (T_{EM}, CD45RO+ CCR7-), and exhausted effector (T_{EM-RA}, CD45RO- CCR7-) T cells and subdivided according to cytokine expression in unstimulated (w/o) and WT1 stimulated (WT1) samples. Total cell count obtained from 5x10^{7} PBMC for donors showing a Th memory response (C) and showing no memory response (D) is given. **(E)** Dot plots of flow cytometric phenotyping of TNF-α- and IFN-γ-producing cells of WT1 stimulated cells of a representative donor showing a memory response against WT1 (n = 3 donors). **(F)** Frequency of TNF-α producing cells within WT1-reactive CD4+ CD154+ cells (background cell count detected in corresponding unstimulated samples was subtracted, n = 24; 12 independent experiments were performed).

Phenotype of cytokine producing WT1-specific T cells was confirmed by direct co-staining of CCR7, CD45RO, TNF-α and IFN-γ (Fig. 3.13F) in additional three healthy donors. WT1-specific TNF-α-producing cells are mostly memory T cells, but also naïve T cells were detected, whereas IFN-γ producers were exclusively found in the memory compartment. Notably, in the "memory response" samples IL-2 production was detected in five out of seven donors tested, IFN-γ production in 5 out of 14 samples and IL-17 production in one out of seven samples tested.

In contrast, in the "no memory response" group (n = 7) only in four of these seven donors few WT1-specific $CD154^+$ $TNF-α^+$ events were identified (two to eight $CD154^+$ $TNF-α^+$ events above background). All $CD154^+$ events recognized above background were of naïve ($CD45RO^-$ $CCR7^+$) phenotype (Fig. 3.13D).

Notably, no WT1-specific IL-4 and IL-10 expression could be observed in the 20 tested donors. Furthermore, $CD8^+$ CD154 expressing WT1-specific T cells could not be detected within this set of experiments (data not shown).

These data confirm that functional $CD4^+$ WT1-specific T cells exist in all healthy donors and furthermore suggest that the majority (>60%) of healthy donors have a $CD4^+$ memory T cell pool reactive for WT.

3.2.1.2 $CD8^+$ WT1-specific T cells derive predominantly from the naïve T cell repertoire in healthy donors

The ARTE protocol described above is a useful tool for *ex vivo* detection of antigen-specific T cells, which fully covers the $CD4^+$ compartment but only a minor subset of antigen-reactive $CD8^+$ T cells. To investigate the *ex vivo* phenotype of the pool of $CD8^+$ WT1-specific T cells, pMHC class I (MHCI) tetramer technology was used for cell identification. The $WT1_{37-45}$-MHCI tetramer was chosen for this purpose, because of high abundance of $WT1_{37-45}$-specific T cells seen in expanded T cells after CD137 enrichment (Fig. 3.17). Due to the expected low frequencies a high number of starting cells and a magnetic enrichment step is required to detect these $WT1_{37-45}$-specific $CD8^+$ T cells at all and to make the assay as sensitive as possible. Therefore, pan T cells were selected from PBMC of $HLA-A2^+$, healthy donors, subsequently $0.8-1.2x10^8$ T cells were labeled with the $WT1_{37-45}$-MHCI tetramer and magnetic beads, and enriched (Fig. 3.14A). In 16 samples $CD8^+$ $WT1_{37-45}$-MHCI tetramer$^+$ events ranged from 1 to 55 cells (mean = 14 cells). As unspecific staining of tetramers is an issue when detecting low frequent T cells, two internal control mechanisms were utilized. First, dual labeling of tetramer$^+$ cells was done, using a PE- and allophycocyanin-conjugated version of the $WT1_{37-45}$-MHCI tetramer. Enrichment was done using anti-PE-MB, but only

allophycocyanin and PE double positive events in the positive fraction were counted as true WT1$_{37-45}$-MHCI tetramer$^+$ events. Secondly, staining of the MHCI tetramer on CD4$^+$ T cells was used as internal negative control (Fig. 3.14B). Substantial background staining on CD4$^+$ T cells, however, was only detected in one sample showing ten CD4$^+$ tetramer$^+$ cells. Moreover, only samples in which at least five CD8$^+$ tetramer$^+$ cells were detected were taken into account for both enumeration and phenotyping (n = 10). Frequencies of WT1$_{37-45}$-specific CD8$^+$ T cells determined with this assay range from 3×10^{-7} up to 3×10^{-6} within CD8$^+$ (mean 1×10^{-6}) (Fig. 3.14C). The majority (70 - 100%) of WT1$_{37-45}$-specific CD8$^+$ T cells detected revealed a naïve phenotype (CD45RA$^+$CCR7$^+$, Fig. 3.14D).

These data suggest that the majority of WT1$_{37-45}$-specific CD8$^+$ T cells in an individual are of naïve phenotype.
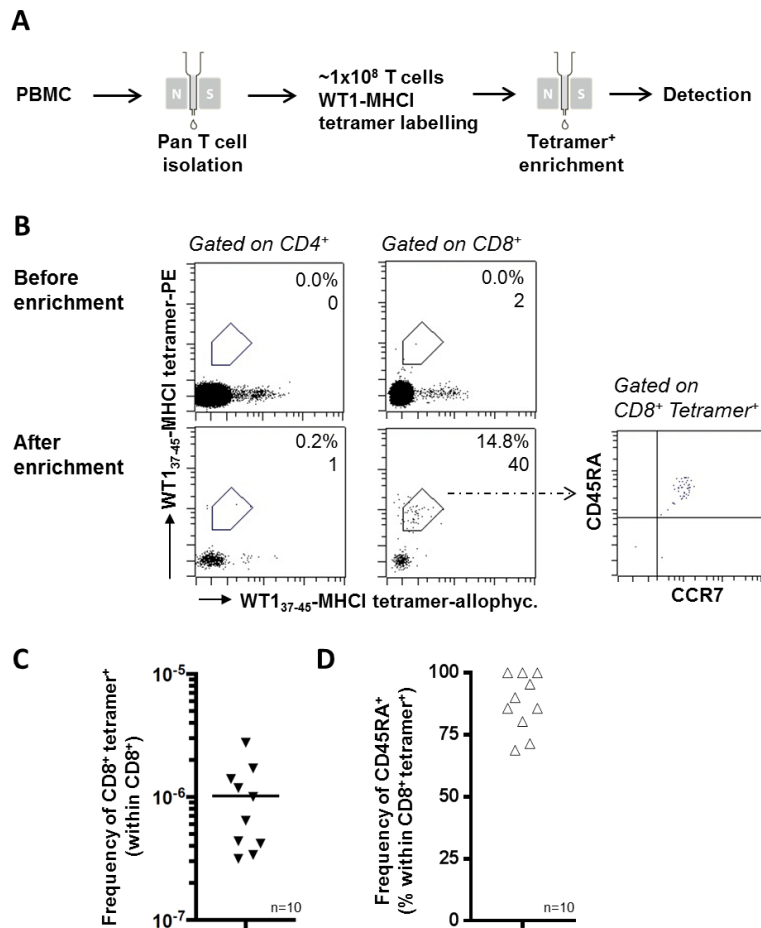
Figure 3.14: MHCI tetramer$^+$ cell enrichment reveals naïve phenotype of most WT1$_{37-45}$-specific CD8$^+$ T cells. WT1$_{37-45}$-MHCI tetramer$^+$ cells have been enriched from $0.8 - 1.2\times10^8$ Pan T cells using anti-PE-MB. **(A)** Workflow for WT1$_{37-45}$-MHCI tetramer$^+$ cell enrichment. **(B)** Representative dot plots of WT1$_{37-45}$-MHCI tetramer$^+$ cell enrichment. Dual staining with WT1$_{37-45}$-MHCI tetramer is shown, cells were gated on CD8$^+$ or CD4$^+$ as internal control for specificity (percentage within CD8$^+$ or CD4$^+$ cells and total count of detected double positive cells is given). CD45RA and CCR7 staining of CD8$^+$ tetramer$^+$ cells (right). **(C)** Frequency of detected CD8$^+$ WT1$_{37-45}$-MHCI tetramer$^+$ within total CD8$^+$ cells is shown for 10 HLA-A2$^+$ donors (6 independent experiments were performed). Mean is given. **(D)** Frequency of CD45RA$^+$ cells within WT1$_{37-45}$-MHCI tetramer$^+$ CD8$^+$ cells is shown (n = 10, 6 independent experiments were performed).

3.2.1.3 Disparity of phenotype in CD4$^+$ and CD8$^+$ T cells specific for WT1

Ex vivo characterization of CD4$^+$ WT1-reactive T cells using ARTE revealed a high proportion of donors exhibiting a memory response against WT1. *Ex vivo* analysis of CD8$^+$ WT1-specific T cells via WT1-MHCI tetramer enrichment proposed a naïve phenotype of WT1$_{37-45}$-specific CD8$^+$ T cells. To obtain a reliable determination of the *in vivo* phenotypic origin of the CD8$^+$ WT1-specific T cells, independent of the WT1$_{37-45}$-specificity used for the tetramer$^+$ enrichment approach, presorting of the T cell subsets before stimulation was done (Fig. 3.15). Sorting of T cell subsets before enrichment of antigen-specific T cells, in addition, circumvents problems with *ex vivo* characterization owing to the exceedingly low frequency, especially of CD8$^+$ WT1-reactive T cells, in healthy donors. Furthermore, this assay allowed for co-detection of CD8$^+$ and CD4$^+$ WT1-reactive T cells simultaneously in one sample. To this end, naïve T cells (CD45RA$^+$ CCR7$^+$) and memory T cells (CD45RO$^+$) were sorted by magnetic cell separation in an untouched manner from PBMC of five healthy donors. Purities of sorted T cell subsets were >99% within CD3$^+$ cells (Fig. 3.15B). Subsequently, 0.5-1x10^8 pure, presorted naïve and memory T cells were separately stimulated with WT1 peptide pool and autologous, CD3-depleted cells for 36 h and CD137$^+$ cells were enriched and expanded for nine days.

Three of the five donors included were HLA-A2 positive (Donor 2, 4, and 5) and allowed for analysis of the presence of WT1-specific T cells using WT1-peptide loaded MHCI tetramers after expansion. Interestingly, in the T cell cultures obtained from naïve T cells a tetramer-staining was detectable in all three tested donors, whereas the memory sorted T cell culture did not show a staining, suggesting that WT1$_{37-45}$-specific T cells in those three donors were derived exclusively from the naïve T cell repertoire (Fig. 3.15C). In the non-sorted fraction, which was also stimulated and enriched for CD137$^+$, WT1-specific T cells could also be detected with the WT1-MHCI tetramer-mix (Fig. 3.15C). Notably, WT1-MHCI tetramer$^+$ cells cannot be detected in either T cell fraction without the enrichment step, since frequencies are below the detection limit. These data confirm the naïve phenotype of WT1-reactive CD8$^+$ T cells in healthy donors.

Investigation on the phenotype of both CD4$^+$ and CD8$^+$ WT1-reactive T cells side-by-side was done via restimulation assays after expansion of both CD4$^+$ and CD8$^+$ T cells. T cells of four out of five donors (donor 1, 3, 4 and 5) were expanded and restimulation assays revealed that the highest frequencies of WT1-reactive CD8$^+$ T cells were detected in the samples derived from naïve T cells. Only one sample (donor 3) exhibited WT1-specific CD8$^+$ T cells in the memory fraction in addition to the WT1-specific T cells detected in the cells derived from the naïve fraction (Fig. 3.15E, left graph). For donor 1, CD8$^+$ WT1-reactive T cells were detected in none of the fractions. In the three other samples also CD8$^+$ WT1-

reactive T cells were detected in the non-sorted sample. These results reflect the results obtained by tetramer detection, namely that *in vivo* occurring CD8$^+$ WT1-specific T cells are of naïve phenotype (Fig. 3.15C).

The CD4$^+$ T cell compartment, however, revealed a strikingly different pattern as highest frequencies of WT1-reactive CD4$^+$ T cells were detected in the cells derived from the memory compartment in three out of four cases (Fig. 3.15D, E and F), confirming the phenotype detected directly *ex vivo* (Fig. 3.13). In each case also reactive CD4$^+$ WT1-specific T cells were detected in the non-sorted sample (Fig. 3.15E).

In summary, these results confirm the data obtained by the *ex vivo* analysis approaches, as they suggest a memory T cell population of WT1-reactive CD4$^+$ T cells (Fig. 3.13) and a naïve phenotype of the CD8$^+$ WT1-specific T cells (Fig. 3.14) in the majority of healthy donors. Furthermore, as the performed assay allows a side-by-side analysis of antigen-reactive CD4$^+$ and CD8$^+$ T cells, it reveals that memory CD4$^+$ and naïve CD8$^+$ T cells with specificity for the WT1 antigen can co-exist in one individual (Fig. 3.15).

Figure 3.15 (next page): Disparity of phenotype in CD4$^+$ and CD8$^+$ T cells specific for WT1 in most healthy donors. 1×10^8 presorted (naïve (CD45RA$^+$CCR7$^+$) or memory (CD45RO$^+$) T cells) or unsorted PBMCs were stimulated with WT1 peptide pool for 36 h and CD137$^+$ cells were enriched. **(A)** Workflow for T cell subset sorting and subsequent enrichment of CD137$^+$ cells. **(B)** Phenotype of T cells after subset sorting, shown for donor 5. Gate is set on living CD3$^+$ cells. **(C)** Analysis of CD8$^+$ WT1-MHCI tetramer$^+$ T cells after expansion of the CD137$^+$ enriched T cells obtained from presorted or non-sorted PBMC. Cells were stained with a mixture of tetramers loaded with four different WT1 epitopes. Cells are gated on CD3$^+$ cells. Percentages of tetramer-mix$^+$ cells within CD8$^+$ cells are given. Dot plots of donor 4 are shown. **(D, E and F)** Analysis of cytokine-producing cells by intracellular staining after restimulation of CD137 enriched and expanded T cell cultures obtained from presorted or non-sorted PBMC as indicated. **(D)** WT1-specific IFN-γ expression after restimulation of expanded cells from one representative donor (donor 4) using either unloaded or differently loaded autologous APC or peptide pulsed T2 cells (PTP = peptide pool). **(E)** Summary of antigen-specific CD4$^+$ TNF-α expression and CD8$^+$ IFN-γ expression after restimulation for 4 different donors. **(F)** Summary of antigen-specific responses after restimulation for four different donors. Ratio of naïve to memory cytokine response after restimulation calculated for CD4$^+$ and CD8$^+$ cells as well as for tetramer$^+$ CD8$^+$ T cells derived from naïve and memory cell populations.

A

PBMC → [N S] → Unsorted / Naive T cells / Memory T cells → 1x10⁸ T cells WT1 stimulation → [N S] CD137⁺ enrichment → Expansion

B

C

D

E

F
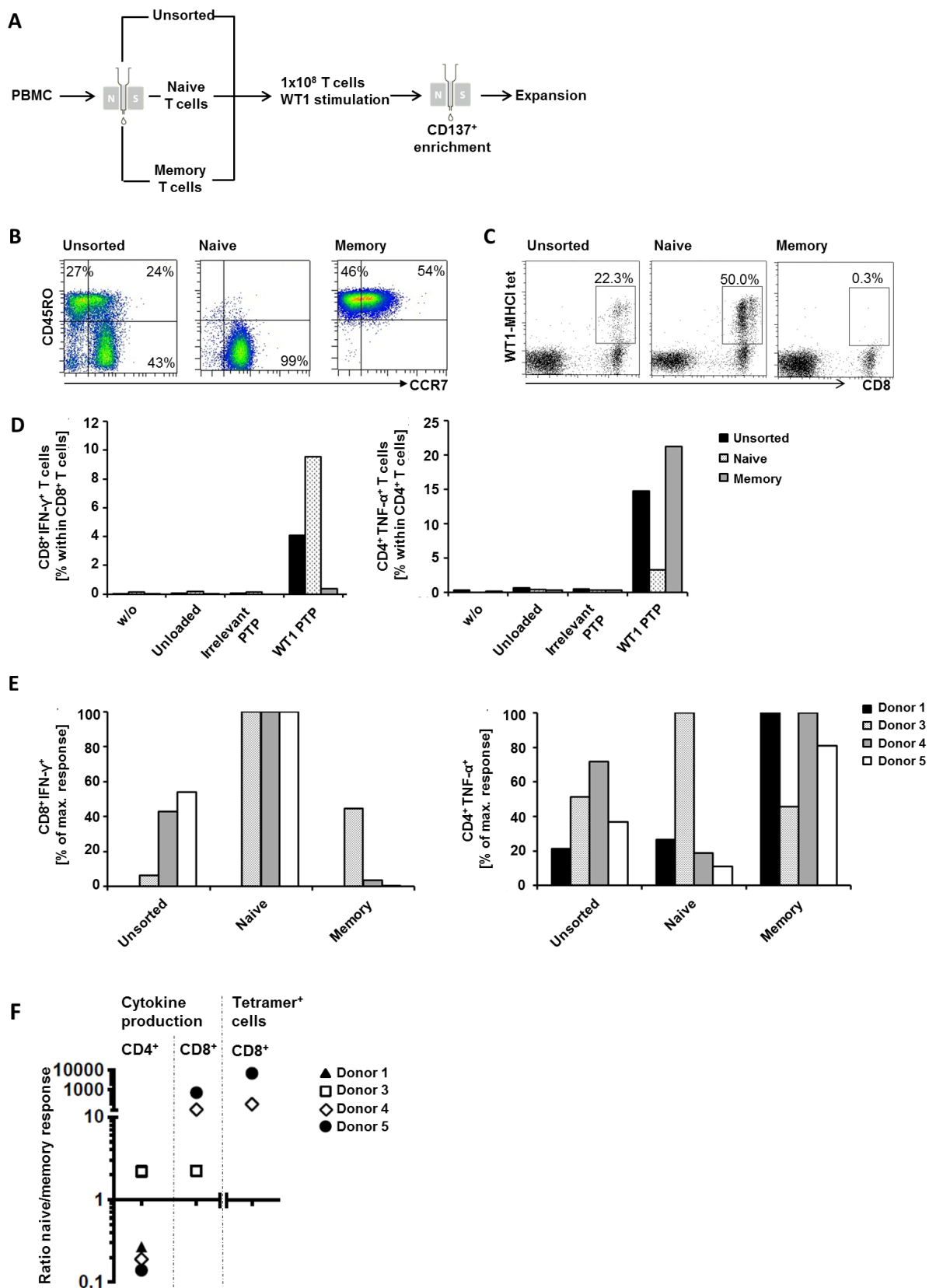
Table 3.2: Schematic overview of WT1-specific T cell responses of five different healthy donors. Given is the fraction (naïve or memory) in which a WT1-specific T cell response could be detected directly after CD137 enrichment (*ex vivo*) or after expansion (restimulation and tetramer staining). Unsorted fractions are not listed. "Highest" marks the fraction showing the highest percentage of WT1-specific T cells after expansion compared between unsorted, naïve, and memory sorted samples.

D	CD4+		CD8+		
	Ex vivo	Restimulation	*Ex vivo*	Tetramerstain	Restimulation
1	Memory	Naïve Memory (highest)	Naïve (CD45RA+)	Not HLA-A2+	No CD8+ response detected
2	Memory (CD45RO+) and Naïve (CD45RO-)	Not done	Naïve (CD45RO-)	Naïve	Not done
3	Memory	Naïve (highest) Memory	Memory (CD45RO+) and naive (CD45RO-)	Not HLA-A2+	Naïve (highest) Memory
4	Memory	Naïve Memory (highest)	Not detectable	Naïve	Naïve (highest)
5	Not detectable	Naïve Memory(highest)	Not detectable	Naïve	Naïve (highest)

3.2.2 *In vitro* generation of WT1-specific T cell cultures

Ex vivo analysis revealed that functional WT1-specific T cells are present in virtually all healthy donors. In the following, the newly established protocol using CD137 as selection marker for propagation of rare TAA-specific T cells was implemented to obtain further knowledge on the WT1-specific T cell repertoire in healthy donors, including cytotoxic potential and functional avidity of the T cells.

3.2.2.1 *In vitro* propagation of WT1-specific T cells by enrichment of CD137+ cells

For the *in vitro* propagation of WT1-specific T cells from blood of healthy donors the CD137 enrichment and expansion approach was implemented (introduced in 3.1.2). 1×10^8 PBMC were stimulated using WT1 peptide pool, CD137+ cells were enriched, and subsequently analyzed by flow cytometry (Fig. 3.16). Frequencies of CD4+ CD137+ and CD8+ CD137+ within T cells were significantly higher in stimulated samples compared to unstimulated control samples (Fig. 3.16B). However, also in the unstimulated control many CD137+ cells were enriched, indicating that the background of enriched, non-WT1-specific T cells is high.
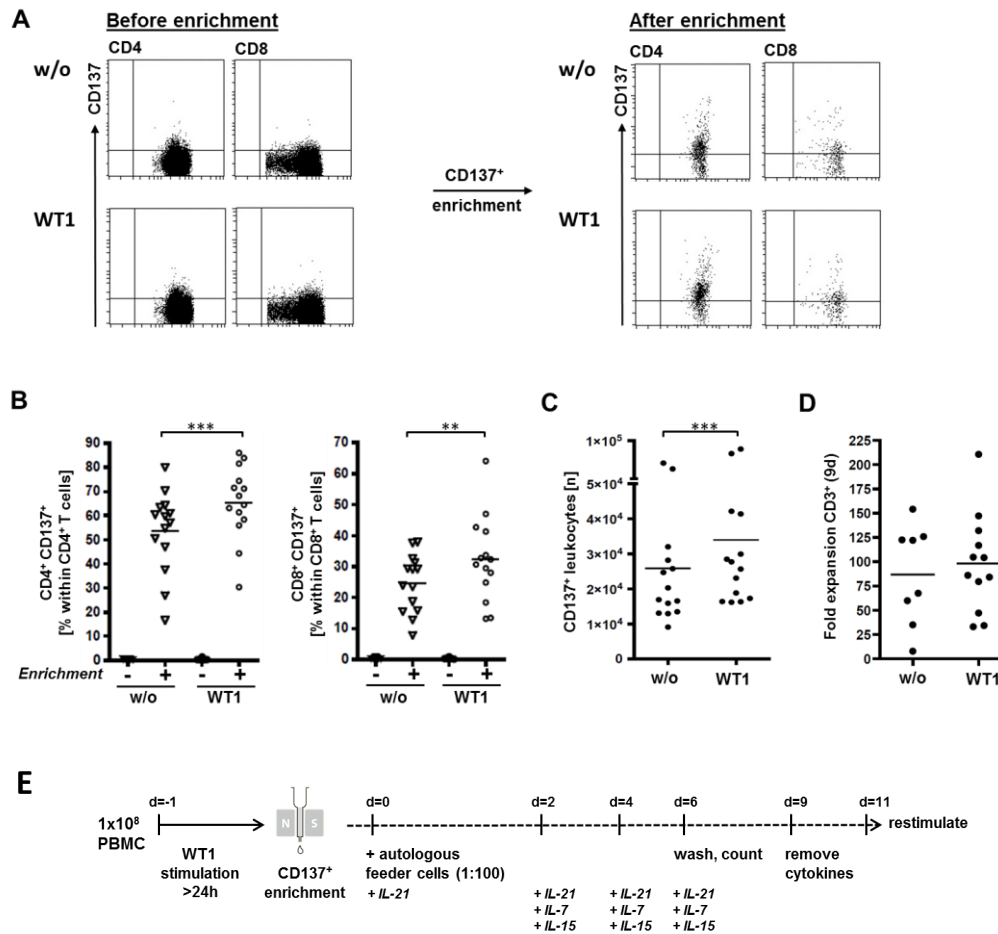
Figure 3.16: Enrichment and expansion of WT1-specific T cells. 1×10^8 PBMC were stimulated using WT1 peptide pool for 24 – 36 h and CD137$^+$ cells were enriched using anti-CD137-PE and anti-PE-MB. **(A and B)** Representative dot plots (as in Fig. 3.9) **(A)** and frequencies **(B)** of CD4$^+$ CD137$^+$ and CD8$^+$ CD137$^+$ cells with and without WT1 stimulation, before and after enrichment. Significance was determined using paired Student's *t*-test. **(C)** Cell count of CD137$^+$ leukocytes after enrichment from 1×10^8 PBMC with and without WT1 stimulation. Significance was determined using paired Student's t-test. **(D)** Fold expansion of CD3$^+$ cells within 9 days of expansion after enrichment of CD137$^+$ cells. **(E)** Scheme of 9 day expansion protocol.

Cell count after enrichment was between 1×10^4 and 1×10^5 leukocytes (mean 3.4×10^4 leukocytes). Fold expansion of CD3$^+$ T cells during the 9 day expansion protocol (depicted in Fig. 3.16E) was between 30- and 210-fold for WT1 stimulated cultures (mean 102-fold) (Fig. 3.16D).

3.2.2.2 WT1-specific T cell cultures can be efficiently generated using CD137 enrichment

After the expansion WT1-specificity was tested by staining with WT1-MHCI tetramers. Four MHCI tetramers loaded with either WT1$_{37-45}$, WT1$_{126-134}$, WT1$_{187-195}$, or WT1$_{235-243}$ peptide were used (Fig. 3.17). The specificity of the staining was controlled by using a CMV pp65$_{495-503}$-MHCI tetramer. In 21 out of 24 expanded T cell cultures from PBMC obtained from HLA-A2$^+$, healthy donors WT1-MHCI tetramer$^+$ CD8$^+$ T cells were detected with frequencies of 0.5

to 38% among CD8$^+$ T cells (Fig. 3.17B), indicating that the WT1 stimulation and CD137 enrichment approach indeed resulted in an enrichment and expansion of WT1-specific T cells. For 3 of these 21 cultures a mixture of the four WT1-MHCI tetramers was used for staining. In all of the remaining 18 T cell cultures CD8$^+$ T cells specific for WT1$_{37-45}$ were found and was the most abundant fraction of WT1-MHCI tetramer$^+$ cells in 16 T cell cultures. Notably, before enrichment no WT1-MHCI tetramer$^+$ cells were detectable in PBMC of those 24 donors.
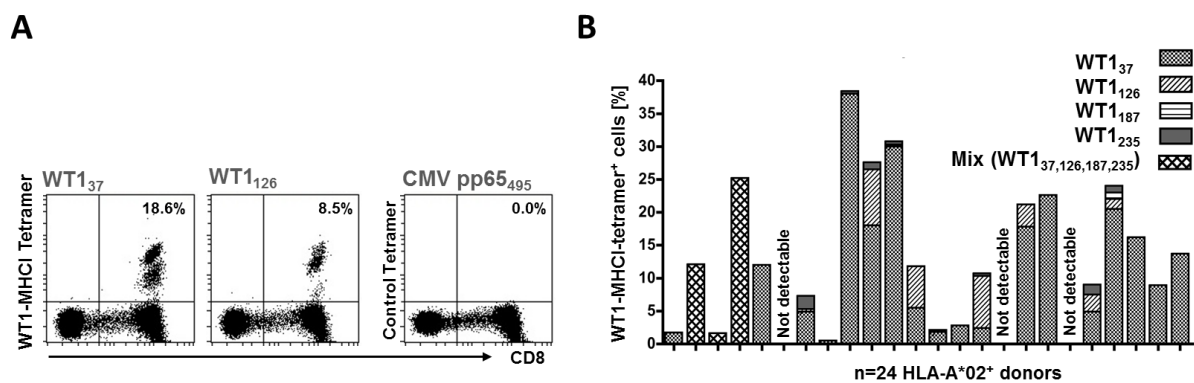
Figure 3.17: Expanded T cells are WT1-specific. T cell cultures generated by stimulation of 1x10^8 PBMC obtained from healthy HLA-A2$^+$ donors with WT1 peptide pool, enrichment of CD137$^+$ cells, and 9 day expansion were stained using MHCI tetramers that have been loaded with the WT1 epitopes WT1$_{37-45}$, WT1$_{126-134}$, WT1$_{187-195}$, and WT1$_{235-243}$ or a mix of all four tetramers. **(A)** Representative dot plots of staining with WT1$_{37-45}$-MHCI and WT1$_{126-134}$-MHCI tetramer and, as negative control, pp65$_{495-503}$-MHCI tetramer. Cells are gated on CD3$^+$ T cells. **(B)** Frequencies of WT1-MHCI tetramer$^+$ cells within CD8$^+$ T cells detected in expanded T cell cultures of 24 donors are given.

3.2.2.3 Expanded WT1-specific T cell cultures are polyfunctional

Functional characterization of the expanded T cell cultures was done by short-term restimulation experiments and subsequent analysis of effector cytokine and activation marker expression, and of the cytotoxic potential.

To this end, expanded T cell cultures were co-cultivated with peptide loaded, autologous APC. Co-cultivation with WT1-loaded APC resulted in activation of CD4$^+$ as well as CD8$^+$ T cells in the expanded cultures (Fig. 3.18A and 3.18B), measured by expression of effector cytokines TNF-α and IFN-γ and upregulation of CD154 and CD137. In contrast, unloaded APC and APC loaded with an irrelevant peptide pool did not trigger activation in most T cell cultures. Frequencies of cytokine- and activation marker-expressing T cells after incubation with unloaded autologous APC were subtracted for the determination of WT-1-specific responses.

WT1-specific cytokine production was detected in cultures generated from all healthy donors. The average antigen-specific TNF-α production was 12.4% within CD4$^+$ T cells (range 2 - 59%) and 6.4% within CD8$^+$ T cells (range 0.5 - 34%). Frequencies of IFN-γ producing cells were 6.0% (range 0.5 - 36%) within CD4$^+$ T cells and 5.1% (range 0.5 - 23%) within CD8$^+$ T cells. Notably, in each donor a WT1-induced cytokine production in either CD4$^+$ or CD8$^+$ T cells was found, and in more than 80% (25 of 30 donors) both CD4$^+$ and CD8$^+$ WT1-reactive T cells were present. Cytokine production correlated with activation marker expression upon restimulation with WT1 peptide pool. WT1-specific CD137 expression was observed on average in 4.9% (range 0.5% - 35%) within CD4$^+$ and 7.3% (range 0.5% - 45%) within CD8$^+$ T cells and CD154 expression in 11.2% (range 1.5% - 50%) on CD4$^+$ and 2.4% (range 0.2% - 30%) on CD8$^+$ T cells. Noteworthy, expression levels were measured after 6 h of stimulation and not all reactive cells might have upregulated CD137 at this point in time, due to the delayed kinetic of CD137 upregulation. Furthermore, CD154 expression on CD8$^+$ T cells is rather low on most expanded, restimulated cells, compared to cytokine production, as it is described as an activation marker mostly found on CD4$^+$ reactive T cells (Frentsch, Arbach et al. 2005), but a special subpopulation of CD8$^+$ T cells was recently described to upregulate CD154 upon stimulation (Frentsch, Stark et al. 2013). In some donors, however, a distinct population of such CD154 expressing CD8$^+$ T cells was detectable after restimulation (Fig. 3.18B). Notably, also in the three samples lacking MHCI-WT1 tetramer$^+$ cells (Fig. 3.17B) WT1-specific cytokine production was detected in either CD4$^+$ T cells only (one of three donors) or in both CD4$^+$ and CD8$^+$ T cells (two of three donors).

Release of further cytokines by T cells restimulated with WT1 peptide pool was determined using a bead-based cytokine detection assay on cell culture supernatants collected from eight donors (Fig. 3.18C). WT1-specific TNF-α, IFN-γ, IL-2, and GM-CSF release was determined, clearly indicating that WT1-specific T$_H$1 cells and/or cytotoxic CD8$^+$ T cells became activated. In some cultures also WT1-specific IL-4, IL-5, IL-6, and IL-10 release was observed, indicating also the presence of functional WT1-reactive T$_H$2 cells. All in all, WT1-specific immunity in those expanded T cell cultures was skewed towards T$_H$1 and CTL cells.
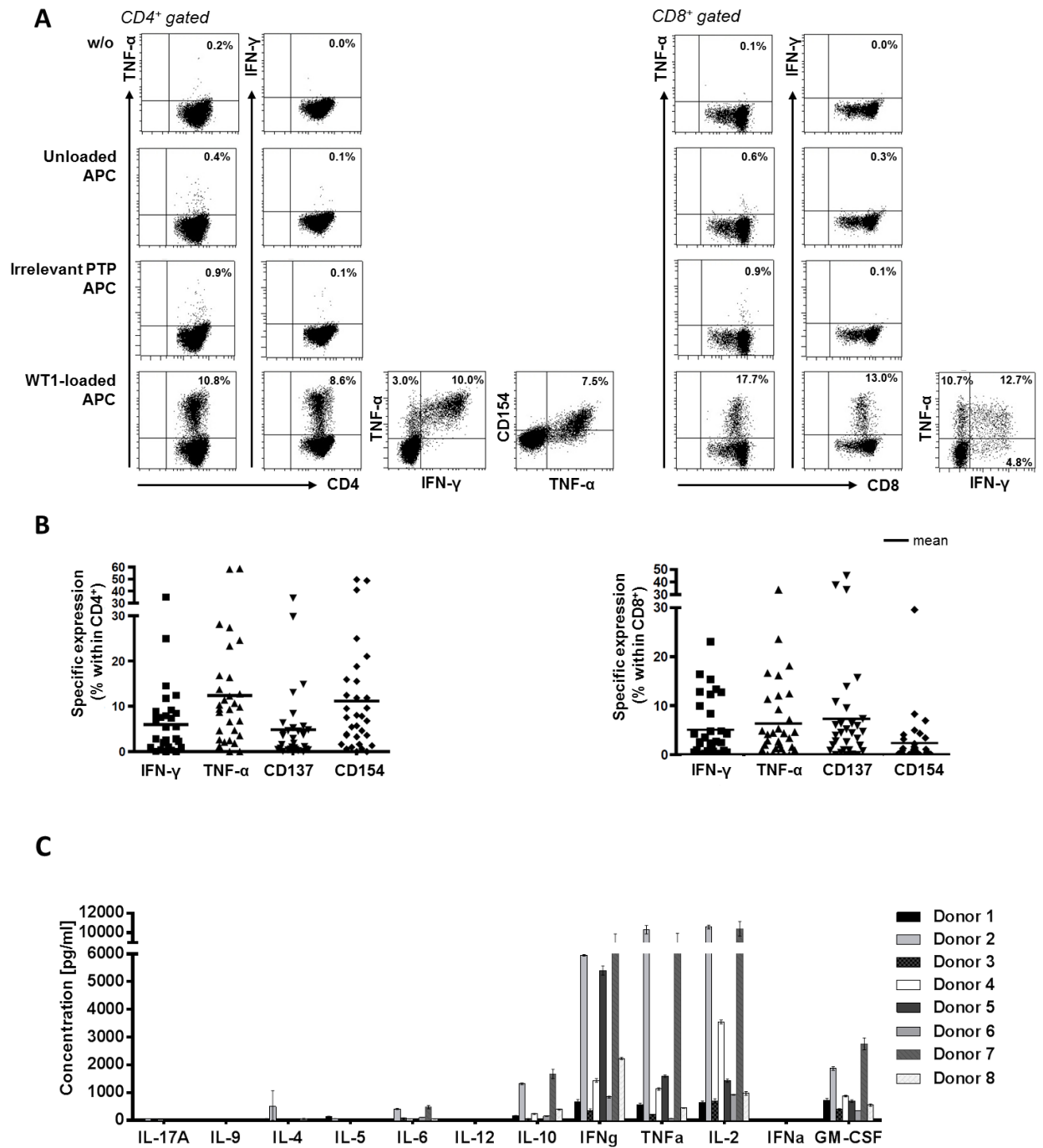
Figure 3.18: Expanded WT1-specific T cells are functional. T cell cultures generated by stimulation of 1x10^8 PBMC obtained from healthy donors with WT1 peptide pool, enrichment of CD137+ cells, and 9 day expansion were restimulated for 6 h by co-cultivation with autologous APC, which were either left unloaded, were loaded with an irrelevant peptide pool, or with WT1 peptide pool. **(A)** Representative dot plots showing intracellular staining of cytokines and CD154 after restimulation, gated on CD4+ (left) or CD8+ (right) T cells. Frequencies of positive cells within CD4+ or CD8+ T cells are given. **(B)** Frequencies of WT1-specific expression of IFN-γ, TNF-α, CD137, and CD154 upon restimulation within CD4+ (left) and CD8+ (right) T cells. Frequencies detected in co-cultures with unloaded APC have been subtracted. Mean of 30 T cell cultures obtained from different healthy donors is given. **(C)** Cytokine concentrations detected in supernatants of WT1-restimulated T cell cultures. Concentrations detected in T cell cultures co-cultivated with unloaded APC were subtracted. 2.5x10^5 T cells obtained from eight donors were used. Bar represents mean of triplicate measurements, standard deviation is given.

WT1-specific cytotoxic potential of the expanded T cells was demonstrated by detection of CD107a expression upon stimulation. CD107a is the lysosome-associated membrane protein (LAMP) and is a marker for T cell degranulation and therefore commonly used as a surrogate marker for cytotoxic activity (Betts, Brenchley et al. 2003). WT1-specific upregulation of CD107a was observed in all tested T cell samples, remarkably both within CD4+ and CD8+ T cells (1.0 to 19.5% and 2.4 to 42.0% within CD4+ and CD8+ T cells, respectively) (Fig. 3.19A). Additionally, direct WT1-specific cytotoxicity was detected by killing of WT1-loaded T2 cells by expanded T cell cultures in co-culture (Fig. 3.19B). Target cell killing was MHC-mediated as MHCI-blocking lead to decreased killing. Unloaded T2 cells were not killed and T cells specific for HPV16 did not kill WT1-loaded T2, clearly proving WT1-specific cytotoxicity and low off-target activity of the expanded T cells. Of note, effector to target ratios were determined for overall T cells used for the assay, however, the T cell culture used for the depicted cytotoxicity experiment displayed 14.6% WT1-MHCI tetramer+ cells within CD8+ (3% among CD3+) T cells and 7.5% WT1-specific TNF-α expression within CD8+ T cells. The given effector to targets ratios might therefore be drastically overestimated and in fact be approximately 35-fold lower.
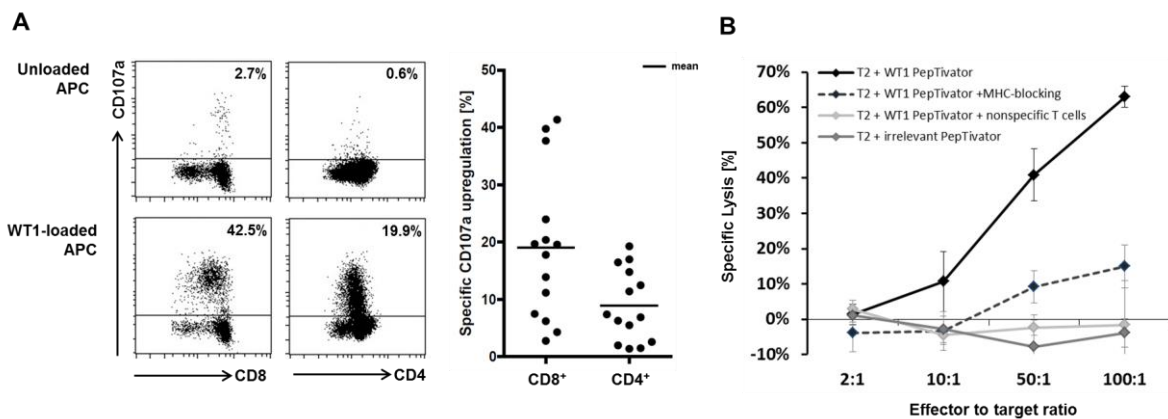
Figure 3.19: Expanded WT1-specific T cells exhibit cytotoxic potential. (A) Representative dot plots of CD107a expression of expanded T cells after 6 h co-cultivation with unloaded or WT1 peptide pool loaded APC, gated on CD4+ or CD8+ T cells. Frequencies of positive cells are given. Graph shows WT1-specific CD107a expression, frequencies detected in co-cultures with unloaded APC were subtracted. Mean of 14 T cell cultures obtained from different healthy donors is given. **(B)** Direct cytotoxicity of expanded T cell cultures towards WT1 peptide pool loaded T2 cells (black line), detected after 4 h of co-cultivation. Different ratios of T cells (effector cells) to T2 cells (target cells) were used. As controls blocking with an anti-MHCI antibody (dotted line), cytotoxicity towards T2 cells loaded with an irrelevant (HPV16) peptide pool (light grey line), and cytotoxicity of non-specific T cells towards WT1-loaded T2 cells (dark grey line) was included. Measurements were done in triplicates and standard deviation is given.

Determining the actual rate of WT1-specific T cells within the expanded T cell cultures is difficult, as every assay most probably detects only a subpopulation of the specific T cells. Frequency of WT1-specific TNF-α and IFN-γ-expressing CD8+ cells was sometimes lower

than the frequency of WT1-MHCI tetramer^{+} cells (Fig. 3.20), indicating that only a subset of cells carrying a WT1-specific TCR produced these effector cytokines upon stimulation. WT1-specific CD107a expression of expanded CD8^{+} T cells was higher than cytokine expression in all T cell cultures tested. Frequencies of CD107a-expressing CD8^{+} T cells was in the range of frequencies of WT1-MHCI tetramer^{+} cells detected, in the depicted sample 38.9% versus 40.5% after 9 day expansion and 72% versus 73.4% after 16 day expansion of CD107a-expressing and WT1-MHCI tetramer^{+} T cells in CD8^{+} T cells, respectively. Therefore, determining frequencies of cytokine-producing CD8+ T cells after WT1 stimulation might underestimate the real frequency of WT1-specific CD8^{+} T cells in the T cell culture.

Furthermore the frequencies of WT1-specific T cells within the expanded T cells cultures could be increased by a pro-longed expansion phase, shown exemplarily for one donor (Fig. 3.20).

Collectively, the data show that the expanded WT1-specific T cells exhibit a multi-functional phenotype.
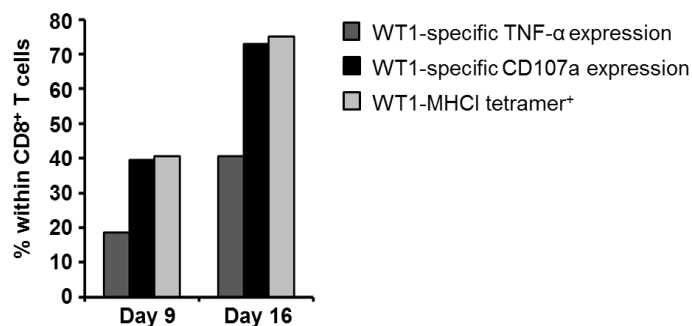
Figure 3.20: Determined frequencies of WT1-specific T cells vary using different read-outs. Frequencies of WT1-specific TNF-α expression and CD107a expression within CD8^{+} T cells after restimulation and frequency of WT1-MHCI tetramer^{+} cells within CD8^{+} T cells detected in expanded T cell cultures of one HLA-A*02^{+} donor, either after 9 day expansion and after 16 day expansion.

3.2.2.4 Expanded WT1-specific T cell cultures show a non-exhausted phenotype

Differentiation status of expanded WT1-reactive T cell cultures was determined, as T cells can acquire an exhausted end-differentiated phenotype during long-term cultivation, especially after repetitive stimulation (Wirth, Xue et al. 2010). Non-exhausted effector cells have been shown to have a better proliferative capacity and therefore provide a more sustained anti-tumor protection when clinically used. The expanded T cell cultures mostly showed an effector memory T cell (CD45RO^{+} CCR7^{-}) phenotype after short-term expansion (9 days), only few cultures showed substantial frequencies of terminally differentiated (CD45RO^{-} CCR7^{-}) CD8^{+} T cells (Fig. 3.21A). Furthermore, co-stimulatory markers CD27 and CD28 were still highly expressed on the expanded T cells (Fig. 3.21B). In contrast exhaustion markers such as CD178 (Fas-L), CD279 (PD-1), and CD57 were only expressed on few expanded CD4^{+} and CD8^{+} T cells (Fig. 3.21C). Additionally, expression of the IL-7

receptor α-chain (CD127) was analyzed, as this marker is described to be an indicator for the proliferative capacity of T cells. CD127 was found to be expressed on a substantial fraction of expanded CD4+ and CD8+ T cells (Fig. 3.21D). Proliferative capacity of the T cell cultures was additionally proven by further expansion (exemplarily shown in Fig. 3.20).

The profile of expression of the tested markers suggests a non-exhausted phenotype of the T cell cultures obtained by short-term expansion.
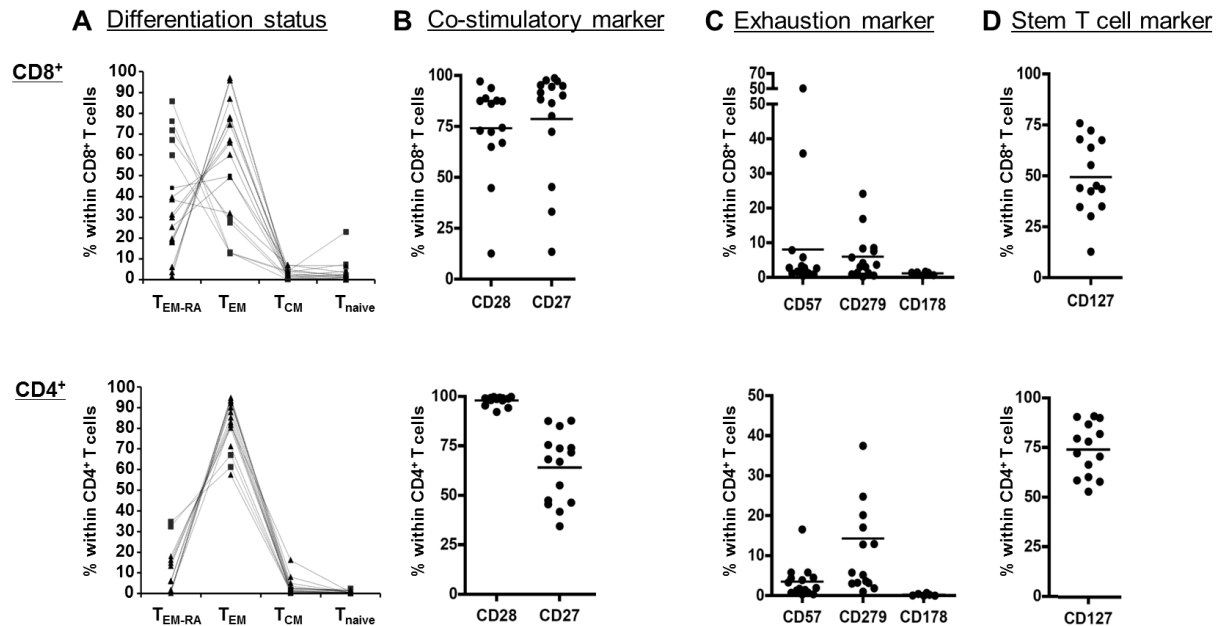
Figure 3.21: Expanded T cells exhibit a non-exhausted phenotype. T cell cultures generated by stimulation of 1x10^8 PBMC obtained from healthy donors with WT1 peptide pool, enrichment of CD137+ cells, and 9 day expansion were stained for expression of surface markers on CD8+ (upper row) and CD4+ (bottom row) T cells. **(A)** Differentiation status of T cells divided into naïve (CD45RO$^-$ CCR7$^+$), central memory (T$_{CM}$, CD45RO$^+$ CCR7$^+$), effector memory (T$_{EM}$, CD45RO$^+$ CCR7$^-$), and exhausted effector (T$_{EM-RA}$, CD45RO$^-$ CCR7$^-$) T cells. **(B)** Frequency of CD28- and CD27-expressing T cells. **(C)** Frequency of CD57-, CD279-, and CD178-expressing T cells. **(D)** Frequency of CD127-expressing T cells.

3.2.2.5 Expanded WT1-specific CD8+ T cells have a functional avidity comparable to CMV-specific T cells

T cells specific bearing a high affinity TCR against a self-antigen are expected to be negatively selected during their development in the thymus to protect the body from severe T cell mediated autoimmunity. However, recently the notion emerged that this negative selection might be incomplete for some antigens. The affinity of the generated WT1-reactive T cells might be crucial for the cells' clinical potential against malignant cells. Therefore, we tested the functional avidity of expanded WT1$_{37-45}$-specific CD8+ T cells derived from eight different donors by restimulation using T2 cells loaded with titrated amount of WT1$_{37-45}$

peptide (Fig. 3.22). The half maximal effective concentration (EC_{50}) for TNF-α release upon restimulation was calculated to range between 4 nM and 2 µM (Fig. 3.22A). However, in four of these T cell cultures also WT1-specific CD107a upregulation was tested and resulted in lower EC_{50} rates (9 nM to 50 nM) for three of the four donors compared to EC_{50} rates calculated based on TNF-α expression (Fig. 3.22B). That different read-outs can result in different EC_{50} values is demonstrated for one T cell culture, comparing TNF-α expression ($EC_{50} = 2.3$ µM) to CD107a expression (Fig. 3.22C, $EC_{50} = 50$ nM) and CD137 expression (Fig. 3.22D, $EC_{50} = 3.3$ nM).
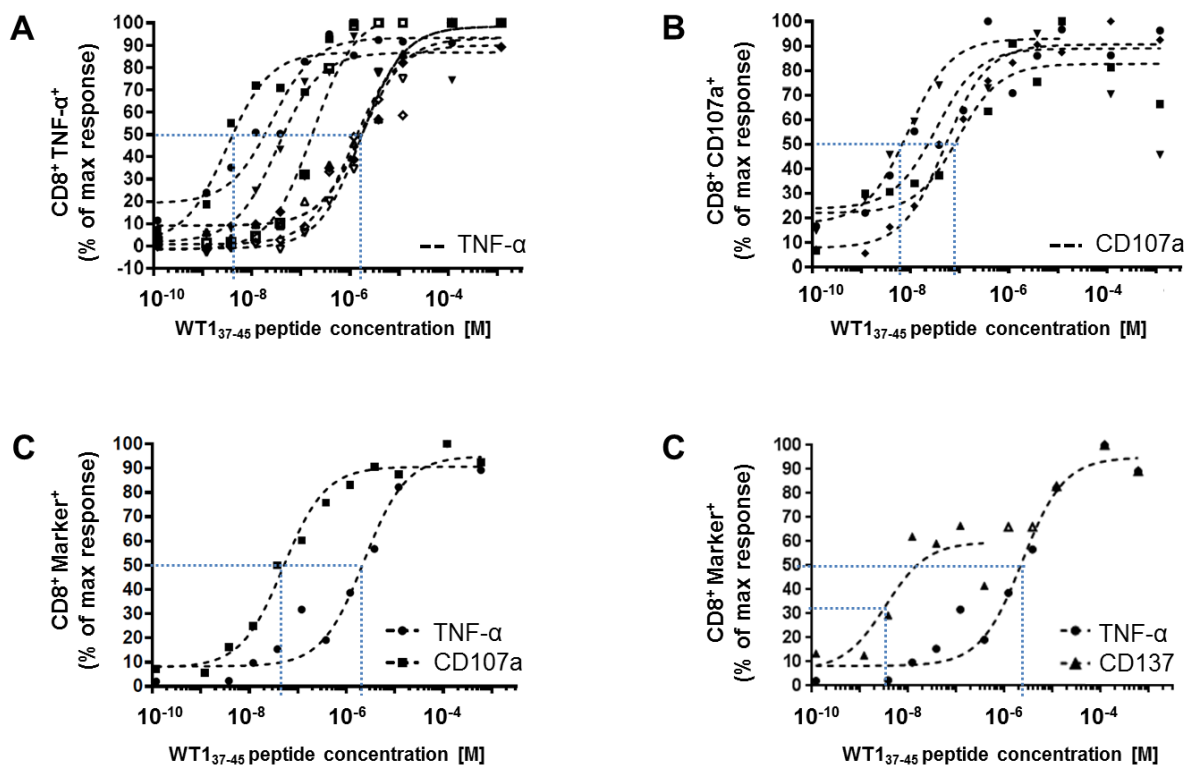
Figure 3.22: Expanded WT1_37-specific T cells show a high functional avidity. T cell cultures generated by stimulation of 1×10^8 PBMC obtained from healthy donors with WT1 peptide pool or WT1_{37-45} peptide, enrichment of CD137+ cells, and 9 day expansion were co-cultivated with autologous APC loaded with titrated amounts of WT1_{35-45} peptide for 6 h. **(A)** WT1-specific TNF-α expression within CD8+ T cells expanded from PBMC of eight donors. **(B)** WT1-specific CD107a expression within CD8+ T cells expanded from PBMC of four donors. **(C)** WT1-specific TNF-α (circles) and CD107a (squares, left) and CD137 (triangles, right) expression within CD8+ T cells expanded from PBMC of one donor. Curves represent non-linear regression curves, based on which EC_{50} values were calculated. Lines illustrate determined EC_{50} values. Open symbols mark values which have not been included in calculation of EC_{50}.

For this reason it might be difficult to compare determined EC_{50} values to EC_{50} values for WT1-specific T cells reported in the literature, as mostly cytotoxicity was used as read-out (Rosenberg). To get a more reliable value to compare the obtained data to, we determined EC_{50} values for CMV pp65_{495-503}-specific T cells using the same experimental setting (Fig. 3.23). CMV-specific T cells are expected be of high affinity, as CMV represents a viral

antigen and T cells specific for foreign antigens should not be affected by negative selection in the thymus. Functional avidity of pp65$_{495-503}$-specific CD8$^+$ T cells can be determined directly *ex vivo* as frequencies for these cells are high in some donors (2.1% among CD8$^+$ T cells for the depicted donor). Two donors were tested and *ex vivo* EC$_{50}$ were as low as 1.2 nM and 8.4 nM for pp65$_{495-503}$-specific TNF-α expression and CD137-expression, respectively. To test whether the enrichment and expansion protocol has any influence on measured functional avidity the functional avidity of pp65$_{495-503}$-specific CD8$^+$ T cells after enrichment and 9 day expansion was also determined. Indeed, the calculated EC$_{50}$ values after expansion were much higher when determining TNF-α release (2 μM), but, interestingly, not when using CD137 expression as read-out (EC$_{50}$ = 6 nM). These data indicate that the enrichment and expansion protocol probably does not *per se* lead to expansion of low avidity clones, but that the functional characteristics of the T cells might change during the expansion phase. The determined EC$_{50}$ values after expansion were similar for WT1$_{37-45}$-specific (determined for 4 T cell cultures) and pp65$_{495-503}$-specific (determined for two T cell cultures) CD8$^+$ T cells. Thus, we conclude that the functional avidity of WT1$_{37-45}$-specific T cells was not strikingly lower than the functional avidity of virus-specific T cells.
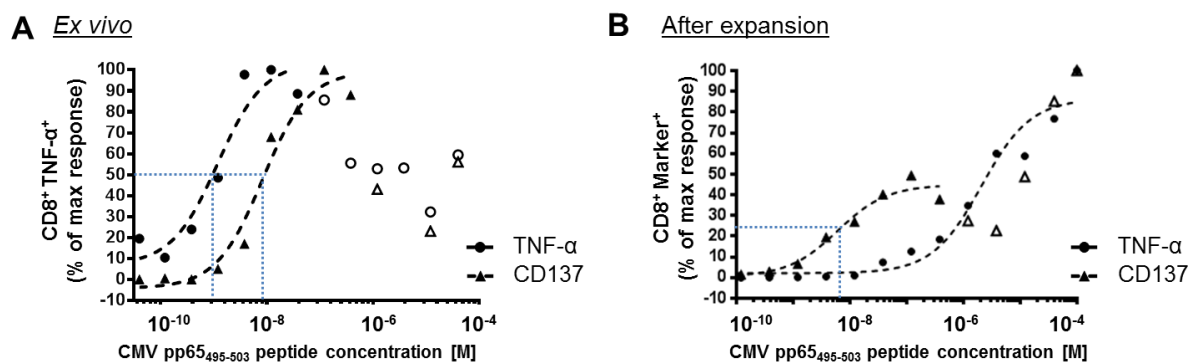
Figure 3.23: Expansion influences read-out but not functional avidity of pp65$_{495}$-specific T cells. (A and B) PBMC of a CMV^{pos} donor were co-cultivated with autologous APC loaded with titrated amounts of pp65$_{495-503}$ peptide for 6 h either **(A)** directly *ex vivo* or **(B)** after stimulation of 1x10^8 PBMC with pp65$_{495-503}$ peptide, enrichment of CD137$^+$ cells, and 9 day expansion. pp65-specific TNF-α (circles) and CD137 (triangles, right) expression within CD8$^+$ T cells expanded from PBMC of one donor is shown. Curves represent non-linear regression curves, based on which EC$_{50}$ values were calculated. Open symbols mark values which have not been included in calculation of EC$_{50}$.

Collectively, the data show that functional WT1-reactive CD4$^+$ and CD8$^+$ T cells are present in peripheral blood of virtually all healthy donors. WT1-reactive T cell populations can be efficiently generated by using an CD137 enrichment and short-term expansion protocol. Furthermore, evidence is provided that the *in vitro* propagated WT1-specific T cells possess a functional and non-exhausted phenotype, exhibit cytotoxic potential and a high or intermediate avidity towards WT1-loaded target cells.

3.3 Characterization of the HPV16-specific T cell immunity in HNSCC patients

Immunity in HNSCC, so far, was mostly studied by immunohistochemistry staining of tumor slices and evaluating strength and quality of overall T cell infiltration, however only few studies have dealt with HPV16-specific immunity in HNSCC. First hints on the presence of systemic and local HPV16-directed T cell responses in some HPV16^{pos} HNSCC patients have been provided recently (Heusinkveld, Goedemans et al. 2012). We aimed at a more precise and detailed characterization of HPV16-specific T cell responses both in the blood and the tumor of HPV16^{pos} HNSCC patients using the highly sensitive method of enrichment and multi-parametric flow cytometry.

3.3.1 Magnitude of HPV16-specific immunity in blood of HPV16^{pos} HNSCC patients varies

To overcome possible detection limits and facilitate an in-depth characterization of presumably rare HPV16-reactive CD4$^+$ T cells directly *ex vivo*, the antigen-reactive T cell enrichment (ARTE) approach (Bacher, Schink et al. 2013) was utilized, which was described already in this work for the analysis of WT1-reactive T cells (Section 3.2.1). For *ex vivo* characterization PBMC of HPV16^{pos} and, as control, HPV16^{neg} HNSCC patients were used. Blood samples were taken directly at time of primary tumor resection before treatment (surgery patients) or taken during a follow-up visit 1 to 57 months after tumor resection (follow-up patients). Details on tumor entities and pre-treatment of patients are given in tables 2.1 and 2.2. PBMC were stimulated using HPV16 E6 and E7 peptide pools for 7 h, CD154$^+$ cells were enriched and analyzed by flow cytometry. In all nine tested HPV16^{pos} HNSCC patients (four follow-up patients and five patients at tumor resection) HPV16-reactive CD4$^+$ T cells could be detected in frequencies ranging from 2.0×10^{-6} to 8.0×10^{-5} within CD4$^+$ T cells. Intriguingly, five of these nine HPV16^{pos} HNSCC patients revealed frequencies of $>2\times10^5$ HPV16-reactive cells within CD4$^+$ T cells (Follow-up patients 17 and 19 and surgery patients 8, 23, and 25, ranging from 2.5×10^{-5} to 8.0×10^{-5} within CD4$^+$ T cells, Fig. 3.24A and B), which are significantly higher compared to frequencies detected in PBMC of healthy donors and HPV16^{neg} HNSCC patients. The five HPV16^{pos} patients bearing this high level of CD4$^+$ HPV16-reactive T cells in the blood will be referred to as high responders, the other four patients as low responders in the course of this thesis. In contrast, only in 23 of 30 tested healthy individuals (=72%) and 7 out of 9 HPV16^{neg} HNSCC patients (=78%) HPV16-reactive T cells could be detected with the ARTE protocol. Frequencies of HPV16-specific CD4$^+$ T cells detected in HPV16^{neg} HNSCC patients (range 1.7×10^{-6} to 1.0×10^{-5} within CD4$^+$ T cells) did not differ significantly from frequencies detected in healthy individuals (range 6.0×10^{-6} to 3.4×10^{-5} within CD4$^+$ T cells) (Fig. 3.24B).
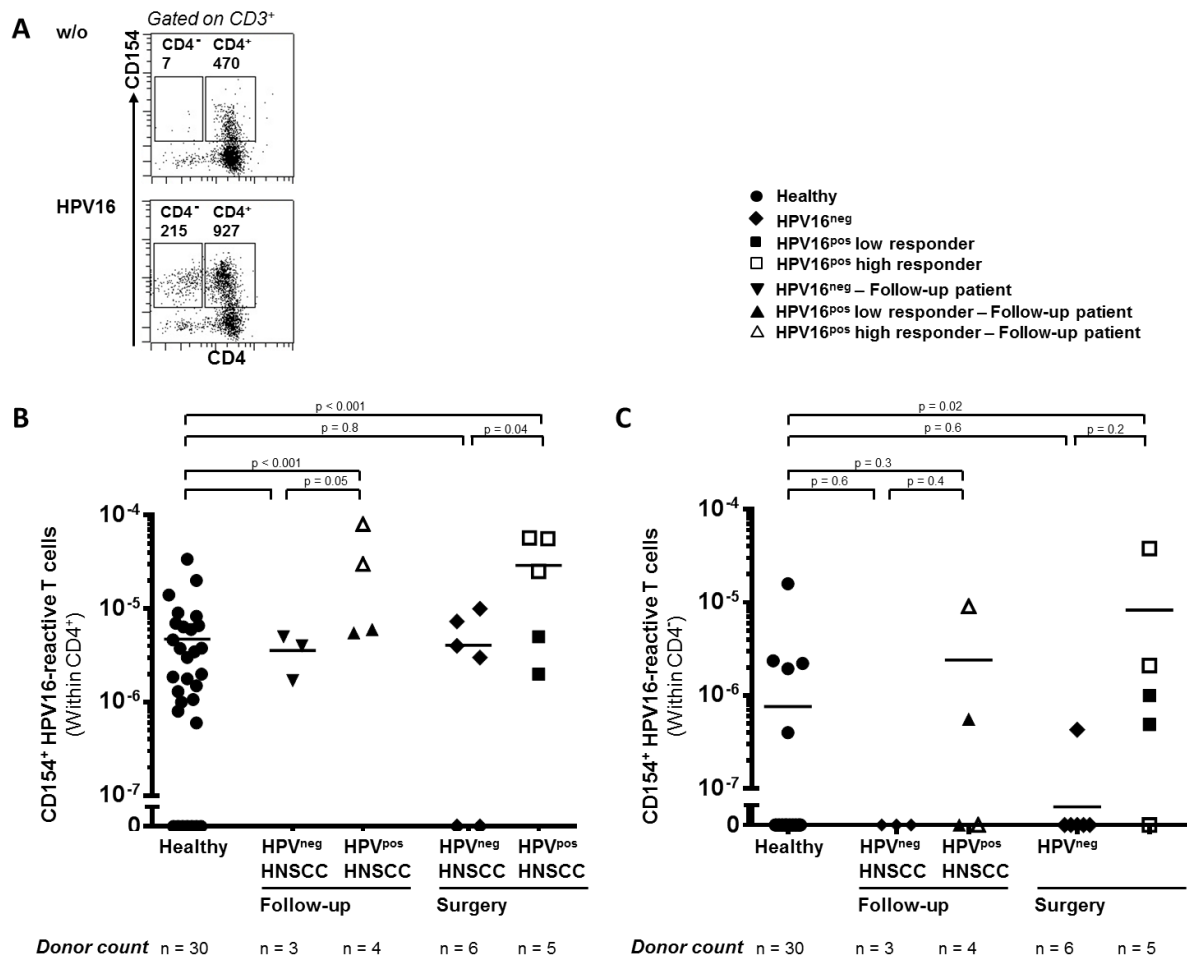
Figure 3.24: High frequencies of HPV16-reactive T cells exist in blood of a subgroup of HPV16^{pos} HNSCC patients. PBMC were stimulated using HPV16 E6 and E7 peptide pools (HPV16) or left unstimulated (w/o) for 7 h and CD154$^+$ cells were enriched. **(A)** Dot plots of positive fractions of CD154 enrichment of PBMC obtained from a HPV16^{pos} HNSCC patient (Patient 8), sequentially gated on lymphocytes, singlets, CD3$^+$ cells, and CD4$^+$ CD154$^+$ or CD4$^-$ CD154$^+$ cells. **(B)** Frequencies of HPV16-reactive CD4$^+$ CD154$^+$ T cells within the CD4$^+$ T cell populations were calculated by first subtracting CD4$^+$ CD154$^+$ cell count in unstimulated sample from CD4$^+$ CD154$^+$ cell count in HPV16 stimulated sample and subsequent division by absolute count of total used CD4$^+$ T cells. Frequencies of HPV16-reactive CD154$^+$ T cells within the CD4$^+$ T cells for PBMC from healthy donors (n = 30), HPV16^{neg} HNSCC (n = 3) and HPV16^{pos} HNSCC follow-up patients (n = 4), HPV16^{neg} HNSCC patients (n = 6) and HPV16^{pos} HNSCC patients (n = 5) at time of tumor resection (surgery) are given. **(C)** Frequencies of HPV16-reactive CD4$^-$ CD154$^+$ T cells were determined according to (B), shown for healthy donors (n = 30), HPV16^{neg} HNSCC (n = 3) and HPV16^{pos} HNSCC follow-up patients, HPV16^{neg} HNSCC patients (n = 6) and HPV16^{pos} HNSCC patients (n = 5) at time of tumor resection (surgery). Significance was determined using unpaired Student's t-test.

To investigate also on the presence of CD8$^+$ HPV16-reactive T cells, CD3$^+$ CD4$^-$ CD154$^+$ cells were determined after enrichment. HPV16-reactive CD3$^+$ CD4$^-$ T cells were found in six out of nine HPV16^{pos} HNSCC patients (Fig. 3.24C; range 5x10^{-7} to 3.8x10^{-5} within CD4$^-$ cells, follow-up patients 17 and 21 and surgery patients 8, 15, 16, and 23). Patient 8 showed exceedingly high frequencies (3.8x10^{-5} within CD4$^-$ cells, Patient 8). We assume that those

CD3$^+$ CD4$^-$ CD154$^+$ cells are indeed CD8$^+$ T cells, as detection of CD8$^+$ CD154$^+$ cells was shown before (Fig. 3.1).

To determine the differentiation status of HPV16-reactive T cells, expression of the differentiation markers CD45RO and CCR7 on CD154$^+$ T cells was determined (Fig. 3.24). The majority of HPV16-reactive T cells detected in the high responder surgery patients at tumor resection are effector memory T cells (CD45RO$^+$ CCR7$^-$) (Fig. 3.25B). In the low responder HPV16^{pos} surgery patients HPV16-reactive CD4$^+$ T cells are central memory (CD45RO$^+$ CCR7$^+$) and effector memory (CD45RO$^+$ CCR7$^-$) T cells (Fig. 3.25B). This is in contrast to HPV16-reactive CD4$^+$ T cells detected in healthy individuals. Among the 30 healthy donors, 15 showed no HPV16-reactive memory T cells, but only naïve HPV-specific T cells. In the 12 of 15 healthy donors showing a memory response, the naïve HPV16-specific precursor cells make up the majority of the total detected cells (Fig. 3.25D). Apart from the fact that the high responders clearly show a strong effector memory response against HPV16, also the low responder patients, who do not have a stronger HPV16-directed CD4$^+$ T cell response in terms of frequency, do indeed show a memory response, which is distinctly different from the majority of healthy individuals. In contrast, in one of the two follow-up high responder patients HPV16-reactive CD4$^+$ T cells showed an exhausted T$_{EM-RA}$ (CD45RO$^-$ CCR7$^-$) phenotype (Fig. 3.25C, Patient 19). HPV16-specific T cells in low responder follow-up patients were of central memory (CD45RO$^+$ CCR7$^+$) and naïve (CD45RO$^-$ CCR7$^+$) phenotype, similar to healthy donors (Fig. 3.25C).
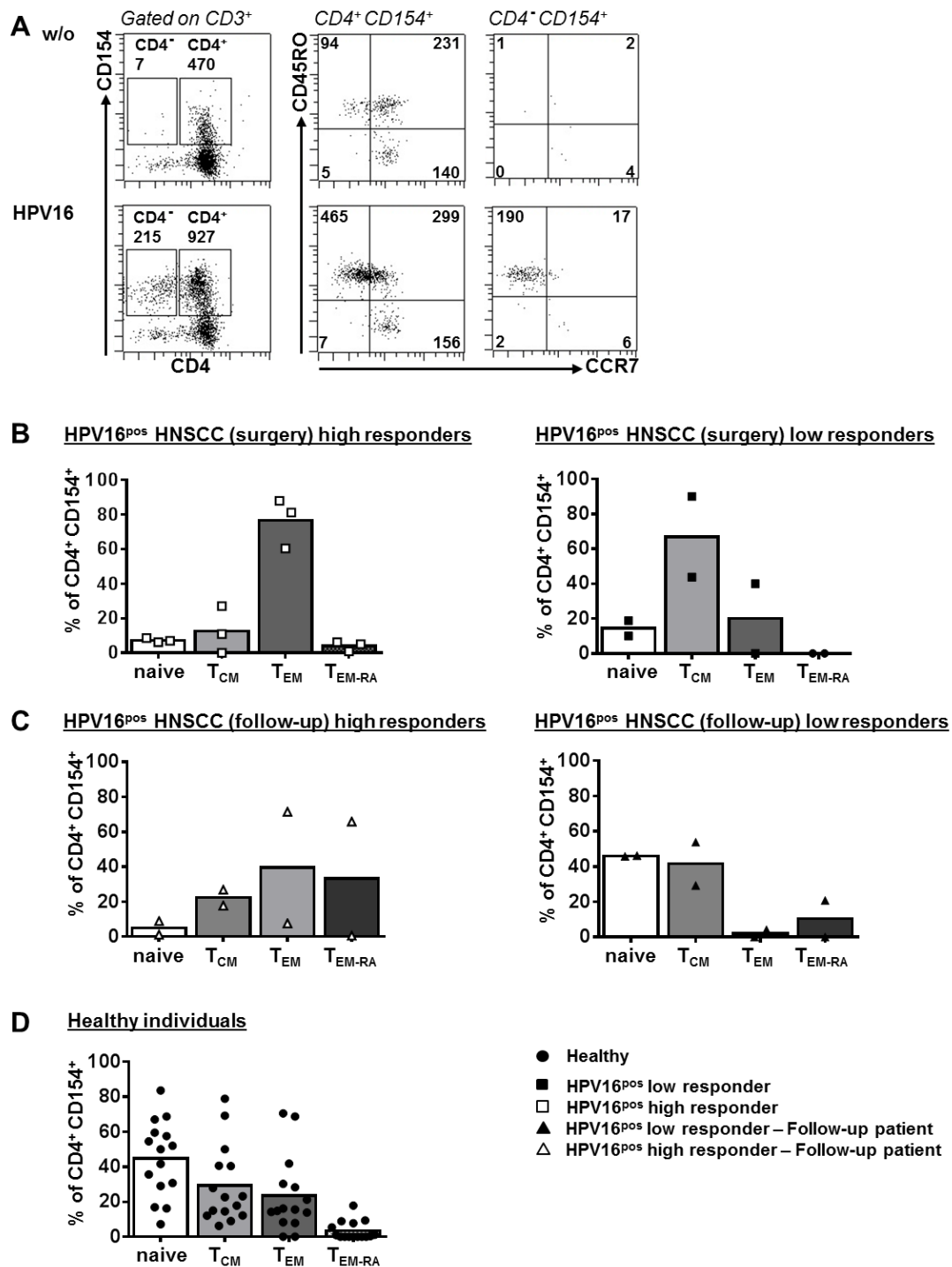
Figure 3.25: HPV16-specific T cells in blood of HPV16^{pos} HNSCC patients are memory T cells.
(A) Dot plots of positive fractions of CD154 enrichment of PBMC obtained from a HPV16^{pos} HNSCC patient (Patient 8), sequentially gated on lymphocytes, singlets, CD3$^+$ cells, and CD4$^+$ CD154$^+$ or CD4$^-$ CD154$^+$ cells. Frequencies and total cell counts of CD154$^+$ naïve (CD45RO$^-$ CCR7$^+$), central memory (CD45RO$^+$ CCR7$^+$), effector memory (CD45RO$^+$ CCR7$^-$), and exhausted effector (CD45RO$^-$ CCR7$^-$) T cells among CD154$^+$ cells are depicted. **(B to C)** Contribution of T cell subsets to total HPV16-reactive CD4$^+$ T cells: naïve (CD45RO$^-$ CCR7$^+$, white bars), central memory (CD45RO$^+$ CCR7$^+$, light grey bars), effector memory (CD45RO$^+$ CCR7$^-$, dark grey bars) and exhausted effector (CD45RO$^-$ CCR7$^-$, black bars) T cells, shown for HPV16^{pos} HNSCC patients **(B)** at time of tumor resection and **(C)** follow-up patients and **(D)** healthy donors bearing a memory response. Bars represent mean.

Although all HPV16^{pos} HNSCC patients showed a HPV16-reactive memory response the question remains why some donors show a strikingly stronger effector memory response than others? Recently, it was shown for epitopes of *Bacillus anthracis* that the number of naïve precursor T cells can determine the strength of memory T cells response after vaccination (Kwok, Tan et al. 2012). Therefore, frequencies of naïve HPV16-specific T cells in the HPV16^{pos} HNSCC surgery patients were checked. Higher frequencies of HPV16-specific precursors were found in high responders (3.6×10^{-6} to 5.0×10^{-6} within CD4$^+$ T cells) compared to low responders (6.6×10^{-7} to 7.0×10^{-7} within CD4$^+$ T cells, Fig. 3.26B). The detected frequencies of naïve HPV16-reactive CD4$^+$ T cells for both groups, the high and low responders, lie within the range of healthy donors (4.4×10^{-7} to 7.7×10^{-6} within CD4$^+$ T cells, Fig. 3.26A). For the five HPV16^{pos} HNSCC surgery patients included in this study a positive correlation between HPV16-specific T cell precursor numbers and memory formation in HPV16^{pos} HNSCC patients was found (Fig. 3.26C).

These data reveal that all nine HPV16^{pos} HNSCC patients included in this study show a clear memory T cell response against HPV16 in the blood. However, the magnitude and phenotype of this HPV16-directed CD4$^+$ T cell response varies dramatically between individual HPV16^{pos} HNSCC patients.
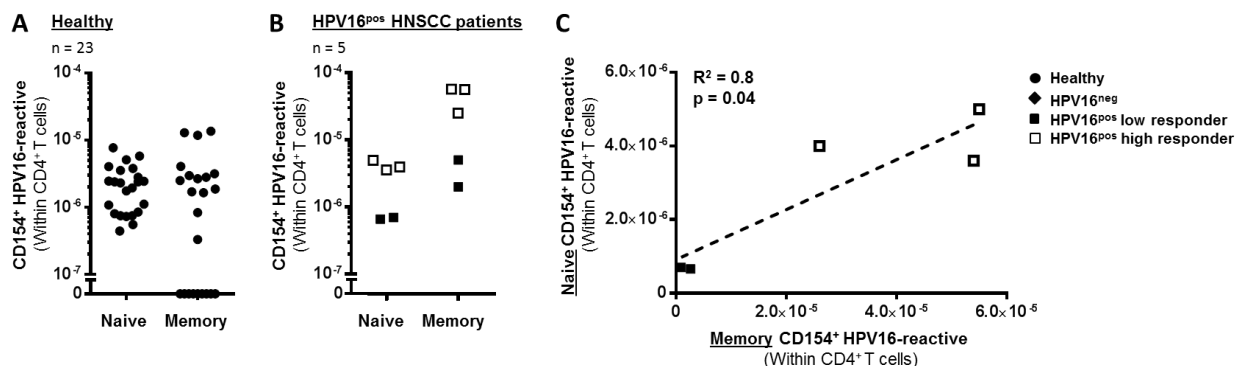
Figure 3.26: Frequencies of naïve and memory HPV16-specific T cells correlate. Frequencies of CD4$^+$ CD154$^+$ HPV16-reactive among naïve and memory T cells determined according to Fig. 3.25, shown for **(A)** healthy donors (n = 23) and **(B)** HPV16^{pos} HNSCC patients (n = 5). **(C)** Correlation of frequency of naïve CD4$^+$ CD154$^+$ HPV16-reactive T cells to frequency of memory CD4$^+$ CD154$^+$ HPV16-reactive T cells for HPV16^{pos} HNSCC patients (n = 5). Correlation was determined by Pearson correlation coefficients.

3.3.2 HPV16-reactive T cells detected in high responder HPV16^{pos} HNSCC patients are highly functional

To investigate on the functionality of blood CD4$^+$ HPV16-reactive T cells, the production of effector cytokines, such as TNF-α and IFN-γ, by HPV16-specific T cells detected with the ARTE protocol produced was tested (Fig. 3.27A). Nearly 100% of the CD4$^+$ HPV16-reactive

T cells detected in the high responders (Patient 8, 23, and 25) at time of surgery produced TNF-α (range from 89.6% to 96.7%, Fig. 3.27B) and a substantial proportion of HPV16-reactive T cells also IFN-γ (range from 27.6% to 50.0%, Fig. 3.27C). The low responders within the HPV16^{pos} HNSCC patients (Pat 15 and 16) at time of surgery contained smaller proportions of TNF-α producing cells (22% and 31%), which was in the range also observed for HPV16^{neg} HNSCC patients and healthy individuals (up to 63%) and hardly any co-produced IFN-γ. HPV16-specific T cells detected in follow-up patients showed cytokine expression in one of the high responder patients (patient 17, 85% TNF-α- and 15% IFN-γ-producing T cells), whereas the patient exhibiting high frequencies of CD4^{+} T$_{EM-RA}$ cells (Patient 7) hardly produced any cytokines, the same was true for HPV16^{neg} HNSCC follow-up patients. Additional information on the cytokine profile of the HPV16-specific T cells could be obtained for HPV16^{pos} patients 8 where the cytokines IL-2, IL-17, and IL-10 could be co-stained as enough cells were available, 41% of HPV16-reactive CD4^{+} T cells produced IL-2 and 1.5% IL-10. No IL-17 producers were detected within the HPV16-reactive T cells (data not shown). CD4^{-} HPV16-reactive T cells from patient 8 also produced effector cytokines (79% TNF-α, 88% IFN-γ and 87% IL-2 within HPV16-specific CD154^{+}) (Fig. 3.27D and E). Analysis of *ex vivo* HPV16-specific release of cytokines is available for high responder patients 17 and 23 (Fig. 3.27F) and reveals a HPV16-specific production of IL-10, IL-12, IL6, and IL-9 in addition to TNF-α and IFN-γ production of the stimulated PBMC of patient 23.

These data show that indeed highly functional HPV16-reactive T$_H$1 effector memory cells exist in the blood of a subgroup of HNSCC patients bearing an HPV16^{pos} HNSCC tumor.
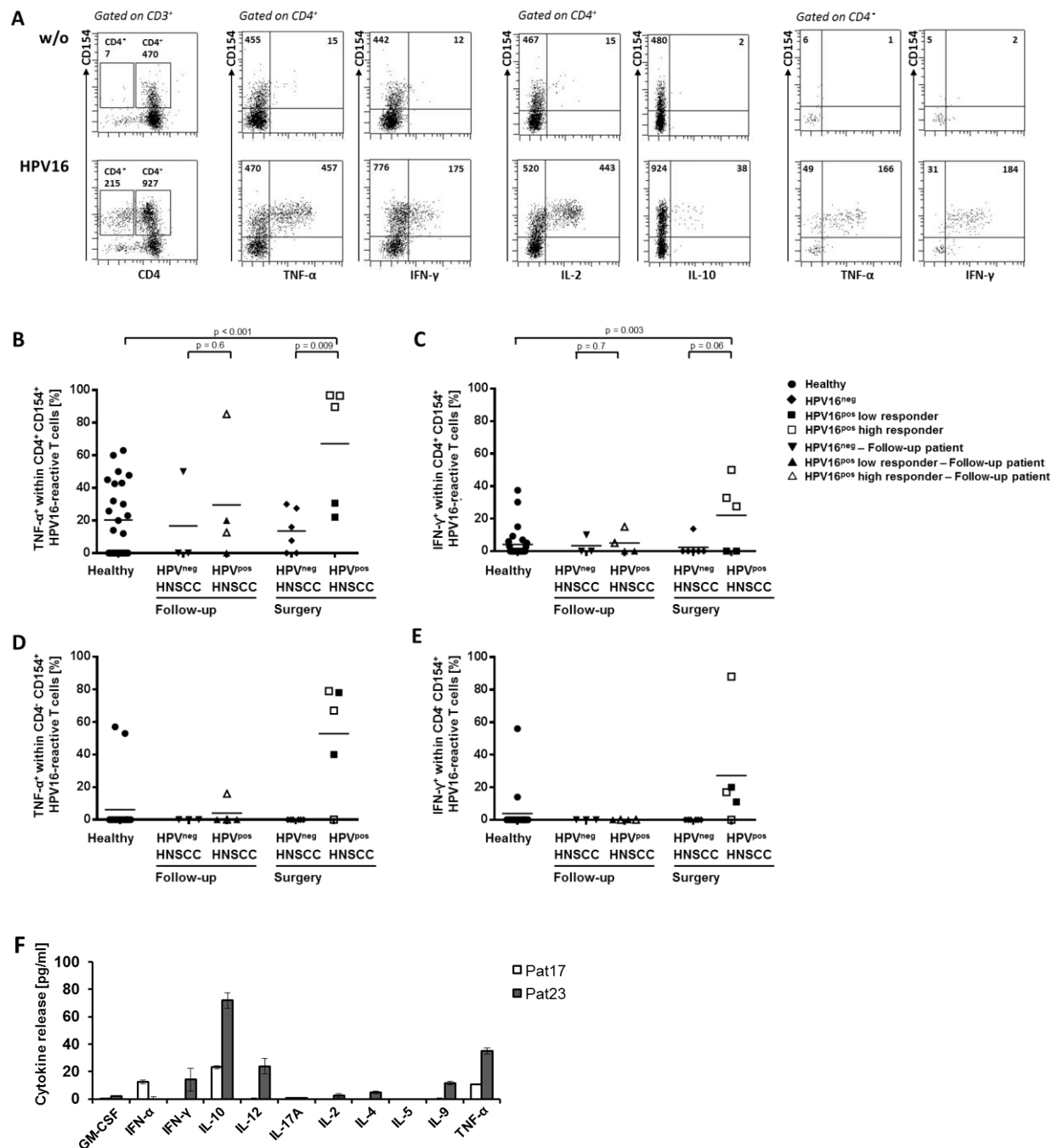
Figure 3.27: Functional HPV16-reactive T$_H$1 cells exist in blood of HPV16^{pos} HNSCC patients.
PBMC were stimulated using HPV16 E6 and E7 peptide pools (HPV16) or no peptide pool (w/o) for 7 h and CD154$^+$ cells were enriched. **(A)** Dot plots of positive fraction after CD154 enrichment of PBMC obtained from a HPV16^{pos} HNSCC patient (Patient 8), gated on lymphocytes, singlets, CD3$^+$, and CD4$^+$ CD154$^+$ or CD4$^-$ CD154$^+$ cells. Cell count is given. **(B to E)** Percentage of **(B)** TNF-α and **(C)** IFN-γ producing T cells within the HPV16-reactive CD4$^+$ CD154$^+$ T cells and percentage of **(D)** TNF-α and **(E)** IFN-γ producing T cells within the HPV16-reactive CD4$^-$ CD154$^+$ T cells shown for PBMC from healthy donors, HPV16^{neg} HNSCC (n = 3) and HPV16^{pos} HNSCC follow-up patients, HPV16^{neg} HNSCC patients (n = 6) and HPV16^{pos} HNSCC patients (n = 5) at tumor resection (surgery). Significance was determined using unpaired Student's *t* test. Significances for CD4$^-$ cells were not determined as in many donors no HPV16-reactive CD4$^-$ T cells were detected. **(F)** Cytokine concentrations detected in PBMC supernatants after 7 h of stimulation using HPV16 E6 and E7 peptide pools (HPV16), concentrations detected in unstimulated samples were subtracted. Shown for two high responder HPV16^{pos} HNSCC patients (patient 17 and 23). Bar represents mean of triplicates, standard deviation is given.

3.3.3 Favorable cell composition of the tumor tissue in high responder HPV16^{pos} HNSCC patients

For HPV16^{pos} cervical carcinoma it has been suggested that patients bearing a systemic HPV16-directed CD4^{+} immune response have a higher CD8^{+} T cell infiltration and a higher CD8^{+} to T_{reg} ratio and both this is correlated to less metastases and hence a better prognosis (Piersma, Jordanova et al. 2007). To test whether or not there are differences in infiltration of the tumor by T cells between the high and low responder HPV16^{pos} HNSCC patients and between HPV16^{pos} and HPV16^{neg} HNSCC patients, the presence of different T cell subsets in freshly dissociated tumor material was analyzed. No significant difference both between HPV16^{neg} and HPV16^{pos} and between tumors of low and high responder patients for CD3^{+} T cells, CD4^{+} T cells, CD8^{+} T cells, and CD4^{+} FoxP3^{+} cells was detected, indicating that the overall T cell infiltration is not substantially varied (Fig. 3.28A). However, when we determined the CD8^{+} to T_{reg} ratio in these tumors, the three high responding patients (but also one of the low responding) HPV16^{pos} patients had higher ratios compared to HPV16^{neg} tumors (Fig. 3.28B), although not statistically significant. Still, these data hint at a favorable T cell composition in the high responder patients.

Furthermore, the activation status of TIL was analyzed. To this end, expression of the activation markers CD137 and CD279 was determined, which were recently reported to mark TIL with anti-tumor function, especially CD137 identifying a subpopulation of highly tumor-reactive T cells (Gros, Robbins et al. 2014, Ye, Song et al. 2014). Additionally, high levels of PD-1^{+} TIL are correlated to a good prognosis in HNSCC (Badoual, Hans et al. 2013). HPV16^{pos} high responders had rather high populations of CD137-expressing (6.9% to10.6% within CD3^{+} cells) and PD-1-expressing (52.5% to 75.6% within CD3^{+} cells) T cells, indicating an activated status of the TIL. However, no significant difference was found both between HPV16^{neg} and HPV16^{pos} and between tumors of low and high responder HPV16^{pos} patients (Fig. 3.28C) for CD279 and CD137 expression.
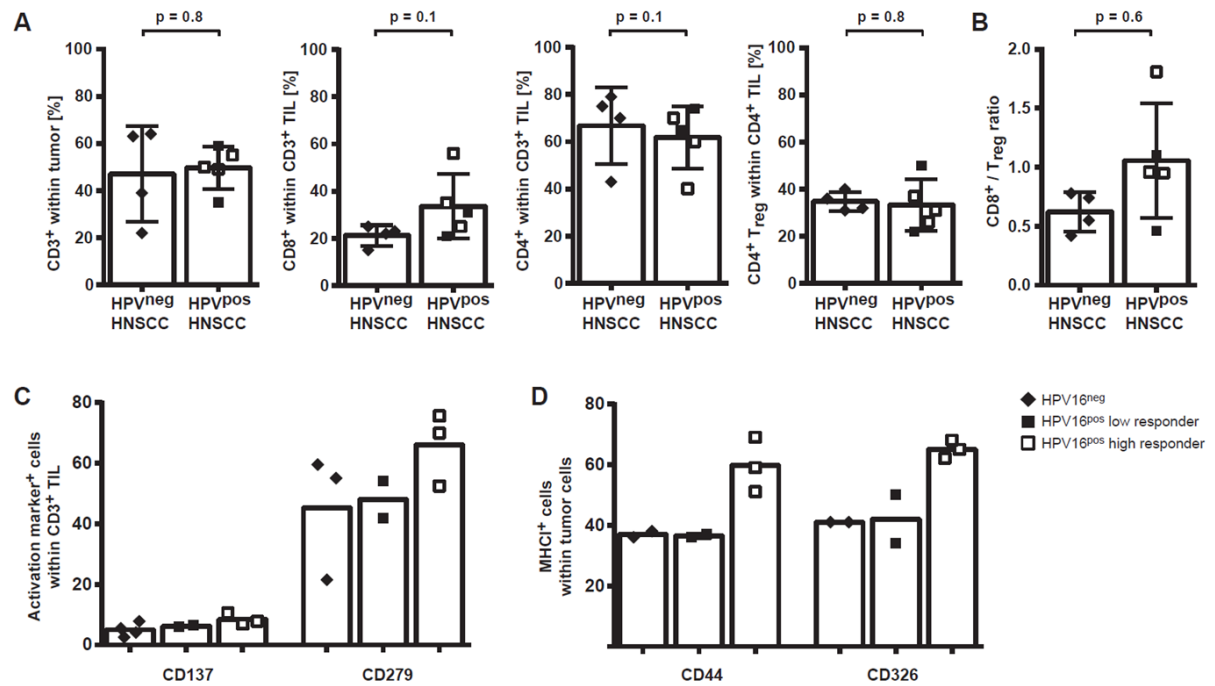
Figure 3.28: T cell infiltration and MHC class I expression in HNSCC tumors. Freshly dissociated tumor material of HPV16^{pos} and HPV16^{neg} HNSCC patients was analyzed by flow cytometry. (**A**, **B**) The number of T cells (CD3$^+$ cells among all living cells), CD4$^+$ and CD8$^+$ cells (within CD3$^+$ cells), and CD25$^+$ FoxP3$^+$ T$_{reg}$ cells (within CD4$^+$ cells) was determined by flow cytometry. Significance was determined using unpaired Student t test. (**C**) Percentage of CD137 and CD279 expressing CD3$^+$ cells. (**D**) Percentage of MHC class I expressing CD44$^+$ and CD326$^+$ tumor cells.

HPV16 induced tumors are known to interfere with the antigen-presentation machinery in host (tumor cells), thereby preventing activation of effector T cells. We checked for MHC expression on tumor cells and detected significantly elevated levels of MHC class I expression on the tumor cells of the high responder patients on both CD326 epithelial cells and a subpopulation of CD44$^+$ putative cancer stem cells (Prince, Sivanandan et al. 2007) (Fig. 3.28D).

Although the strength of overall T cell infiltration in the tumor tissue was not strikingly different in the tested patients, the higher expression of MHC class I and the higher CD8$^+$ to T$_{reg}$ ratios detected in the tumor of high responder HPV16^{pos} patients hint at an on-going HPV16-directed anti-tumor response in those patients compared to the HPV16^{neg} and low responder HPV16^{pos} patients.

3.3.4 HPV16-directed T cell immunity in blood of HNSCC patients reflects intratumoral immunity

To investigate the HPV16-specific immunity at the tumor site and to compare HPV16-reactivity in the periphery to intratumoral immunity, T cell cultures from PBMC and tumor

tissue of HNSCC patients were expanded. HPV16-reactive T cell cultures from patient material were generated by utilizing enrichment via the activation marker CD137. PBMC of HNSCC patients were stimulated directly *ex vivo* with HPV16 E6 and E7 peptide pools and CD137^{+} cells were enriched. To expand HPV16-reactive tumor-infiltrating lymphocytes (TIL) fresh tumor pieces were dissociated and likewise stimulated and enriched for CD137-expressing cells. In parallel, direct TIL expansion from tumor fragments without enrichment was performed, adapted to established protocols (Dudley, Wunderlich et al. 2003) (Fig. 3.29A). Starting cell numbers were between 0.8×10^7 and 6×10^7 for PBMC and 1×10^6 to 4×10^6 total cells obtained after tumor dissociation. Obtained total cell counts after expansion ranged between 4.3×10^5 to 1.4×10^7 for cells obtained from PBMC, between 2.8×10^4 to 5.0×10^6 for cells obtained by CD137 enrichment of dissociated tumor material and between 2.7×10^6 to 1.5×10^7 for cells grown from tumor pieces (Fig. 3.29B).
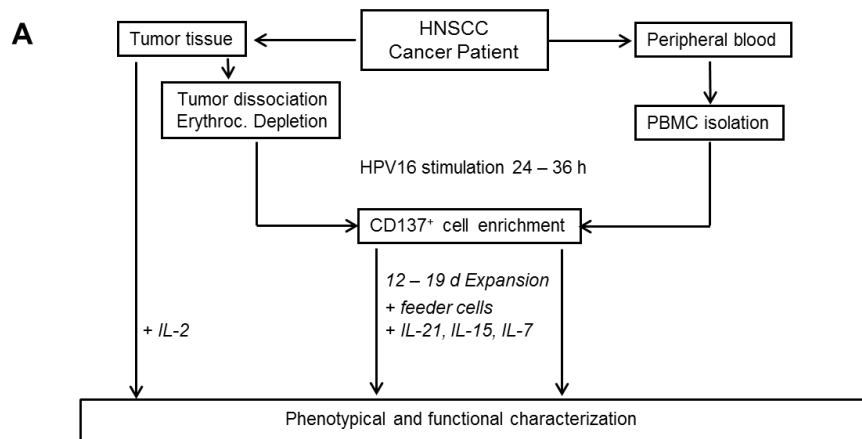
Figure 3.29: Expansion of peripheral blood T cells, tumor-infiltrating T cells. (A) Scheme of expansion strategy. **(B)** Cell count at day 12 or day 19 is depicted.
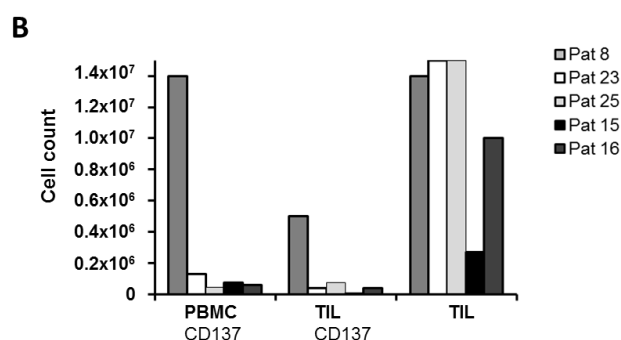
Expanded T cell cultures were tested for HPV16 reactivity by co-cultivation with autologous CD3-depleted PBMC, which have been either loaded with HPV16 peptide pools or left unloaded (Fig. 3.30). HPV16-specific TNF-α expression was determined via intracellular staining and flow cytometric analysis after 6 h of co-cultivation. In all five tested HNSCC patients bearing an HPV16-positive tumor TNF-α-producing HPV16-reactive T cells could be generated from blood and tumor material by using the enrichment strategy (Fig. 3.30B),

clearly indicating that potentially functional HPV16-directed T cells exist in these patients. CD4+ HPV16-reactive T cells were detected in all five cultures derived from PBMC (range HPV16-specific TNF-α production 3.6 – 20% within CD4+ T cells), in four of five cultures derived from CD137-enriched tumor material (range HPV16-specific TNF-α production 6.6 – 23% within CD4+ T cells, no data for patient 15) and weakly in one culture directly expanded from tumor pieces (HPV16-specific TNF-α production 2.3% within CD4+ T cells). CD8+ HPV16-reactive T cells were detected in all five cultures derived from PBMC (range HPV16-specific TNF-α production 1.0 – 7.2% within CD8+ T cells), in four of five cultures derived from CD137-enriched tumor material (range HPV16-specific TNF-α production 0.5 – 27% within CD8+ T cells, no data for patient 15), and in one culture (patient 8) directly expanded from tumor pieces (HPV16-specific TNF-α production 15.2% within CD8+ T cells). Except from patient 8 the HPV16-directed T cell immunity in the tested patients seems to be skewed to CD4+ T cells within the blood. Expansion of the CD137-negative fraction did not result in expansion of HPV16-specific T cells (data not shown), indicating that this approach selects for HPV16-reactive T cells. In HNSCC patients bearing an HPV16-negative tumor HPV16-specific T cells could be generated from PBMC in three out of four donors, but not from tumor material, indicating that HPV16-specific T cells selectively infiltrate the tumor tissue of HPV16pos patients.

The HPV16-reactivity of the T cell cultures was investigated in more depth by determining the reactivity against each of the used HPV16 antigens separately (Fig. 3.30C). In the T cell cultures obtained from blood and tumor by CD137 enrichment the same protein specificities could be detected for each patient. Four donors (patient 8, 15, 23, and 25) showed CD4+ T cell reactivity both against HPV16 E6 and E7 and CD8+ T cell reactivity against HPV16 E7. Patient 16 showed CD4+ T cell reactivity only against HPV16 E6 and also CD8+ T cell reactivity against HPV16 E6. The distribution of CD4+ and CD8+ T cell reactivity and also the distribution of E6 and E7 protein responses vary remarkably between T cell cultures obtained from blood and tumor in most donors. Nonetheless, concerning the presence of protein specificities in the CD4+ and CD8+ T cell compartment, the HPV16-directed T cell immunity detected in the blood seems to reflect the tumor resident HPV16-reactive T cells.

In the cell cultures expanded from both PBMC and tumor tissue the dominant HPV16-specifically released cytokines were IL-2, TNF-α, and IFN-γ (Fig. 3.30D).

For the high responding patients 8, 23, and 25 the *ex vivo* data obtained with the ARTE approach (Fig. 3.24) reflect the data obtained by CD137 enrichment and expansion (Fig. 3.30). In patient 8 a strong CD4+ and CD8+ HPV-reactivity was detected *ex vivo* as well as after expansion of both PBMC and enriched TIL. In contrast, patients 23 and 25 seem to

have a CD4^{+} skewed HPV16 response, detectable both *ex vivo* and after expansion of PBMC and enriched TIL.

Figure 3.30 (A – C): For figure legend see next side.
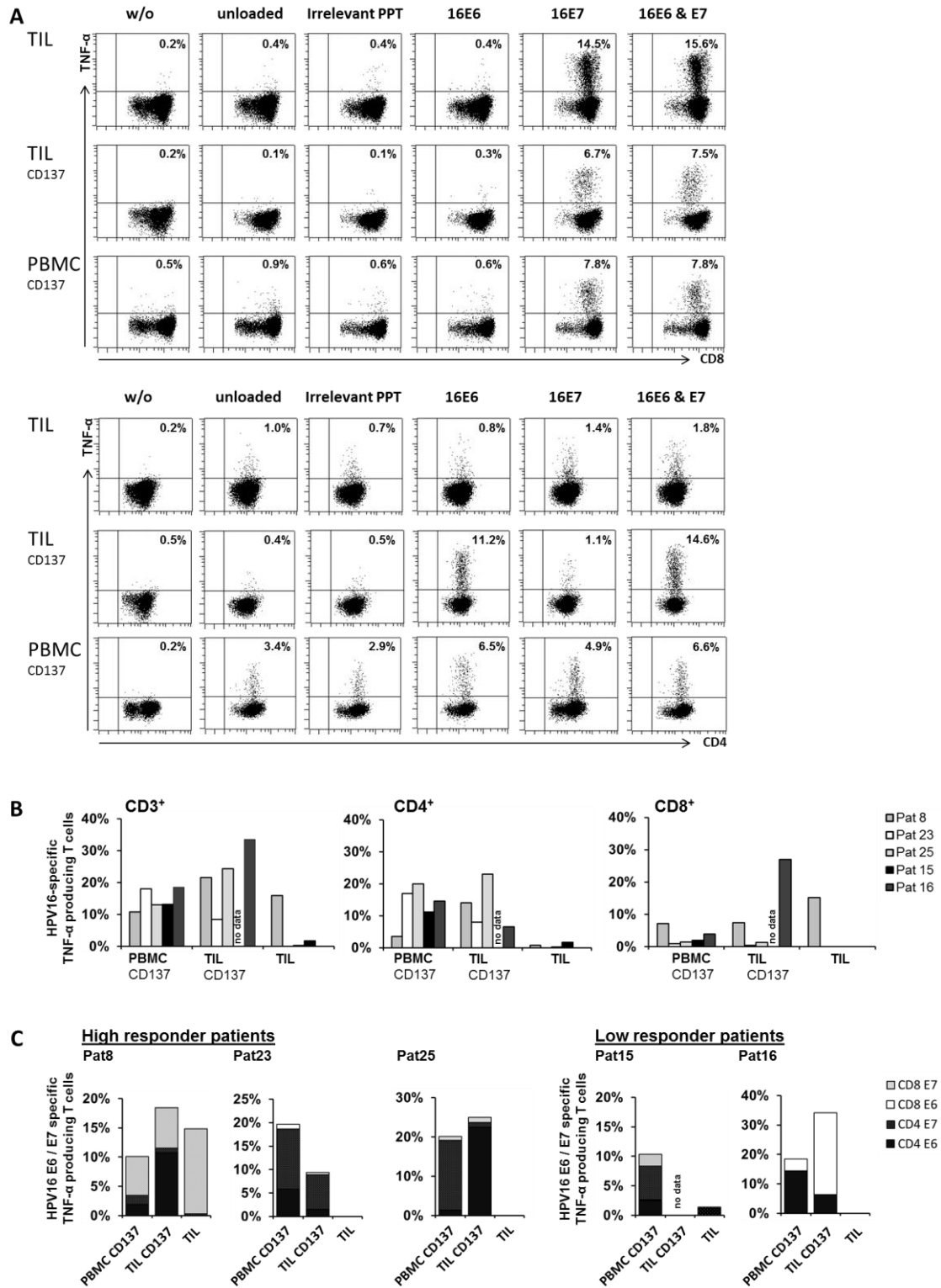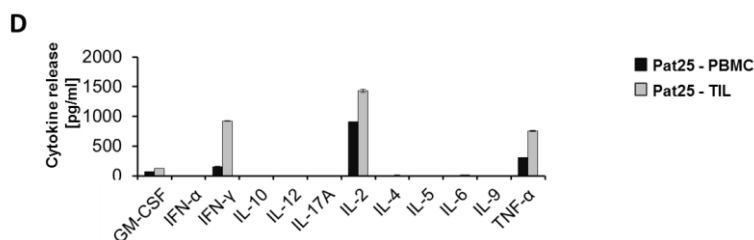
Figure 3.30: HPV16-specific reactivity of expanded T cells from blood and tumor. T cells expanded from PBMC or dissociated tumor material of five HPV16pos HNSCC patients. PBMC (PBMC CD137) and dissociated tumor material (TIL CD137) were stimulated using HPV16 E6 and E7 peptide pools, subsequently CD137+ cells were enriched, and expanded for 19 days. In parallel T cells from tumor pieces (TIL) were expanded without stimulation and enrichment. HPV16-specific TNF-α production was determined after 6 h co-cultivation of T cell cultures with autologous antigen-presenting cells either loaded with HPV16 E6 or HPV16 E7 peptide pool or both peptide pools, additionally as controls APC loaded with an irrelevant peptide pool and unloaded APC were used. **(A)** Dot plots of restimulated T cell cultures obtained from patient 8. Gated on CD8+ T cells (top) or CD4+ T cells (bottom). **(B)** HPV16-specific TNF-α production of expanded overall CD3+ (left), CD4+ (middle), and CD8+ (right) T cells. **(C)** Composition of CD4+, and CD8+ T cell responses against E6 and E7 peptide pools, shown for all five HPV16pos HNSCC patients' T cell cultures. **(D)** Cytokine concentrations in supernatants after restimulation using HPV16 E6 and E7 peptide pools, concentrations detected in unstimulated samples were subtracted. Shown for T cell culture obtained from PBMC (black) and tumor tissue (grey) of one high responder HPV16pos HNSCC patients (patient 25). Bar represents mean of triplicates, standard deviation is depicted.

In summary, these results show that functional HPV16-reactive T cells can be generated from all HPV16-positive HNSCC patients, both from blood and tumor tissue, independent of the magnitude of HPV16-directed T cell immunity in the periphery.

3.3.5 T cells expanded from blood and tumor tissue exhibit a similar phenotype

To further investigate whether HPV16-specific T cells from one particular source, blood or tumor tissue, have favorable characteristics for potential clinical use, expression of co-stimulatory markers and exhaustion markers and differentiation status of the expanded T cells was determined. After expansion of T cells no striking difference in the expression of the co-stimulatory markers CD27, CD28, and the IL-7 receptor α-chain (CD127), which marks a putative stem T cell population, was detected both for CD4+ and CD8+ T cells between HPV16-reactive T cell cultures expanded from blood or tumor tissue of HPV16pos HNSCC patients (Fig. 3.31). Likewise, the exhaustion markers CD57, CD279, and TIM-3 were not differentially expressed. The majority of expanded T cells exhibited a CD45RO+ CCR7- T_{EM} differentiation status. So overall, no striking differences in terms of expression profile of the tested phenotypic markers was observed depending on which source, blood or tumor, was used for the generation of HPV16-reactive T cell cultures. A cluster analysis revealed that the difference between donors were more profound than differences of T cell cultures derived from different sources of one donor (cluster analysis not depicted).
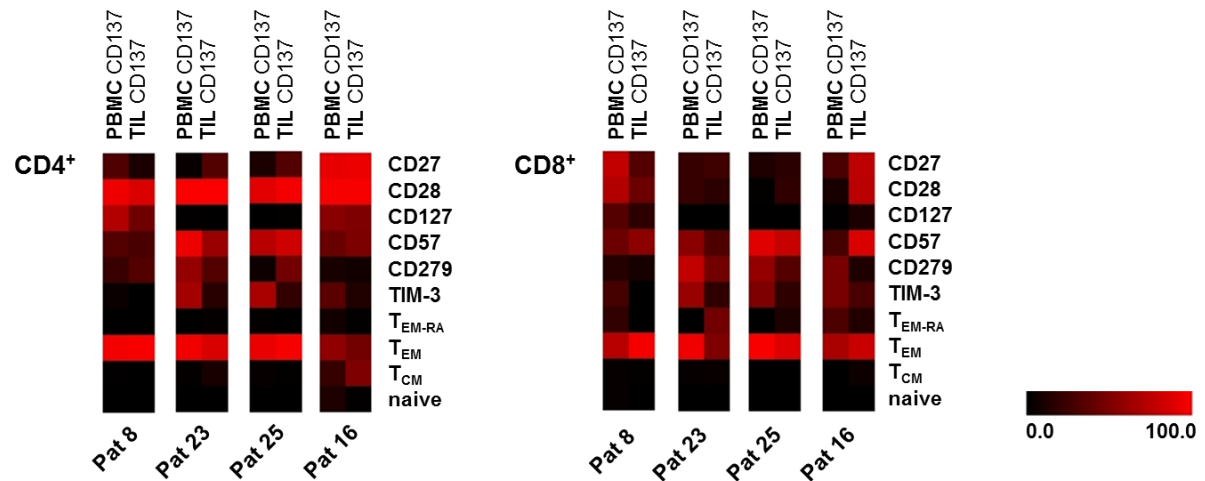
Figure 3.31: Surface marker expression of expanded T cells from blood and tumor. Heat map analysis of flow cytometric analysis of expression of surface markers in expanded T cells obtained from blood (PBMC CD137) and tumor tissue (TIL CD137), shown for CD4+ T cells (left) and CD8+ T cells (right). Black indicates 0% of T cells express the respective marker and red indicates 100% of T cells express the respective marker. Differentiation status was distinguished as CD45RO- CCR7- (T_{EM-RA}), CD45RO+ CCR7- (T_{EM}), CD45RO+ CCR7+ (T_{CM}) and CD45RO- CCR7+ (naïve). Analysis was done using TIGR Multi Experiment Viewer 4.9.

3.3.6 T cells expanded from blood and tumor tissue show HPV16-specific cytotoxic potential

To check for cytotoxic potential, CD107a expression after restimulation of expanded T cell cultures from HPV16pos HNSCC patients with HPV16 peptide loaded autologous APC was determined (Fig. 3.32). HPV16-specific CD107a expression was observed on CD8+ and, although with lower mean fluorescence intensity, also on CD4+ T cells in all five cultures derived from PBMC (range HPV16-specific CD107a expression 6.8 – 16% within CD4+ T cells, 2.4 – 19.2% within CD8+ T cells) and in four of five cultures derived from CD137-enriched tumor material (range HPV16-specific CD107a expression 2.5 – 16.7% within CD4+ T cells, 0.2 – 41% within CD8+ T cells, no data for patient 15).

To investigate on cytotoxicity against tumor cells, CD107a expression after co-cultivation with cultivated autologous, primary tumor cells was determined (Fig 3.32C) for T cell cultures obtained from HPV16pos HNSCC patients. *In vitro* expansion of autologous tumor cells was successful only for tumors of patients 23 and 25. MHC class I expression on CD324+ CD326+ was observed after expansion of autologous tumor cells, allowing recognition by specific CD8+ T cells (Fig. 3.32C). Both T cell cultures showed tumor cell-specific CD107a expression on CD8+ T cells (shown for patient 23 in Fig. 3.32D). For patient 23 5.3% of CD8+ T cells obtained from PBMC and 1.5% of CD8+ T cells expanded from tumor tissue showed tumor cell-specific expression of CD107a, for patient 25 2.5% and 3.5%, respectively. As negative control unloaded APC and autologous fibroblast cultures were used (not shown). The

obtained results indicate that the expanded T cell cultures exhibit cytotoxic potential against autologous tumor cells.
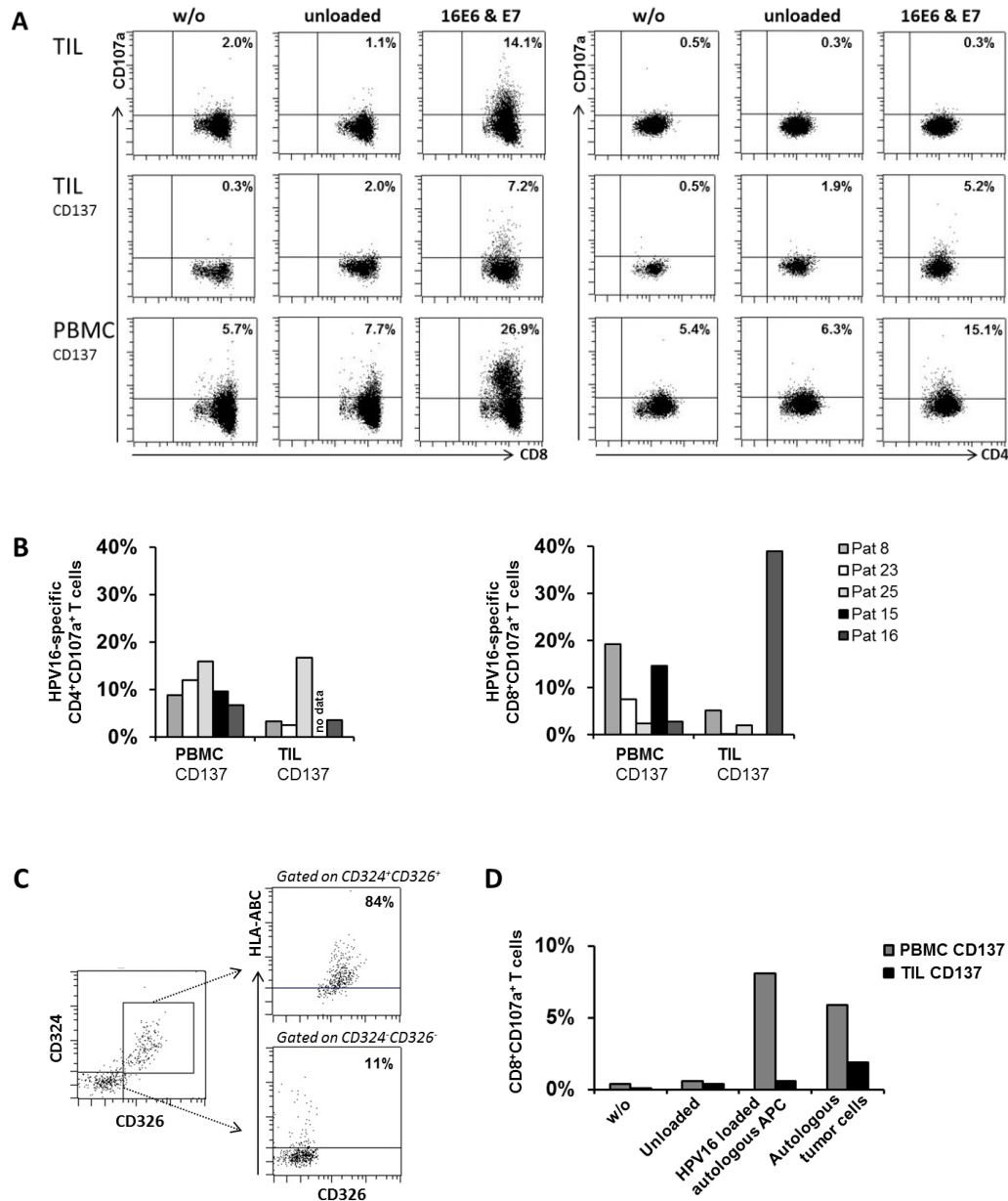
Figure 3.32: HPV16-specific T cells from blood and tumor exhibit cytotoxic potential. T cell cultures were generated according to Fig. 3.29. HPV16-specific expression of CD107a was tested after 6 h of co-cultivation. **(A)** Dot plots of CD107a expression of T cell cultures derived from PBMC (PBMC CD137) and tumor tissue with enrichment (TIL CD137) and without enrichment (TIL) of patient 8. Gated on CD8+ (left) and CD4+ (right) T cells. **(B)** CD107a expression of CD4+ (left) and CD8+ (right) T cells upon co-cultivation with antigen-loaded APC, shown for the five HPV16pos HNSCC patients. **(C)** CD107a expression of CD8+ T cells obtained from PBMC and tumor tissue of patient 23 upon co-cultivation with autologous tumor cells (left). **(D)** HLA-ABC expression on a tumor cell line from patient 23. Dead cells, CD45+, CD31+ cells, and fibroblasts were excluded from the analysis (right).

3.3.7 Immunosuppressive tumor microenvironment in HPV16^{pos} HNSCC impairs T cell functions

To test intratumoral HPV16-directed T cell activity for HPV16^{pos} patients, the cytokine profile of freshly dissociated tumor MNC after 24 h of cultivation *ex vivo* with addition of HPV16 peptide pool was analyzed (Fig. 3.33). As the number of cells available from the patients varied, direct comparison of cytokine concentrations between the patient samples is difficult, however it became obvious that not only pro-inflammatory cytokines, such as IFN-γ, are prominent, but also the suppressive cytokine IL-10 was detected in high amounts. Elevated IFN-γ to IL-10 ratios were detected for two of the high responder HPV16^{pos} patients compared to the two low responder HPV16^{pos} patients (Fig. 3.33B). These data indicate that there are either differences in the strength of immunosuppression, e.g. by IL-10 release, or a difference in the strength of HPV16-directed T cell reactivity. In either case the data imply a stronger anti-tumor response in the high responder HPV16^{pos} patients. Unfortunately for three of these four donors an unstimulated control sample is not available to judge on the strength of non-HPV16-specific background activation.

That immunosuppression is a prominent feature also of HPV16^{pos} high responder tumors was manifested by an experiment in which CD25^{+} cells were depleted from the tumor MNC before stimulation and enrichment of CD137^{+} cells (Fig. 3.33C). Depletion of CD25^{+} cells lead to a strong increase of HPV16-specific IFN-γ (5-fold) and IL-2 (45-fold) release and decrease of IL-10 (2-fold) release of the tumor MNC (Fig. 3.33B and D). As the IFN-γ concentrations detected in the unstimulated sample were low these data indicate an increased functionality of HPV16-directed T cells after depletion of immunosuppressive cells from the tumor tissue. Interestingly, also the expansion of CD137 enriched TIL increased 6-fold when CD25^{+} cells were depleted before stimulation (Fig 3.33E). This reflects the prominent role of suppressive cells in impairing HPV16-specific T cell activation in the tumor.
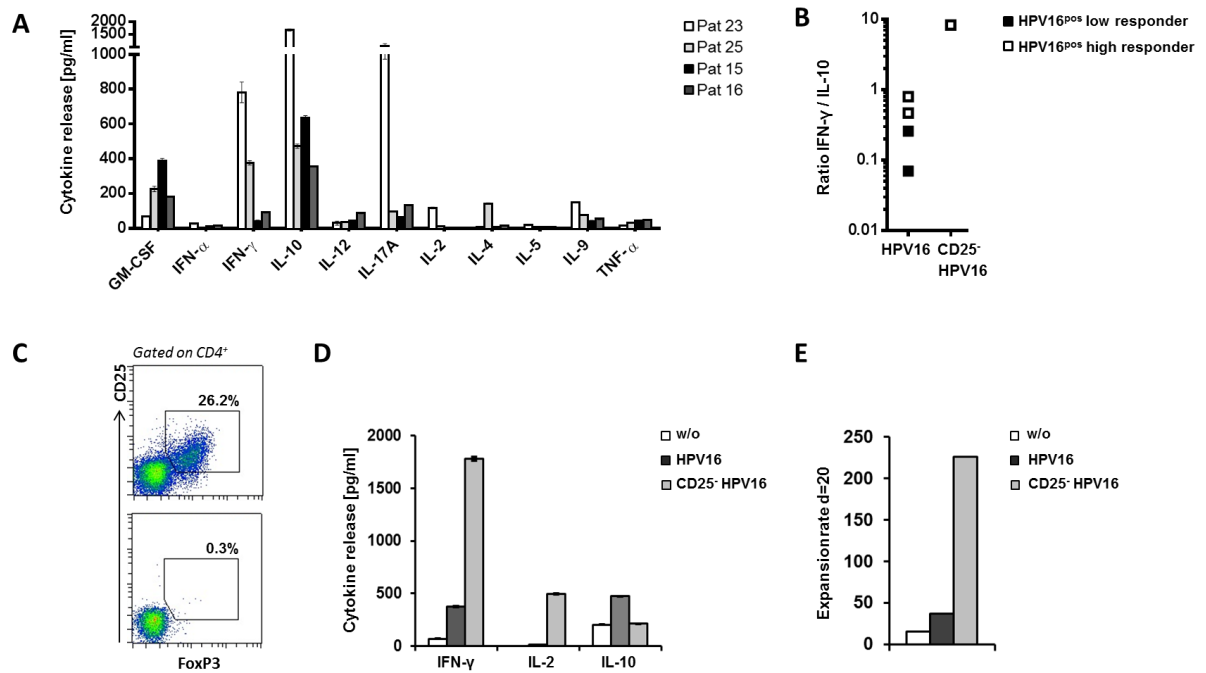
Figure 3.33: Suppressive cytokine milieu present in HNSCC tumors. Dissociated HNSCC tumor material was cultivated for 24 h with addition of HPV16 peptide pools and cytokine concentrations in the supernatants were determined. **(A)** Cytokine concentrations in HPV16 stimulated samples of dissociated HPV16^{pos} tumors. Between $1x10^6$ and $4x10^6$ total cells were stimulated. Cytokine measurements were done in triplicates, standard deviation is depicted. **(B)** Ratio of IFN-y to IL-10 concentrations of two low responders (patients 15 and 16, dark squares), high responders (patients 23 and 25, white squares) (left), and patient 25 with CD25$^+$ cell pre-depletion before cultivation (right). **(C)** Frequency of CD25$^+$ FoxP3$^+$ cells within CD4$^+$ T cells in dissociated tumor material of patient 25, before (top) and after (bottom) depletion of CD25$^+$ cells. **(D)** IFN-y, IL-2, and IL-10 concentration for patient 25 without HPV16 stimulation and with HPV16 stimulation, both with and without CD25$^+$ cell pre-depletion. **(E)** Expansion rate of CD137 enriched TIL with and without pre-depletion of CD25$^+$ cells.

Strong immunosuppressive mechanisms impair the HPV16-directed T cell immunity in the tested HNSCC tumor. A release of some of these immunosuppressive features, as shown for CD25$^+$ cell depletion, or the removal of the T cells from the suppressive microenvironment, as shown by expansion experiment (Fig. 3.30), restores the functionality of the HPV16-directed tumor-resident T cells.

4 Discussion

4.1 Establishment of activation marker-based enrichment strategies for the detection of rare antigen-specific T cells

In this study, an in-depth analysis of the full repertoire of rare TAA-specific T cells is provided. Magnetic cell enrichment strategies were implemented to overcome sensitivity hurdles of conventional methods. By using enrichment based on activation marker expression after antigenic stimulation using peptide pools, the full-repertoire of both CD4$^+$ and CD8$^+$ naïve and memory T cells was investigated. Subsequent multi-parametric flow cytometry enabled an in-depth analysis of the TAA-specific T cells in terms of prevalence, functionality, and differentiation status. Such an in-depth characterization of TAA-specific T cell repertoires is valuable for diagnostic, prognostic, and also therapeutic intervention strategies.

Ex vivo detection and comprehensive characterization was achieved by stimulation of primary peripheral blood cells and enrichment of CD154$^+$ cells. Propagation of TAA-specific T cell cultures from blood and tumor tissue was established by *in vitro* stimulation, enrichment of CD137$^+$ cells, and subsequent short-term expansion. With the help of the newly established, highly sensitive methods novel, comprehensive insights in both the WT1- and HPV16-specific T cell repertoire were obtained.

4.1.1 *Ex vivo* enumeration and characterization of rare antigen-specific T cells via CD154 enrichment

Presence and functionality of presumably rare TAA CD4$^+$ T cells was investigated directly *ex vivo* with the help of the antigen-reactive T cell enrichment (ARTE) approach. ARTE facilitates *ex vivo* analysis of the complete antigen-specific Th cell compartment regarding their cytokine expression profile and expression of cell surface markers down to frequencies of 10^{-5} to 10^{-6} specific T cells within 10^7 to 10^8 PBMC after magnetic enrichment of antigen-activated, CD154$^+$ cells (Bacher, Schink et al. 2013). CD154 enrichment was established for detection of T cells specific for recall antigens. By the use of 15-mer peptide pools for stimulation, CD4$^+$ T$_H$ cells were activated independent of their HLA status. Thus, this approach allows for the detection of the full-repertoire of antigen-specific T cells without any epitope restriction. Besides CD4$^+$ T$_H$ cells also antigen-activated CD8$^+$ T cells were detected. It was recently reported that those CD154-expressing CD8$^+$ T cells can compose up to 25% of the total CD8$^+$ compartment and that these cells probably bear helper functions comparable to T$_H$ cells (Frentsch, Stark et al. 2013). A reliable enumeration of antigen-

specific CD4$^+$ T cells is feasible via 15mer peptide pool stimulation, enrichment of CD154$^+$ cells, and subsequent flow cytometric analysis.

In a next step, the established system was transferred to less frequent antigen-specificities. In principle, the CD154 enrichment strategy is a suitable method for detection of rare TAA-specific T cells in healthy donors. Due to the enrichment step the sensitivity of the method is 10- to 100-fold higher compared to commonly used methods, such as direct pHLA tetramer staining and also ELISPOT. However, at least $5x10^7$ PBMC should be used as input when low frequent T cells are to be detected, as their frequencies lie between $1x10^{-7}$ and $1x10^{-5}$ within T cells.

The ARTE approach combined with analysis via multiparametric flow cytometry allows direct functional and/or phenotypical analysis of the enriched T cells. However, for rare cells an educated gating strategy has to be implemented to identify the right cells by exclusion of debris and non-target cells and requires at least four detection channels in flow cytometry. With the instruments used in this study eight different fluorophores could be detected, leaving four channels for the markers of interest. Co-staining of the effector cytokines TNF-α, IFN-γ, and IL-2 was feasible and allowed for functional characterization of the enriched antigen-specific T cells.

Furthermore, the differentiation status of the enriched, antigen-specific T cells can be determined via co-staining of CCR7 and CD45RO, clearly indicating that both naïve and memory T cells can be detected with ARTE. Naïve cells can have slower kinetics of cytokine production compared to memory T cells (Bachmann, Barner et al. 1999), nonetheless, also naïve TNF-α-producing T cells were detected after antigen-specific stimulation.

4.1.2 Detection of rare antigen-specific T cells via CD137 enrichment

CD137 has been described as a marker of activated T cells upon TCR engagement (Pollok, Kim et al. 1993) and was previously used to detect antigen-specific memory and naïve CD4$^+$ and CD8$^+$ T cells (Wolfl, Kuball et al. 2007, Wolfl, Kuball et al. 2008). Detection of antigen-specific T cells after CMV peptide stimulation was confirmed, as CD137 was co-expressed with other established T cell activation markers. However, several feature of CD137 hinder an accurate *ex vivo* characterization of rare antigen-specific T cells using this activation marker. Firstly, for rare antigen-specific T cells an enrichment step has to be implemented, which results in relatively high background of pre-activated, CD137-expressing cells in both antigen-stimulated and unstimulated control samples. This background of pre-activated CD137$^+$ T cells hinders an accurate enumeration of rare antigen-specific T cells. Secondly, prolonged stimulation times lead to changes in the expression of differentiation markers,

consequently accurate phenotyping is hardly possible. Thirdly, co-staining of cytokines holds also limited capacity due to the fact that stimulation times >12 h are needed for expression of CD137 on the surface of activated effector T cells. Expression of effector cytokines in memory T cells, in contrast, peaks at approximately 6 h of stimulation (Pala, Verhoef et al. 2000). Simple addition of a secretion inhibitor to allow for accumulation of cytokines in the cell to enhance fluorescent signals for detection, as done for CD154 enrichment, is not possible as it hinders CD137 expression. Hence, CD137 was chosen as a marker to generate TAA-specific T cell cultures, but was not used for *ex vivo* characterization.

4.1.3 Influence of T_{reg} on enrichment of antigen-specific effector T cells via CD137

CD137 is not only upregulated on T_{eff}, but also on T_{reg}, even with a faster kinetic upon antigen stimulation (Schoenbrunn, Frentsch et al. 2012). Indeed, FoxP3-expressing cells were enriched via CD137 enrichment after 24 – 36 h of stimulation. In experiments in which T_{reg} (CD25$^+$ cells) were depleted before stimulation and CD137 enrichment, indeed a lot of these CD4$^+$ FoxP3$^+$ CD137^{dim} cells were lost. We assume that those T cells are T_{reg}, but most likely not antigen-specific T_{reg}. The hypothesis that those CD137^{dim} cells are most likely no antigen-specific T_{reg} is based on the following findings. Firstly, this phenomenon was especially pronounced when recall antigens were used for stimulation and many antigen-specific effector T cells were activated. Secondly, far higher "antigen-specific" CD4$^+$ CD137^{dim} cell numbers were detected compared to CD4$^+$ CD137$^+$ cells after depletion of CD25$^+$ cells, presumably suggesting a dominance of antigen-specific T_{reg}. However, this is highly unlikely, as previous studies clearly show that antigen-specific T_{reg} to T_{eff} ratios usually lie below one. Even for particular antigens for which rather high T_{reg} frequencies have been reported, presumably to prevent allergies or autoimmune diseases, the T_{reg} to T_{eff} ratios lay close to one (Belkaid and Tarbell 2009, Bacher, Kniemeyer et al. 2014). Thirdly, it was found that the CD137^{high} fraction contained much higher frequencies of antigen-specific T cells, when antigen-specificity of CD137^{dim} and CD137^{high} cells was investigated after sorting of both fractions and expansion (personal communication Anne Schoenbrunn, Charité, Berlin). Therefore, we hypothesize that the CD4$^+$ FoxP3$^+$ CD137^{dim} cells get dimly activated via bystander mechanisms, probably mediated by soluble factors, and are not antigen-specific T_{reg}.

Antigen-specific T_{reg} might also be present, but not in such a high magnitude. Indeed, pre-depletion of CD25$^+$ cells in some cases led to higher numbers of activated T_{eff}. Indicating that the activation of antigen-specific T_{eff} in some cases is diminished by antigen-specific T_{reg}. However, such differences were only detected in the experiments where T cell specific for recall antigens were stimulated, but not for rare antigen-specific T cells. Indicating either that

the effect is just not strong enough to be visible in the rare T cell setting or that higher amount of antigen-specific T_{reg} exist for recall antigens to provide a natural balance between activation and regulation of a T cell response under inflammatory conditions (Belkaid and Tarbell 2009).

However, efficiency of WT1- and HPV16-specific T cell generation was not altered by CD25^{+} cell depletion, as expansion rates and frequencies of antigen-specific T cells was similar to unsorted PBMC. So both the activation and proliferation efficiency were obviously not altered; indicating that the numbers of antigen-specific T_{reg} indeed is low for those TAA-specific T cells in healthy donors and the conditions for expansion were favorable for T_{eff}, not T_{reg}.

4.1.4 Generation of TAA-specific T cell cultures

In contrast to existing protocols for the expansion of TAA-specific T cells, which are mainly based on repetitive antigen stimulation cycles and subsequent cloning of T cells, this study introduces a rapid and efficient protocol based on enrichment of rare antigen-specific T cells and short-term expansion.

Traditionally, T cells were expanded *in vitro* by addition of IL-2, which is the main cytokine responsible for overall T cell proliferation. However, in the last decade, there have been multiple reports stating that extensive *in vitro* culturing, especially in high doses of IL-2, leads to an exhausted phenotype of obtained T cells. At the same time studies proved the favorable characteristics of other cytokines for T cell expansion for clinical purposes. IL-15 has been reported to maintain functional CD8^{+} T cells with enhanced *in vivo* anti-tumor activity compared to T cells expanded using IL-2 in a mouse model (Klebanoff, Finkelstein et al. 2004). Additionally, IL-15 was found to rescue anergic T cells and restore their activity against TAA (Teague, Sather et al. 2006). IL-21 was reported to promote the expansion of cytotoxic TIL, which retain expression of the co-stimulatory molecules CD27 and CD28 (Santegoets, Turksma et al. 2013). Several groups than used these and other cytokines in combination to generate T cells with a non-exhausted phenotype in short-term expansion approaches. In this study the cytokine replenishment was adapted from Wölfl et al. (Wolfl, Merker et al. 2011), where tumor-reactive multifunctional CD8^{+} T cells were generated specific for the TAA MART-1 using IL-7, IL-15, and IL-21, and the expanded CD8^{+} T cells retained a non-exhausted CD62L^{+} CCR7^{+} CD28^{+} phenotype. Indeed, by using IL-7, IL-15, and IL-21 for the expansion of TAA stimulated and CD137 enriched T cell cultures expressing co-stimulatory markers CD27 and CD28 at a high level were obtained both within the CD4^{+} and CD8^{+} T cell compartment. In addition, surface markers indicating T cell exhaustion or senescence were not profoundly upregulated by the implemented expansion

protocol. Expression of CD57, a marker indicating limited proliferative ability (Brenchley, Karandikar et al. 2003), remained low. Likewise, CD279 (PD-1) expression was observed only on a minority of both CD4$^+$ and CD8$^+$ T cells after expansion. CD279 is a co-inhibitory molecule and can be upregulated after prolonged antigen encounter, presumably *in vivo* in chronic infections or cancer and during *in vitro* culturing. PD-1 can actively suppress T cell functionality when binding to its ligand PD-L1 (Barber, Wherry et al. 2006).

The used cytokine panel did not drive the expansion of T$_{reg}$, as no T$_{reg}$ were detected after 9 day expansion, although T$_{reg}$ were clearly also enriched via CD137 enrichment. This is in line with published reports stating that IL-7 does not promote T$_{reg}$ expansion, as T$_{reg}$ commonly have only low expression level of the IL-7 receptor α-chain (CD127) (Liu, Putnam et al. 2006, Seddiki, Santner-Nanan et al. 2006). IL-2, in contrast, clearly drives the expansion of T$_{reg}$ (de la Rosa, Rutz et al. 2004).

Therefore, it is assumed that TAA-specific T cells generated by peptide pool stimulation, CD137 enrichment and expansion under supplement of IL-7, IL-15, and IL-21 bear favorable features in terms of functionality and *in vivo* persistence for a potential clinical use of the expanded T cell product. Furthermore, the introduced protocol can be easily transferred to GMP-conform conditions, as all needed reagents are available at clinical grade quality.

Percentage of CD4$^+$ T cells directly after enrichment step was strongly increased, due to high unspecific background expression of CD137 on CD4$^+$ T cells (discussed in 4.1.3). However, the enriched antigen-specific T cells received a proper TCR trigger and therefore were driven into proliferation in contrast to dimly activated or non-activated T cells. Therefore, enriched unspecific or non-activated T cells did not attenuate expansion of antigen-specific T cells. After expansion the ratio of CD4 to CD8 T cells was highly variable, probably depending on the repertoire of naïve and memory antigen-specific T cell of the individual donor. But no general bias to propagation of either CD4$^+$ or CD8$^+$ T cells was observed with the used enrichment and expansion conditions.

4.1.5 Peptide pools for stimulation of the full repertoire of antigen-specific T cells

According to basic literature only professional APC, such as DC, are able to prime naïve antigen-specific T cells as they provide the right co-stimulatory molecules. Until now, peptide stimulation of T cells *in vitro* was done with peptide loaded DC. These DC have to be prepared using a laborious protocol, commonly from peripheral blood monocytes, as DC mainly reside in the tissue *in vivo* and only few are found in the circulation. Furthermore, it is believed that cross-presentation of extracellular peptides onto MHC class I to CD8$^+$ T cells is a feature unique to DC. In contrast to these classical beliefs, the activation of both naïve and

memory antigen-specific T cells was possible using peptide pools of overlapping 15-mers without separate preparation of DC, simply by adding the 15-mers to isolated PBMC. Additionally, an efficient stimulation of CD4 and CD8 T cells was feasible, indicating that antigen-presentation, presumably including antigen-processing and cross-presentation, was fully functional even without separately matured DC. When the described method was established experiments using separately matured DC, loaded with the peptide pools, were also included, but did not lead to a striking difference in efficiency of propagation of rare antigen-specific T cell. As no direct comparison of both protocols, with and without separate DC preparation, was done the results are not shown. Thus, peptide pool stimulation and enrichment of activation marker-expressing cells presents a straightforward and easy approach, which allows for the detection of the full-repertoire of antigen-specific T cells without separate DC preparation and without any epitope or HLA restriction.

4.2 WT1-specific T cell repertoire in healthy donors

This study gains comprehensive insight into the naturally existing WT1-specific T cell pool in healthy individuals. The key findings are: (i) WT1-specific T cells are present in the vast majority of healthy donors; (ii) WT1-specific CD4$^+$ T cells are commonly present in the memory pool; (iii) WT1-specific CD8$^+$ T cells reside primarily in the naïve pool; and (iv) WT1-specific memory CD4$^+$ and naïve CD8$^+$ T cells can co-exist in the same individual, which implies that distinct mechanisms control the differentiation of the auto-reactive WT1-specific CD4$^+$ and CD8$^+$ T lymphocytes from naïve into memory cells; (v) functional WT1-specific T cell lines can efficiently be generated *in vitro*. Collectively, the obtained data argue for the usage of the natural WT1-reactive T cell repertoire for immune therapy, such as vaccination or adoptive T cell transfer, of WT1-expressing cancers.

4.2.1 Prevalence and functionality of WT1-specific T cells

Ex vivo detection of the naturally existing WT1-specific T cell pool in healthy individuals revealed frequencies as low as 10^{-6} to 10^{-5} within the T cell compartment. Additionally, functionality of the WT1-specific T cells was proven and their phenotype was determined. Notably, the first evidence of co-existence of both memory CD4$^+$ T cells and naïve CD8$^+$ T cells with the same self-antigen-specificity within one individual donor is provided.

Functional CD4$^+$ WT1-specific T cells in healthy donors were detected by enrichment of CD154$^+$ T cells (ARTE) after WT1-specific short-time stimulation. By utilizing ARTE, CD4$^+$ WT1-specific T cells could be characterized directly *ex vivo,* comprising determination of frequency, phenotype, and functionality. The ARTE method was highly reproducible and thus reliable, even if the number of detected activated cells after WT1 stimulation in some samples was elevated only by as few as 30 CD154$^+$ T cells compared to the unstimulated control (range 30 – 370 WT1-reactive CD154$^+$ T cells above background). Frequencies of WT1-specific T cells in healthy donors ranged from 10^{-6} to 10^{-5} within CD4$^+$ T cells. These determined frequencies are in consistency with published data, both for WT1-specific CD4$^+$ T cells (Bacher, Schink et al. 2013), which have been detected using the same method, as well as CD4$^+$ T cells specific for other self- or neo-antigens (gp100, fibrinogen, preproinsulin (Su, Kidd et al. 2013) and *Bacillus anthracis* (Kwok, Tan et al. 2012), detected with MHCII tetramer enrichment strategies.

CD8$^+$ WT1-specific T cells, detected with the help of WT1-MHC tetramer enrichment, were determined to be present in approximately one magnitude lower frequencies (10^{-7} to 10^{-5} within CD8$^+$ T cells) than CD4$^+$ WT1-specific T cells detected via ARTE, keeping in mind that MHCI tetramer enrichment only covers one epitope-specificity, whereas for the ARTE

approach a pool of peptides spanning the whole WT1 protein was used to activate and identify WT1-reactive $CD4^+$ T cells. The determined frequencies of naïve $CD8^+$ $WT1_{37-45}$-specific T cells are comparable to frequencies reported for self- or unexposed viral antigens (NY-ESO ($10^{-6} - 10^{-5}$), HIV ($10^{-7} - 10^{-5}$)) (Alanio, Lemaitre et al. 2010).

T cells specific for the self-antigen WT1 exist in virtually all healthy donors. There is evidence that the WT1-specific $CD8^+$ T cells are of quite high avidity (see section 3.2.2.5 and (Chapuis, Ragnarsson et al. 2013). The presence of high-avidity WT1-specific T cells in peripheral blood of healthy donors argues for an incomplete negative selection of these self-antigen specific T cells, as high-affinity clones against self-antigens are classically believed to be deleted during their development in the thymus in a mechanism known as central tolerance (Wiegers, Kaufmann et al. 2011). Therefore, the question arises why those WT1-reactive T cells have not been negatively selected in the thymus? There are several mechanisms reported that can lead to high levels of auto-reactive T cells because of insufficient negative selection in thymus: (1) very low expression of the antigen in mTEC as reported for the myosin heavy chain 6 in autoimmune myocarditis (Lv, Havari et al. 2011) and the glutamate decarboxylase 2 (GAD2) in type I diabetes (Gotter, Brors et al. 2004); (2) differential splicing or mis-initiation of transcription in mTEC reported for MART-1 (Klein, Klugmann et al. 2000, Pinto, Sommermeyer et al. 2014); (3) missing post-translational modifications of antigens in mTEC as shown for aggrecan and vimentin in rheumatoid arthritis (Scally, Petersen et al. 2013) or insulin in type I diabetes (Van Lummel, Duinkerken et al. 2014) (List taken from (Klein, Kyewski et al. 2014)). Whether any of these mechanisms is involved in the development of WT1-specific T cells remains matter of future investigation. However, it was shown that activation of self-reactive T cells can also occur in the absence of any defects in negative selection and in the presence of functional T_{reg} (Enouz, Carrie et al. 2012). T cells that escape negative selection, as their avidity is below negative selection threshold, are quiescent due to sustained encounter of antigen, which can render mature T cells tolerant to the antigen by constant signals through their T cell receptors. These auto-reactive T cells are therefore ignorant to self under steady-state conditions in the periphery. Such tolerant T cells can be activated, e.g. during an infection due to cross-reactivity to foreign antigens or when their threshold for activation is lowered by co-activating factors. One such stimulus could be infection or in case of TAA-specific T cells tumor formation accompanied by inflammatory conditions. Self-reactive T cells can then cause autoimmunity resulting in tissue destruction or, in the case of WT1-specific T cells, in tumor cell destruction. WT1-specific T cells can at least *ex vivo* clearly be activated by stimulation with WT1 peptides, as shown in this study, indicating that the T cells are not anergic. So far, no autoimmune complications were reported emerging from WT1-specific T cells, although WT1 is expressed on $CD34^+$ hematopoietic precursors. This could be due to the fact, that expression levels of WT1 are

just too low on normal cells compared to tumor cells. WT1 expression levels have been reported to be comparable to leukemic cells in about 1% of CD34$^+$ hematopoietic precursors, the vast majority of cells expressing far lower levels (Hosen, Sonoda et al. 2002). Therefore, normal WT1-expressing cells seem to not provide a stimulus, which is above the activation threshold of WT1-specific T cells. Severe autoimmunity resulting in leukopenia has been observed after vaccination with WT1$_{126-134}$ peptide in myelodysplastic syndrome (MDS) patients (Oka, Tsuboi et al. 2003). This leukopenic effect is a sign of the anti-tumor functionality of WT1-specific T cells rather than a safety concern, as this side-effect was so far only observed in MDS patients, but not in other patients treated (Oka, Tsuboi et al. 2004). MDS patients have only a few normal hematopoietic precursors as this disorder is marked by mutations already in the stem cells in bone marrow, which give rise to all blood cells.

The ARTE assay revealed that CD4$^+$ WT1-reactive memory T cells exist in over 60% of healthy donors in addition to the prevalent naïve WT1-specific T cell pool. These memory CD4$^+$ T cells could be shown to have a functional phenotype as they readily expressed the effector cytokine TNF-α and partially also IFN-γ.

4.2.2 Discrepancy in differentiation status of CD4$^+$ and CD8$^+$ WT1-specific T cells

This work comprises, for the first time to my knowledge, phenotyping of both CD4$^+$ and CD8$^+$ T cells with the same antigen-specificity. This study discovers, via the ARTE assay, that over 60% of healthy donors exhibit a CD4$^+$ memory T cell response additionally to CD4$^+$ T cells of naïve phenotype specific for WT1. In contrast, virtually all WT1$_{37-45}$-specific CD8$^+$ T cells, detected by pMHCI tetramer, are of naïve phenotype. Additionally, a direct discrepancy in CD4$^+$ and CD8$^+$ phenotype of WT1-specific T cells was identified in four out of five tested donors using presorted naïve or memory T cell subsets. In all five donors included in this assay CD4$^+$ WT1-specific memory T cells were identified, whereas detected CD8$^+$ WT1-specific T cells arose solely from the naïve T cell compartment in four of the five tested donors. Such a discrepancy in phenotype of CD4$^+$ and CD8$^+$ T cells with the same antigen-specificity is in sharp contrast to the classical model of antigen-specific T cell memory formation. The classical model states that antigen-specific T cell memory is formed solely after recent exposure to the antigen to protect the body from a potential re-encounter with the particular specimen. Such an exposure would presumably trigger the formation of both CD4$^+$ and CD8$^+$ memory T cells. Recent data introduced alternative ways of memory generation into the T cell field, indicating that T cell memory must not necessarily be a result of previous cognate antigen encounter. On the one side, memory-like CD8$^+$ antigen-specific population were reported in unexposed mice. These memory CD8$^+$ T cells were generated by homeostatic mechanisms and were named "virtual memory" (Haluszczak, Akue et al. 2009,

Lee, Hamilton et al. 2013). On the other side, Su et al. (Su, Kidd et al. 2013) recently introduced a distinct mechanism of memory formation of human virus-specific CD4^{+} T cells by demonstrating their cross-reactivity against common environmental antigens. Our results would fit to the latter model, i.e. in the case of the self-antigen WT1, CD4^{+} memory T cells might be a result of cross-reactivity. One reason for this assumption is the absence of CD8^{+} WT1-specific memory seen in the experiments, which argues for the absence of a previous systemic WT1-specific T cell response, e.g. due to tumor cell growth. Furthermore, formation of a so-called "virtual memory" CD4^{+} T cells is contradicted by two facts. Firstly, effector cytokines were readily produced upon antigen encounter of those T cells. Secondly, the fact that they represent a major part of CD4^{+} WT1-specific T cells (ratio of memory to naïve WT1-specific CD4^{+} detected was in a range of 0.6 to 5.2), in contrast to virtual memory T cell repertoire, which was reported to comprise only 5-20% of the respective antigen-specific population (Haluszczak, Akue et al. 2009, Lee, Hamilton et al. 2013). Intriguingly, the existence of memory T cells specific for self-antigens, including WT1, was demonstrated recently (Bacher, Schink et al. 2013, Su, Kidd et al. 2013). However, prove for cross-reactivity as the reason for memory formation of such self-antigen specific T cells remains elusive. For CD8^{+} T cells specific for viral antigens cross-reactivity has been demonstrated to exist (Wedemeyer, Mizukoshi et al. 2001, Clute, Watkin et al. 2005). However, CD8^{+} T cells specific for self-antigens (NY-ESO, MART-1) have been reported to exhibit a naïve phenotype in the periphery (Zippelius, Pittet et al. 2002, Alanio, Lemaitre et al. 2010). The findings presented here indicate that memory formation due to cross-reactivity does not occur as frequently for WT1-reactive CD8^{+} T cells as for CD4^{+} T cells. The hypothesis that cross-reactivity might be more abundant in the CD4^{+} T cell compartment than in the CD8^{+} T cell compartment was already raised by others in the past (Wilson, Wilson et al. 2004, Welsh, Che et al. 2010), however, until now, conclusive evidence is missing.

The lack of CD8^{+} WT1-specific memory T cells could also be a result of a more effective central tolerance for CD8^{+} T cells compared to CD4^{+} T cells, as it has been suggested for p53 in mice (Lauwen, Zwaveling et al. 2008). Such a more stringent negative selection of CD8^{+} T cells could serve as a safety mechanism to prevent autoimmunity caused by self-reactive cytotoxic T cells. However, although a recent study provided interesting insights into the human thymic peptide repertoire, such as differences between epitopes and individuals, clear prove for such a systemic difference in tolerance induction for CD8^{+} and CD4^{+} T cells has not been provided for humans (Adamopoulou, Tenzer et al. 2013).

4.2.3 *In vitro* generation of WT1-specific T cell lines

Enrichment of T cells expressing CD137 out of PBMC obtained from healthy donors after *in vitro* WT1 peptide pool stimulation allowed for the generation of oligoclonal WT1-reactive T cell cultures within ten days. The generated T cell populations consisted of CD4$^+$ and CD8$^+$ T cells, which produced effector cytokines upon restimulation with WT1 peptides, thus arguing for the existence of a functional WT1-specific immunity in virtually all healthy donors, which can potentially be utilized for immunotherapeutic approaches. Possible areas of application for WT1-specific T cells are, on the one hand, adoptive T cell transfer, preferentially in leukemia, and, on the other hand, therapeutic vaccination for numerous tumor entities.

To judge the therapeutic potential of natural WT1-specific T cells, knowledge about their avidity is crucial, as it might determine *in vivo* anti-tumor efficacy (Pedersen, Sorensen et al. 2013). The process of clonal deletion during central tolerance was shown to be TCR-affinity dependent (Starr, Jameson et al. 2003), suggesting that WT1-specific T cells might be of rather low or intermediate affinity towards their antigen. Intriguingly, other groups have reported the generation of CD8$^+$ WT1-specific T cell clones of high avidity. These results have been obtained by using different assays. Weber et al. (Weber, Karbach et al. 2009) reported EC$_{50}$ values of 0.1 nM for a WT1$_{37-45}$-specific T cell clone and Chapuis et al. (Chapuis, Ragnarsson et al. 2013) reported even higher functional avidities. In contrast to the approach used in this study, published results were obtained by testing the specific lysis of T2 cells of a WT1-specific single cell clone. However, cytotoxicity of T cells can be triggered at 10- to 100-fold lower peptide concentrations than needed for cytokine production (Betts, Price et al. 2004). Indeed, in this study, discrepancies in determined EC$_{50}$ values were discovered depending on whether cytokine production or CD107a upregulation, a surrogate marker for cytotoxicity, was used as read-out. Studying the functional avidity of CMV pp65$_{495-503}$-specific T cells *ex vivo* and after CD137 enrichment and expansion revealed that T cells might change certain activation properties during *in vitro* culture. Unfortunately, determination of functional avidities of WT1-specific T cells *ex vivo* is hindered owing to their exceedingly low frequencies. However, the comparison of functional avidities of CMV- and WT1-specific T cells after expansion indicated that WT1$_{37-45}$-specific T cells were indeed not of low avidity, as one might expect due to negative selection of high avidity clones during development, but had similar functional avidities to CMV-specific T cells. Weber et al. (Weber, Karbach et al. 2009) proved sufficient avidities of generated WT1-specific T cells towards leukemia cell lines, which express WT1 endogenously. Reactivity against natural targets such as primary tumor cell killing could, unfortunately, not be tested in this study. Further support for the therapeutic capacity of natural existing WT1-specific immunity comes from immunmonitoring studies. Here, an induction of WT1-specific CD8$^+$ T cell response after alloSCT and or donor

lymphocyte infusion (DLI) clearly proved the immunogenicity of WT1 in cancer patients. Moreover, the induced WT1-specific T cells presumably mediated graft versus leukemia effects in leukemia patients, demonstrating their therapeutic potential (Rezvani, Yong et al. 2007, Kapp, Stevanovic et al. 2009, Tyler and Koehne 2013). Vaccination strategies, which naturally rely on exploiting the pre-existing WT1-specific T cell pool for therapy, likewise showed promising results in several clinical studies, reporting clinical response rates of 63% in hematological diseases (Van Driessche, Berneman et al. 2012).

In the past, several studies already established WT1-specific T cell cultures. However, all of them used *in vitro* priming approaches including DC preparation and loading, repetitive stimulation cycles using WT1 peptide-loaded DC in some studies followed by cloning of single CD8^{+} T cells (Weber, Karbach et al. 2009, Krishnadas, Stamer et al. 2011, Weber, Gerdemann et al. 2013). The described protocols demand laborious DC preparation and take several weeks of expansion time. Krishnadas et al.(Krishnadas, Stamer et al. 2011) for the first time included an enrichment step, however, enrichment was done after several weeks of repetitive stimulation cycles and the obtained T cell culture only contained 3 - 5% of WT1 tetramer^{+} T cells. In this study, a new, improved protocol for the efficient generation of WT1-specific T cell cultures via CD137 enrichment and short-term expansion is introduced, which has several advantages over established protocols: (i) The protocol avoids prolonged *in vitro* culture, which typically results in an exhausted T cell phenotype associated with limited *in vivo* efficacy (as discussed in 4.4.5). With the efficient protocol used in this study functional, non-exhausted T cells cultures were obtained. (ii) The expanded T cell cultures contain high frequencies of WT1-specific T cells, up to 60% of WT1-reactive T cells. (iii) The described protocol employs the full-repertoire of WT1-specific T cells instead of using clonal culture specific for only one particular epitope. Multi-epitope-specificity can be beneficial for *in vivo* efficacy of the T cell product. (iv) The protocol includes enrichment and expansion of both CD4^{+} and CD8^{+} WT1-specific T cells. In order to provide optimal anti-tumor efficacy it is desirable to include CD4^{+} T cells, as it has been shown that CD4^{+} T cells can be powerful anti-tumor effector cells in mouse (Perez-Diez, Joncker et al. 2007, Xie, Akpinarli et al. 2010, Goldstein, Varghese et al. 2011) and human (Tran, Turcotte et al. 2014). The importance of CD4^{+} T cell inclusion has been supported by studies demonstrating that CD4^{+} T cell help is crucial for a maintained CD8^{+} T cell functionality (Bourgeois, Veiga-Fernandes et al. 2002, Shedlock and Shen 2003, Sun and Bevan 2003) and also by studies proving an *in vivo* anti-tumor effect of adoptively transferred CD4^{+} tumor-specific T cells (Tran, Turcotte et al. 2014). To this end, utilizing the broad repertoire of pre-existing CD4^{+} and CD8^{+} might be beneficial. The generation of such WT1-specific CD4^{+} and CD8^{+} mixed T cell cultures has been proven to be feasible by using a 15mer peptide pool of WT1 (Krishnadas, Stamer et al. 2011), our data). (v) Our simplified protocol does not require laborious isolation and maturation of DC.

Therefore, the protocol for propagation of WT1-specific T cell cultures, based on *in vitro* stimulation using 15mer peptide pools and enrichment of CD137^{+} cells, established in this study is superior to previously used protocols for the generation of WT1-specific T cells in terms of production efficiency and quality of the T cell product. Notably, the introduced protocol could be easily transferred to GMP-conform conditions as all needed reagents are available at clinical grade.

4.2.4 Expanded WT1 specific T cells for adoptive anti-cancer therapy

The generation of such WT1-specific T cells out of the natural existing pool has been of great interest for therapeutic approaches, such as adoptive therapy and vaccination. A compelling opportunity for which the research results presented here could directly be implemented is the use of WT1-specific T cells as DLI after HSCT of leukemia patients. DLI, consisting of total lymphocytes of the stem cell donor, is a routine treatment when relapse occurs after HSCT and does successfully fight small amounts of recurrent tumor cells in many cases due to the so called graft-versus-tumor effect. However, a major drawback of standard DLI is the mixed nature of the cell product, containing many different T cell antigen-specificities. Therefore unsorted DLI often cause severe autoimmunity due to graft-versus-host properties. A more specific, targeted DLI product, such as expanded WT1-specific T cells, could prevent these complications (Bornhauser, Thiede et al. 2011). A typical DLI consists of 1×10^7 to 1×10^8 T cells or total PBMC per kg bodyweight (Luznik and Fuchs 2002, Bachireddy, Hainz et al. 2014). In this study up to 1×10^7 mostly WT1-specific T cells after expansion from 1×10^8 starting PBMC were obtained. However, higher starting cell numbers would result in higher T cell numbers, which is easily possible by using a leukapheresis product of the healthy stem-cell donor. For a defined, specific T cell product such high numbers of transferred T cells might not be needed, this needs to be evaluated in the future.

WT1-specific T cells can also be used for adoptive T cell therapy of other cancer entities which is a field of ongoing research. A successful first clinical trial using naturally derived, avidity selected, $WT1_{126-134}$-specific CD8^{+} T cell clones recently demonstrated the feasibility and safety of adoptive T cell therapy with WT1-specific T cells derived from the natural, autologous repertoire in leukemia (Chapuis, Ragnarsson et al. 2013).

4.2.5 Employing WT1-specific T cells for therapeutic anti-cancer vaccination

Therapeutic vaccination using WT1 as an antigen is discussed currently as a potential treatment of myeloid leukemias (Oka, Tsuboi et al. 2004, Rezvani, Brenchley et al. 2005, Keilholz, Letsch et al. 2009, Yasukawa, Fujiwara et al. 2009, Maslak, Dao et al. 2010, Van

Tendeloo, Van de Velde et al. 2010, Kitawaki, Kadowaki et al. 2011, Kuball, de Boer et al. 2011, Rezvani, Yong et al. 2011), but also other cancer entities including breast cancer (Oka, Tsuboi et al. 2004, Morita, Oka et al. 2006) and lung cancer (Oka, Tsuboi et al. 2004, Krug, Dao et al. 2010).

The insights into the natural occurring WT1-reactive T cell repertoire have direct implications on the design of WT1-based vaccination approaches. In this study, CD8+ T cells specific for the $WT1_{37-45}$ epitope were much more abundant than T cells specific for $WT1_{126-134}$, both after CD137 enrichment and expansion (Fig. 3.17) and in *ex vivo* WT1-MHCI tetramer enrichment approaches (Fig. 3.14). This might have implications on the design of therapeutic and immunmonitoring strategies, as many published studies solely concentrate on CD8+ T cell clones specific for $WT1_{126-134}$. Multiple vaccination studies that used the $WT1_{126}$ epitope alone or in combination achieved only limited T cell responses in humans (Keilholz, Letsch et al. 2009, Rezvani, Yong et al. 2011, Uttenthal, Martinez-Davila et al. 2014). In contrast, studies including WT1 stimuli, which cover a multitude of WT1 epitopes, such as long peptides ((Maslak, Dao et al. 2010) in AML, (Krug, Dao et al. 2010) in mesothelioma] and WT1 mRNA DC vaccination (Van Tendeloo, Van de Velde et al. 2010), lead to broader WT1-specific CD4+ and CD8+ T cell responses. The vaccination studies using long peptides successfully induced both CD8+ and CD4+ WT1-specific T cell responses *in vivo* (Krug, Dao et al. 2010, Maslak, Dao et al. 2010), indicating that the success of such vaccination strategies is not impaired by the discrepancy in the differentiation status of CD4+ and CD8+ preexisting WT1-specific T cell populations, which was disclosed in this study. On the contrary, one might speculate that pre-existing memory CD4+ WT1-specific T_H cells might help to generate a CD8+ T cell response from the naïve pool. In consistence with these reported clinical findings, both CD4+ and CD8+ WT1-specific T cells could be readily activated *ex vivo* by stimulation with WT1 peptide pool in this study. The results obtained in this study together with the mentioned previous studies argue for the usage of WT1 stimuli, which cover the whole WT1 protein, for vaccination rather than single peptides.

In order to reveal clinically relevant cell responses of applied vaccinations the techniques described in this paper provide compelling tools for immunmonitoring. The ARTE approach is a suitable tool to monitor not only frequency but remarkably also functionality of antigen-specific CD4+ T cell with high resolution. Usage of peptide pools additionally provides the opportunity to monitor oligoclonal T cell responses circumventing HLA-restriction.

4.3 HPV16-specific T cell immunity in HNSCC patients

In this study an in-depth characterization of peripheral blood and intratumoral HPV16-directed T cell immunity in HPV16^{pos} HNSCC patients was conducted. Major results are: (i) HPV16-specific CD4^{+} T cells are present in the blood of all patients; (ii) a subgroup of this cohort bears exceedingly high numbers of effector memory HPV16-reactive CD4^{+} T cells compared to other HPV16^{pos} HNSCC patients and HPV16^{neg} HNSCC patients, which (iii) might be related to different frequencies of HPV16-reactive naïve T cells; furthermore (iv) HPV16-directed T cell immunity in blood of HNSCC patients reflects intratumoral immunity; (v) CD25^{+} cells, most likely T$_{regs}$, impair intratumoral HPV16-directed effector T cell responses *in vivo*; nonetheless, (vi) functional HPV16-reactive T cells can be expanded *ex vivo* from blood and tumor tissue of all HPV16^{pos} HNSCC patients after their enrichment. In summary, this data support the therapeutic utilization of the existent HPV16-reactive T cells in HPV16^{pos} HNSCC patients.

4.3.1 Prevalence and functionality of HPV16-reactive T cells in HPV16^{pos} HNSCC patients

The highly sensitive method based on enrichment of CD154-expressing, activated T cells enabled the detection of HPV16-specific memory T cells in blood of all HPV16^{pos} HNSCC patients, independent of whether the blood was derived from patients at the time of tumor resection or several month after surgery. Intriguingly, five of the nine HPV16^{pos} HNSCC patients revealed exceedingly high frequencies of HPV16-reactive CD4^{+} T cells, which were significantly higher compared to frequencies detected in PBMC of healthy donors and HPV16^{neg} HNSCC patients. In addition, in blood of two of the five high responders CD3^{+} CD4^{-} HPV16-reactive T cells were found. In the other four of the nine HPV16^{pos} HNSCC patients the level of HPV16-reactive CD4^{+} T cells did not exceed the level determined in healthy donors.

The obtained results clearly show that HPV16-reactive T$_{H}$ cells detected in the blood of the high responder HPV16^{pos} HNSCC patients at time of tumor resection were fully functional T$_{H}$1 cells. This is in contrast to data obtained for HPV16^{pos} cervix carcinoma patients, where an impaired functionality of circulating HPV16-directed T cells has been suggested (Clerici, Merola et al. 1997, de Jong, van Poelgeest et al. 2004, Bais, Beckmann et al. 2005, Sharma, Rajappa et al. 2007). However, multiple publications speculate that immunity to HPV16^{pos} HNSCC tumors might be profoundly different to immunity against HPV16^{pos} cervix carcinoma, simply because HPV16^{pos} HNSCC tumors are mostly located closely or within lymphoid tissue of the tonsils. In a recent study on HPV16-reactive T cell immunity in blood of

HPV16[pos] HNSCC patients only in a subgroup of these patients circulating HPV16-reactive T cells were detected (Heusinkveld, Goedemans et al. 2012), the detected lack of a peripheral HPV16-specific T immunity in some patients might be due to the inability to detect antigen-specific T cells at low frequencies with the used assay. Therefore, data from Heusinkveld et al (Heusinkveld, Goedemans et al. 2012) are in line with data in this study, as they reflect remarkable differences in the strength of HPV16-directed T cell immunity in HPV16^{pos} HNSCC patients. However, data obtained in the study presented here clearly show, for the first time, that a subgroup of HPV16^{pos} HNSCC patients has highly functional HPV16-reactive T cells, thereby contrasting the notion that T cell immunity is generally impaired in HPV16^{pos} cancer patients.

Concerning frequencies of HPV16-reactive CD4$^+$ and CD8$^+$ T cells in the peripheral blood, samples taken from HPV16^{pos} patients at the time of tumor resection showed similar results to samples taken from HPV16^{pos} follow-up patients, as in both groups in approximately half of the samples elevated frequencies of CD4$^+$ HPV16-reactive T cells and in approximately a quarter of the samples elevated frequencies of CD8$^+$ HPV16-reactive T cells were detected compared to HPV16^{neg} patient samples and healthy donors. However, T cells of one high responding HPV16^{pos} follow-up patient revealed an exhausted phenotype (T_{EM-RA}, CD45RO$^-$ CCR7$^-$) and limited functionality, as only a very small proportion of CD4$^+$ HPV16-reactive T cells produced TNF-α and IFN-γ upon stimulation. Also the other HPV16^{pos} high responding follow-up patient showed somewhat functional impairment, as the CD4$^+$ HPV16-reactive T cells produced hardly any IFN-γ and the CD4$^-$ HPV16-reactive T cells produced hardly any TNF-α, even though the differentiation status of both the CD4$^+$ and CD4$^-$ population did not primarily indicate an exhausted state of the T cells, but a T_{EM} (CD45RO$^+$ CCR7$^-$) phenotype. The samples of these two high-responding follow-up patients had been taken 15 and 31 months after diagnosis, respectively. The data might indicate that the tumor load was low, i.e. infection was not acute anymore in the follow-up patients, but decaying. Notably, the tested follow-up patients were in complete remission without relapse.

Frequencies of HPV16-reactive T_H cells in low-responders within the HPV16^{pos} HNSCC surgery patients were similar to frequencies in healthy patients. However, all HNSCC patients show clear memory formation, indicating that indeed an on-going HPV16 infection was sensed by the immune system and induced the formation of memory T cells.

CD4$^+$ HPV16-reactive T cells of low-responder HPV16^{pos} follow-up patients were of T_{CM} and naïve phenotype with rather a higher proportion of naïve T cells compared to HPV16^{pos} low-responder surgery patients, supporting the idea that in follow-up patients the HPV16 infection was decaying. The two low-responder follow-up patients were sampled 36 and 57 months after diagnosis and were without relapse until this time point.

4.3.2 HPV16-reactive T cells in healthy individuals

Some healthy individuals also showed quite high frequencies of HPV16-reactive T cells in the periphery. In detail, three healthy individuals (of 32 donors tested) had frequencies of >1x10^{-5} within CD4$^+$ T cells, the majority of those HPV16-reactive T cells were of T_{CM} or T_{EM} phenotype. This high frequency of memory HPV16-reactive T cells indicates that these healthy donors might have had an HPV16 infection. However, for the used healthy individuals it was impossible to determine whether those individuals had ever encountered an HPV16 infection or were currently HPV16 infected. It is believed that more than 50% of people are infected by any type of HPV once during their life time. As most of these infections are cleared without any symptoms and are therefore not noticed, exact infection rates in the normal population cannot be determined accurately. Additionally, reliable detection of HPV infection is hardly possible. The only reliable detection of HPV infection is DNA detection in the infected tissue. Additionally, anti-HPV16 antibody titers in the blood can be determined as surrogate marker, however, seroconversion of infected individuals does not necessarily occur. Even women with HPV16^{pos} or HPV18^{pos} cervical lesions do only develop anti-HPV-antibodies in about 60% of cases (Porras, Bennett et al. 2010).

4.3.3 Correlation between HPV16-specific naïve and memory T cell frequencies

Although all HPV16^{pos} HNSCC patients showed an HPV16-reactive memory response the question remains why some donors showed a strikingly stronger effector memory response than others? Recent publications provided growing evidence that the T cell response is directly proportional to the antigen-specific naïve T cell pool. In detail, the size of the naïve T cell pool for one particular epitope is correlated to the size of the resulting memory T cell response against this epitope, both in mouse (Moon, Chu et al. 2007, Kotturi, Scott et al. 2008, Obar, Khanna et al. 2008) and human (Kwok, Tan et al. 2012). Kwok et al. (Kwok, Tan et al. 2012) determined frequencies of naïve T cell precursors for different epitopes of *Bacillus anthracis*, to which individuals normally have no contact, and correlated those frequencies to frequencies of *Bacillus anthracis*-specific memory T cells in vaccinated subjects. In the study presented here, a positive correlation of naïve and memory HPV16-reactive T cell frequencies in the HPV16^{pos} HNSCC patients at time of surgery was found. Our data cannot be directly compared to the published data, as frequencies of naïve T cells were determined in already infected individuals in contrast to individuals before antigen contact as in the study of Kwok et al. According to the classical model of T cell development a naïve T cell encounters its antigen and differentiates into a memory T cell and is therefore lost from the naïve repertoire. Consequently, memory formation would go along with a decrease in antigen-specific naïve T cell frequencies. However, a naïve T cell bearing one

particular specificity undergoes homeostatic proliferation and therefore builds up a small clonal population bearing the exactly same TCR. Not all members of this clonal population undergo differentiation at once, but only a subset of naïve T cells gets activated and is therefore "lost" from the naïve repertoire. Intriguingly, naïve HPV16-reactive T cells were not detectable in HPV16^{pos} follow-up patients, maybe indicating that with prolonged time of infection the whole naïve repertoire is recruited to the memory T cell compartment. Activation and differentiation of naïve antigen-specific T cells by encounter of the epitope-presenting DC in a lymphatic tissue is most likely a stochastic process. Single-cell cloning and TCR sequencing of the naïve and memory T cells could give interesting insights into this issue. As only five HPV16^{pos} HNSCC patients could be included in this analysis, no conclusive prove for an existing correlation between HPV16-specific T cell precursor numbers and memory formation in HPV16^{pos} HNSCC patients can be provided. However, the discrepancy in HPV16-specific precursor numbers could be one of the factors affecting the strength of HPV16-specific immunity in tumor patients.

An appealing question is whether the frequency of HPV16-reactive T cells in the periphery is related to clinical outcome or relapse-free survival of patients? However, the follow-up time of the patients included at time of surgery was only a few months and all patients were alive and without relapse at the endpoint of this study. Therefore, no correlation can be drawn in the course of this study. Knowledge about such a correlation would be of prognostic value for patients treated with conventional therapies and also novel immunotherapeutic interventions.

4.3.4 *In vitro* generation of HPV16-reactive T cell populations from blood and tumor

Propagation of HPV16-reactive T cell lines was performed in this study to: Firstly, enable investigation on the functionality of CD8^{+} HPV16-reactive T cell pool in the blood, which was possible only in a restricted way with the ARTE approach; secondly, to extend the analysis to T cells in the tumor lesions, and thirdly, to examine, whether blood or tumor tissue are suitable sources for functional HPV16-reactive T cell populations for adoptive immunotherapy. Strikingly, functional HPV16-reactive T cells could be expanded from the tumor tissue and from blood of all HPV16^{pos} HNSCC patients. Expansion of HPV16-reactive T cell from blood of oropharyngeal cancer patients was previously reported by Ramos et al. (Ramos, Narala et al. 2013), who used a traditionally approach including DC preparation and weekly antigen restimulation of PBMC. With this approach they were able to expand HPV16-reactive T cells from 73% of HPV16^{pos} oropharyngeal cancer patients. *Ex vivo* no HPV16-reactive T cells were detected when PBMC of HNSCC patients were incubated with 15-mer peptides. Ramos et al. claim that this is due to an anergized state of the HPV16-reactive T

cells in cancer patients. However, another reason could be the limited sensitivity of the used assay, as an IFN-γ ELISpot was used, which was accounted to be positive when >10 spots were detected in 10^5 PBMC. However, the frequency of HPV16-reactive T cells as determined with ARTE was about 2×10^{-5} within CD4+ T cells in high responders and IFN-γ production was detected in approximately 30% of these HPV16-reactive CD4+ T cells; this accounts for "only" one IFN-γ producing CD4+ T cell in about 1.5×10^5 CD4+ T cells, so less than one HPV16-reactive IFN-γ producing CD4+ T cells in 1×10^5 PBMC. The frequency of CD8+ HPV16-reactive T cells did not seem to be strikingly higher in most HPV16pos HNSCC patients. Consequently, frequencies of HPV16-specific IFN-γ-producing T cells are too low to be detected with the IFN-γ ELISpot, as used in the Ramos et al study. Ramos et al. claim that HPV16-reactive T cells need to be reactivated *in vitro* by addition of cytokines (IL-6, IL-7, IL-12, and IL-15), which then enabled them to generate T cell cultures containing up to 7% of T cells showing HPV16-specific IFN-γ production after five rounds of weekly antigen-specific restimulation. This *in vitro* assay most probably just amplified the number of HPV16-specific T cells, rather than re-activating them, and thus allowed their detection after expansion. In the study presented here the functionality of HPV16-specific T cells was clearly demonstrated *ex vivo*.

Expansion of TIL from tumor tissue for clinical use has been initially established at the National Institute of Health (NIH, (Dudley, Wunderlich et al. 2003)). A protocol adapted to this established technique was also used in this study. In contrast to the protocol based on enrichment of CD137+ cells after HPV16 peptide pool stimulation, the classical NIH protocol without enrichment only resulted in substantial propagation of HPV16-reactive TIL in one patient. We conclude that the protocol for antigen-specific T cell expansion established in this study is feasible to selectively expand HPV16-reactive T cells also from tumor material.

Few studies have, until now, dealt with the selective expansion of tumor-reactive TIL populations. pHLA tetramer selection of epitope specific T cells based on mutations found in individual melanoma patients demonstrates a novel appealing approach for personalized adoptive therapy treatment with a highly tumor-specific T cell product (Heemskerk, Kvistborg et al. 2013, Van Rooij, Van Buuren et al. 2013). However, this elaborate approach might be too laborious and cost intensive for clinical routine. More general approaches using enrichment strategies based on enrichment of activation marker expressing T cells have been introduced recently. Such enrichment strategies can, on the one hand, be used to enrich *in vivo* preactivated T cells to enrich the whole population of presumably *in vivo* tumor-reactive T cells. Or, on the other hand, also TAA-reactive T cells can be enriched after *in vitro* stimulation using peptides, as demonstrated in this study.

Enrichment of tumor-reactive TIL via the activation marker CD137 was recently described in a melanoma mouse model (Ye, Song et al. 2014). Ye et al. also exemplarily proved in an *in vitro* model that enrichment of TAA-specific T cells is feasible. *In vitro* stimulation of established MART-1-specific TIL cell lines with MART-1 expressing melanoma cell lines resulted in CD137 expression in all MART-1-MHCI tetramer^{+} TIL. Furthermore, enhanced tumor control of CD137^{pos} fraction compared to CD137^{neg} fraction after 7 days of expansion in a mouse xenograft model was detected.

Another marker which proved to be suitable to enrich the overall tumor-reactive CD8^{+} TIL was found to be PD-1 (CD279) (Inozume, Hanada et al. 2010). Rosenberg et al (Gros, Robbins et al. 2014), who were the first to report on sorting of TIL subsets of human melanoma, found both CD137^{+} and PD-1^{+} enriched populations to contain many tumor-reactive T cells. In detail, they clearly showed that PD-1^{+} CD137^{+} TIL contained higher percentages of tumor-reactive TIL compared to PD1^{+} CD137^{-} TIL. In line, sorting of CD137^{+} PD-1^{+}, CD137^{+} PD-1^{-}, and CD137^{-} PD-1^{+} TIL done by Ye et al. (Ye, Song et al. 2014) revealed that CD137^{-} PD-1^{+} TIL show diminished *in vitro* reactivity against target tumor cell lines compared to CD137^{+} PD-1^{+} and CD137^{+} PD-1^{-} sorted TIL. However as CD137 is only expressed on a tiny fraction of CD8^{+} melanoma cells (mean 10.8%) compared to PD-1 (mean 32.4%), CD137^{+} cells representing a subpopulation of PD-1^{+} CD8^{+} TIL. Rosenberg et al. therefore claimed that CD137 as marker misses a large proportion of tumor-reactive T cells as sorted PD-1^{+} CD137^{-} TIL also contained tumor-reactive T cells. Consequently, they postulated that PD-1 is a better marker for enrichment of CD8^{+} tumor-reactive T cells compared to CD137.

Different tumor entities have different expression patterns of CD137 and/or PD-1, which might be crucial for the decision which enrichment strategy should be chosen. In TIL of dissociated HNSCC tumor tested in this study 4 – 25% of CD4^{+} (mean 10.0%) and 1 – 7.2% of CD8^{+} (mean 2.7%) TIL expressed CD137. PD-1 expression was observed on 20 – 70% of CD4^{+} TIL (mean 48%) and 35 – 85% of CD8^{+} TIL (mean 58%), indicating that PD-1 expression on T cells in HNSCC tumors is higher than in melanoma tissue. For HNSCC tumors enrichment of PD-1^{+} TIL might be redundant, as the majority of TIL express PD-1 without sorting. In line with data for melanoma, CD137 is only expressed on a minority of TIL in HNSCC tumors and therefore enrichment of CD137^{+} cells selects for a small subpopulation of T cells. Data of Rosenberg et al. proved that the CD137^{+} TIL subpopulation represents a population containing high amounts of effective tumor-reactive T cells. Only drawback pointed out by Rosenberg et al. is that some tumor-reactive might be lost in the CD137^{-} fraction and therefore obtained cell numbers after CD137^{+} sorting are lower compared to PD-1^{+} cell selection and too low for clinical application. However, the more specific the T cell product is the less cells presumably need to be applied. For unsorted TIL,

about 10 – 100x10^9 TIL are given to an adult melanoma patient (Hong, Rosenberg et al. 2010, Dudley, Gross et al. 2013). Therefore, despite this recently published data in melanoma patients, for HNSCC we argue for a usage of the CD137 enrichment and expansion protocol established in this study for the generation of HPV16-specific TIL cultures rather than a PD-1 enrichment approach.

Of note, in contrast to previous studies enrichment of activated CD137$^+$ cells in this study was done after *in vitro* antigen stimulation, thus selecting mostly HPV16-specific TIL. A T cell product, which is highly specific for HPV16-expressing tumor cells, can be achieved after expansion with this enrichment approach.

4.3.5   Cytotoxicity of expanded HPV16-reactive T cells from blood and tumor

Expanded CD4$^+$ and CD8$^+$ T cells showed cytotoxic potential towards HPV16 E6 and E7 peptide loaded autologous peripheral blood cells. Additionally, cytotoxicity against autologous tumor cells was shown for T cells obtained from both blood and tumor tissue of two HPV^{pos} HNSCC patients. However, such autologous tumor cells could only be grown efficiently for these two HNSCC donors. For both cytotoxic potential against loaded APC and autologous tumor cells seems to be higher for T cells grown from blood compared to T cells grown from tumor tissue (Patient 8 and 23). This higher cytotoxic potential might be due to differences in differentiation status of expanded T cells, as end-differentiated T cells can have diminished effector functions. However, phenotypic analysis after expansion did not reveal striking differences in differentiation status of T cell obtained from blood compared to T cells expanded from tumor tissue.

4.3.6   Role of T$_{reg}$ in activation and expansion of HPV16-specific T cells

In healthy donors TAA-specific effector T cells could be efficiently enriched and expanded from blood of healthy donors and the presence and enrichment of activated T$_{reg}$ did not result in diminished activation and expansion of antigen-specific effector T cells (see section 3.1.2). However, for the enrichment of HPV16-reactive T cells via the CD137 enrichment and expansion protocol from tumor tissue T$_{reg}$ might indeed be an issue. Within the tumor tissue not only HPV16-specific effector T cells but also HPV16-specific T$_{reg}$ might be selectively enriched and T$_{reg}$ mediated effector T cell inhibition is most likely a mechanism of major importance within HNSCC tumors. For one patient sample depletion of CD25$^+$ cells, which include T$_{reg}$, resulted in substantially enhanced antigen-specific stimulation. Most likely high T$_{reg}$ frequencies are responsible for inhibition of activation of HPV16-specific effector T cells. Interestingly, also the expansion of CD137 enriched effector TIL was much stronger when

CD25$^+$ cells were depleted before stimulation. This is in stark contrast to results observed for CD137 enrichment and expansion of T cells from PBMC of healthy donors where CD25 depletion did not result in changed expansion rates. Therefore, a depletion of CD25$^+$ cells is strongly recommend when HPV16-specific T cells are enriched via the CD137 enrichment and expansion protocol from HPV16^{pos} HNSCC tumors.

4.3.7 Quantity and quality of T cell immunity in tumor lesions

To what extent peripheral HPV16-directed immunity is connected to intratumoral immunity and prognosis is not well established so far. For cervical carcinoma it was shown that patients with a systemic HPV16-specific T_H response have higher numbers of CD8$^+$ T cells infiltrating the tumor and higher CD8$^+$ to T_{reg} ratios (Piersma, Jordanova et al. 2007). Furthermore, higher CD8$^+$ T cell infiltration and higher CD8$^+$ to T_{reg} ratios were correlated to the absence of metastases. Likewise, for HNSCC patients a positive correlation of CD8$^+$ to T_{reg} ratio with prognosis of HNSCC patients was reported (Watanabe, Katou et al. 2010, Nasman, Romanitan et al. 2012), but a clear correlation of systemic HPV16-directed immunity to favorable prognosis is missing so far. In this study no statistically significant differences in overall T cell infiltration between the HPV16^{pos} HNSCC low and high responders were detected. Nevertheless, higher CD8$^+$ to T_{reg} cell ratios, higher levels of activated TIL, higher levels of MHC class I expressing tumor cells, and higher IFN-γ to IL-10 ratios in tumor supernatants observed for high responder HPV16^{pos} patients hint at a favorable cell composition of tumors of high responder patients and an on-going anti-tumor response in those patients compared to low responder HPV16^{pos} patients.

4.3.8 Comparison of HPV16-reactive T cell immunity in the blood and tumor

The results strongly suggest that the HPV16-directed T cell immunity detected in the blood reflects HPV16-directed immunity within the tumor tissue. Firstly, favorable T cell composition and elevated T cell activity within the tumor was detected in HPV16^{pos} high responder HNSCC patients. Secondly, data from *ex vivo* detection of HPV16-reactive T cells from the blood (ARTE) show the same skewing of the ratio of CD4$^+$ to CD8$^+$ T cells of the HPV16-directed T cell response as seen within TIL. Thirdly, data on composition of CD4$^+$ and CD8$^+$ T cell response against both HPV16 E6 and E7 antigen reveal the presence of the same specificities in T cell cultures obtained from blood and tumor tissue. Accordingly, we hypothesize that peripheral HPV16-directed T cell immunity reflects intratumoral T cell immunity. However, our data also suggest that certain tumor-antigen-specific T cells are enriched in the tumor tissue as also suggested recently (Tjin, Krebbers et al. 2014). On the

one side, the magnitude of the different HPV16 antigen responses was rather different between T cells from PBMC and tumor after expansion. On the other side, only low frequencies of HPV16-reactive T cells were detected in the blood of two HPV16^{pos} HNSCC patients, but nonetheless HPV16-reactive T cells could be expanded from tumor tissue.

In line with earlier studies in HNSCC patients (Heusinkveld, Goedemans et al. 2012, Ramos, Narala et al. 2013), a bias towards CD4^{+} T cells directed against HPV16 in both blood and tumor tissue was detected. CD4^{+} TIL can exert an anti-tumor effect (Tran, Turcotte et al. 2014), but correlations of presence of TIL with better prognosis have mostly be drawn for CD8^{+} TIL, which might be partially due to the fact that many studies did not discriminate between CD4^{+} T_{eff} and T_{reg}. Only one of the five tested donors in this study showed a strong HPV16-directed CD8^{+} T cell response in the blood and in the tumor. Why, for example, the other two high responder HPV16^{pos} HNSCC patients did not mount an HPV16-directed CD8^{+} T cell response is not clear.

Collectively, this data suggest that the tumor-specific T cell repertoire in blood represents tumor-specific TILs in quality, but not necessarily in quantity. In the future, examination of clonotypes from both, blood and tumor tissue, could reveal more precise insight into the relationship of the HPV16-directed T cell repertoires at both sites.

4.3.9 Immunosuppressive conditions in HNSCC tumors

Activation of effector T cells due to tumor-recognition is a critical step for a successful *in vivo* anti-tumor immunity. Especially HPV16-induced tumors are known to evade host immunity by a multitude of mechanisms. One of them is the interference of viral proteins with the antigen-presentation machinery in host (tumor) cells, thereby preventing recognition through tumor-specific T cells. The E7 protein of HPV high-risk types was shown to down-regulate the expression of HLA class I molecules on the surface of tumor cells (Li, Deng et al. 2010). In this study elevated expression of MHC class I on tumor cells obtained from HPV16^{pos} high responder HNSCC patients was found. This difference in antigen-presentation of the tumor cells could either be a reason for the stronger immune response detected in these patients or, more likely, a consequence of an on-going T cell mediated anti-tumor response as IFN-γ, released by activated T cells, triggers the up-regulation of MHC class I molecules on tumor cells (Lopez-Albaitero, Nayak et al. 2006). These three high responder patients also showed high CD8^{+} to T_{reg} ratios, further supporting that in these tumors a higher T cell response is on-going. These data hint at a favorable T cell composition in the high responder patients, where effector T cells are able to partially overcome T_{reg} suppression. High CD8^{+} to T_{reg} ratios have been positively correlated to a good prognosis in HNSCC (Watanabe, Katou et al. 2010, Nasman, Romanitan et al. 2012). However, our small patient cohort does not allow any

conclusive statements concerning a favorable outcome of these high responder patients, especially as at closing of this study all patients were in complete remission and no relapse had occurred.

We and others detected prominent immunosuppressive conditions within the tumor. In general tumors, and HPV16^{pos} tumors in particular, are able to create a prominent immunosuppressive microenvironment within the tumor tissue. Strong IL-10 production could be detected in supernatants of dissociated HPV16^{pos} HNSCC tumors, which hints at an unfavorable, immunosuppressive cytokine profile probably affecting the effector functions of the resident TIL. Higher IFN-γ to IL-10 ratios in tumor supernatants of HPV16^{pos} high responder patients compared to HPV16^{pos} low responder patients further argues for a stronger intratumoral immune response in the high responder patients. The magnitude of immunosuppression might vary in different patients and lead to a different strength in T cell impairment. Furthermore, evidence was provided that CD25^{+} cells, which include CD4^{+} CD25^{+} FoxP3^{+} regulatory T cells, are responsible for a strong suppression of HPV16-reactive T cell response, because removal of CD25^{+} cells enhances IFN-γ release and expansion of specific T cells *in vitro.* These data are in line with other publications reporting a strong immunosuppressive environment in HPV16-positive HNSCC tumors. The immunosuppressive mechanisms most likely hinder the strong HPV16-specific immunity detected in some HPV16^{pos} HNSCC patients to fight the infected tumor cells.

Collectively, a functional HPV16-directed T cell immunity was detected *ex vivo* in both blood and tumor of HPV16^{pos} HNSCC patients. Functionality of tumor resident HPV16-directed T cells might be impaired due to strong immunosuppressive mechanisms. However, functionality can be restored by weakening immunosuppression or removal of the T cells from the suppressive tumor microenvironment.

4.3.10 Implications on immunotherapeutic approaches

In vivo anti-tumor reactivity of the *ex vivo* and *in vitro* detected HPV16-directed TIL seems to be limited in the patients, as the tumor was able to grow. Strikingly, functionally HPV16-reactive T cells can be expanded from the tumor tissue *in vitro*, probably due to removal of the T cells from their suppressive tumor environment, as suggested earlier (Ramos, Narala et al. 2013, Tjin, Krebbers et al. 2014). These immunosuppressive conditions need to be taken into consideration for immune therapy and argue for implementation of combinational therapy. One compelling option would be the combination of immunotherapeutic interventions like vaccination or adoptive transfer of HPV16-specific T cells subsequent to conventional interventions like chemo- or radiotherapy, to partially destroy the compact tumor

microcosm. C. Melief's group already provided first evidence for an enhanced CD8^{+} T cell activity in a mouse cervical cancer model when treated with a combined chemo-immunotherapy including vaccination and cisplatin treatment (Van der Sluis T.C. 2014). Furthermore, it was shown that HPV16^{pos} tumor patients respond better to chemotherapy and combined chemo-radiation therapy (Fakhry, Westra et al. 2008), probably as a partial disruption of the tumor microenvironment by the conventional therapies helps the existent HPV16-directed immunity of the patients to become active in tumor cell defense and provide prolonged protection against relapse.

For pre-stages of cervical cancer exciting results have been achieved using a combination of therapeutic vaccination using a HPV16 E6E7L2 fusion protein and the immunmodulator imiquimod, with this treatment 63% of the women showed complete regression. These responder patients also showed an increased local T cell infiltration, whereas non-responders had higher infiltration of T_{reg} cells in the lesion (Daayana, Elkord et al. 2010).

For one patient sample it could be shown that depletion of CD25^{+} cells lead to an increased TIL *in vitro*. Therefore, strategies to reduce immunosuppression via CD25^{+} cells are especially promising for therapy in HPV16^{pos} HNSCC. Different strategies have been implemented in the past to address the issue of T_{reg}-mediated immunosuppression in cancer patients. Firstly, T_{reg} can be targeted *in vivo* by an antibody, which blocks IL-2 binding to the IL-2 receptor. Such an anti-CD25 antibody (PC61) was shown to reduce infiltration of T_{reg} cells into tumor lesions in mice and thus provides a compelling approach (Onizuka, Tawara et al. 1999). First clinical trials in humans were done using the Food and Drug Administration (FDA)-approved anti-CD25 antibody daclizumab in brain (Sampson, Schmittling et al. 2012) and breast cancer (Rech, Mick et al. 2012). These pilot-studies demonstrated that human T_{reg} can be safely and selectively depleted *in vivo* with daclizumab and indicated a higher immune response rate to vaccination in daclizumab-treated patients. Secondly, cyclophosphamide, used frequently for chemotherapy, was shown to selectively deplete T_{reg} cells in the periphery of cancer patients when applied in low-doses (Ghiringhelli, Menard et al. 2007, Walter, Weinschenk et al. 2012, Heylmann, Bauer et al. 2013). Thirdly, genetically engineered TGF-β-resistant CTL, carrying a malfunctional TGF-β receptor, have been shown to resist the inhibitory effects of tumor-derived TGF-β *in vitro* and *in vivo* (Foster, Dotti et al. 2008).

A skewing of the HPV16-directed immunity rather towards CD4^{+} T cells than CD8^{+} CTLs in some HPV16^{pos} HNSCC patients was detected in this and previous studies (Ramos, Narala et al. 2013) and should be considered when immunotherapeutic interventions are designed. Consequentially, vaccination approaches might be favorable, which focus on the induction of a CD8^{+} T cell response, e.g. through co-administration of DNA encoded antigen or a

xenogenic MHC molecule, which presumably enhances efficient cross-presentation (Kang, Chung et al. 2010). Intriguingly, immunotherapy using CD4$^+$ T cells in epithelial cancer (Tran, Turcotte et al. 2014) has clearly proven the anti-tumor function of CD4$^+$ T cells. However, the exact mechanism of action of those anti-tumor CD4$^+$ T cells remains elusive. Several mechanisms have been described. Firstly, co-activation of CD8$^+$ T cells (Matthew 2012 CancerRes); secondly, recruitment of innate immune cells, such as macrophages (Corthay, Skovseth et al. 2005) and NK cells (Perez-Diez, Joncker et al. 2007); thirdly, direct cytotoxicity of CD4$^+$ T cells (Paludan, Bickham et al. 2002). The latter is hampered by the fact that MHC class II expression is restricted to professional APC, however, other cells are capable of upregulating MHC class II upon pathogen challenge. MHC class II upregulation was reported for epithelial cells when they are activated by infection (Debbabi, Ghosh et al. 2005) or IFN-γ-mediated signals (Cunningham, Zhang et al. 1997).

The obtained results on expansion of blood- and tumor-derived HPV16-reactive T cells in this study strongly argue for the implementation of a CD137 enrichment approach for the generation of a HPV16-targeted T cell product for adoptive T cell transfer to HPV16^{pos} patients. However, CD25$^+$ cell depletion seems to be mandatory to ensure efficient stimulation and expansion of such isolated HPV16-reactive T cells. Which tissue source should be used of generation of HPV16-specific T cells for adoptive therapy of HPV16^{pos} HNSCC patients, blood or tumor? Considering the here presented results both sources are suitable for the generation of HPV16-reactive T cells. However, HPV16-reactive T cells from the blood might have a better anti-tumor function, as they showed higher cytotoxic capacity compared to tumor-derived HPV16-reactive T cells in most patients. Furthermore, enrichment of T_{reg} might be of minor importance when peripheral T cells are enriched compared to tumor-resident T cells. Additionally, generating these HPV16-reactive T cells from blood provides a compelling opportunity as the approach can lead to a cell product faster, as higher starting T cell numbers can be obtained from blood compared to tumor.

In summary, the study shows that a HPV16-directed, functional peripheral and intratumoral T cell immunity exists in HPV16^{pos} patients, which argues for their clinical usage. Based on the obtained results a combinational therapy is favored, as strong immunosuppressive mechanisms in the HNSCC tumor need to be overcome to facilitate functional anti-tumor T cell responses.

4.4 Juxtaposition of WT1-specific T cells and HPV16-specific T cells

The main aim of this study was to characterize WT1- and HPV16-specific T cells regarding their use in immunotherapeutic approaches. Additionally, it also allows a direct comparison of WT1- and HPV16-specific T cells, which are expected to bear distinct features, as these two tumor-associated antigens are of different origin, WT1 being a self-antigen and HPV16 E6 and E7 being viral antigens. Surprisingly, in most healthy donors CD4$^+$ T cells specific for both antigens were found in similar frequencies. For HPV16 some donors (3 of 32 healthy individuals) had extraordinary high frequencies of CD4$^+$ HPV16-specific T cells (>1x10^{-5} within CD4$^+$ T cells), most probably resulting from an (non-persistent) infection with HPV16. Interestingly, concerning the differentiation status of the T cells, in healthy donors the frequency of individuals bearing CD4$^+$ memory T cells was higher for WT1 (65% of healthy donors) compared to HPV16 (50% of healthy donors). For HPV16 this frequency probably represents the frequency of healthy individuals, which have been infected with the virus recently. For the self-antigen WT1 we suggest other mechanisms to be responsible for memory formation, such as cross-reactivity to environmental antigens.

Both antigens have proven to be immunogenic in cancer patients and therefore provide favorable targets for immunotherapeutic approaches. In this study a novel, straight-forward protocol, based on antigen-specific stimulation and enrichment of CD137$^+$ cells, for the efficient propagation of WT1- and HPV16-specific T cells was established, which has great potential for clinical implementation. For both antigens functional and non-exhausted specific T cells could be expanded from blood of healthy individuals. HPV16-specific T cells were additionally expanded from blood and tumor tissue of HPV16^{pos} HNSCC patients. We suggest to use this established expansion protocol for the generation of WT1-specific T cells from healthy stem-cell donors for infusion into leukemia patients after hematopoietic stem cell transplantation to prevent or treat relapse. HPV16-specific T cells can be expanded using our protocol for adoptive HPV16-specific T cell transfer in HPV16^{pos} HNSCC patients after easing the suppressive milieu of the tumors or after tumor resection. For the design of therapeutic vaccination approaches our study also bears valuable insights, as a detailed *ex vivo* analysis of WT1- and HPV16-specific T cells is provided. The broad presence of WT1-specific T cells and their high functional avidity clearly argue for the use of peptide pool- or DNA-based WT1 vaccination as supplemental therapy in leukemia. Therapeutic HPV16 vaccination in HPV16^{pos} HNSCC also present a compelling therapy option when combined with other interventions. Results of currently ongoing clinical trials will give more insights. Furthermore, the here presented highly sensitive detection methods can be implemented for a sensitive monitoring of patients during vaccination and other immunotherapeutic interventions.

5 References

Adamopoulou, E., S. Tenzer, N. Hillen, P. Klug, I. A. Rota, S. Tietz, M. Gebhardt, S. Stevanovic, H. Schild, E. Tolosa, A. Melms and C. Stoeckle (2013). "Exploring the MHC-peptide matrix of central tolerance in the human thymus." <u>Nat Commun</u> **4**: 2039.

Alanio, C., F. Lemaitre, H. K. Law, M. Hasan and M. L. Albert (2010). "Enumeration of human antigen-specific naive CD8+ T cells reveals conserved precursor frequencies." <u>Blood</u> **115**(18): 3718-3725.

Albers, A., K. Abe, J. Hunt, J. Wang, A. Lopez-Albaitero, C. Schaefer, W. Gooding, T. L. Whiteside, S. Ferrone, A. DeLeo and R. L. Ferris (2005). "Antitumor activity of human papillomavirus type 16 E7-specific T cells against virally infected squamous cell carcinoma of the head and neck." <u>Cancer Res</u> **65**(23): 11146-11155.

Allan, S. E., S. Q. Crome, N. K. Crellin, L. Passerini, T. S. Steiner, R. Bacchetta, M. G. Roncarolo and M. K. Levings (2007). "Activation-induced FOXP3 in human T effector cells does not suppress proliferation or cytokine production." <u>Int Immunol</u> **19**(4): 345-354.

Arstila, T. P., A. Casrouge, V. Baron, J. Even, J. Kanellopoulos and P. Kourilsky (1999). "A direct estimate of the human alphabeta T cell receptor diversity." <u>Science</u> **286**(5441): 958-961.

Bacher, P., O. Kniemeyer, A. Schonbrunn, B. Sawitzki, M. Assenmacher, E. Rietschel, A. Steinbach, O. A. Cornely, A. A. Brakhage, A. Thiel and A. Scheffold (2014). "Antigen-specific expansion of human regulatory T cells as a major tolerance mechanism against mucosal fungi." <u>Mucosal Immunol</u> **7**(4): 916-928.

Bacher, P., C. Schink, J. Teutschbein, O. Kniemeyer, M. Assenmacher, A. A. Brakhage and A. Scheffold (2013). "Antigen-reactive T cell enrichment for direct, high-resolution analysis of the human naive and memory Th cell repertoire." <u>J Immunol</u> **190**(8): 3967-3976.

Bachireddy, P., U. Hainz, M. Rooney, O. Pozdnyakova, J. Aldridge, W. Zhang, X. Liao, F. S. Hodi, K. O'Connell, W. N. Haining, N. R. Goldstein, C. M. Canning, R. J. Soiffer, J. Ritz, N. Hacohen, E. P. Alyea, 3rd, H. T. Kim and C. J. Wu (2014). "Reversal of in situ T-cell exhaustion during effective human antileukemia responses to donor lymphocyte infusion." <u>Blood</u> **123**(9): 1412-1421.

Bachmann, M. F., M. Barner, A. Viola and M. Kopf (1999). "Distinct kinetics of cytokine production and cytolysis in effector and memory T cells after viral infection." <u>Eur J Immunol</u> **29**(1): 291-299.

Badoual, C., S. Hans, N. Merillon, C. Van Ryswick, P. Ravel, N. Benhamouda, E. Levionnois, M. Nizard, A. Si-Mohamed, N. Besnier, A. Gey, R. Rotem-Yehudar, H. Pere, T. Tran, C. L. Guerin, A. Chauvat, E. Dransart, C. Alanio, S. Albert, B. Barry, F. Sandoval, F. Quintin-Colonna, P. Bruneval, W. H. Fridman, F. M. Lemoine, S. Oudard, L. Johannes, D. Olive, D. Brasnu and E. Tartour (2013). "PD-1-expressing tumor-infiltrating T cells are a favorable prognostic biomarker in HPV-associated head and neck cancer." <u>Cancer Res</u> **73**(1): 128-138.

Bains, I., H. M. van Santen, B. Seddon and A. J. Yates (2013). "Models of self-peptide sampling by developing T cells identify candidate mechanisms of thymic selection." <u>PLoS Comput Biol</u> **9**(7): e1003102.

Baird, P. N. and P. J. Simmons (1997). "Expression of the Wilms' tumor gene (WT1) in normal hemopoiesis." <u>Exp Hematol</u> **25**(4): 312-320.

Bais, A. G., I. Beckmann, J. Lindemans, P. C. Ewing, C. J. Meijer, P. J. Snijders and T. J. Helmerhorst (2005). "A shift to a peripheral Th2-type cytokine pattern during the carcinogenesis of cervical cancer becomes manifest in CIN III lesions." J Clin Pathol **58**(10): 1096-1100.

Barber, D. L., E. J. Wherry, D. Masopust, B. Zhu, J. P. Allison, A. H. Sharpe, G. J. Freeman and R. Ahmed (2006). "Restoring function in exhausted CD8 T cells during chronic viral infection." Nature **439**(7077): 682-687.

Barnes, E., S. M. Ward, V. O. Kasprowicz, G. Dusheiko, P. Klenerman and M. Lucas (2004). "Ultra-sensitive class I tetramer analysis reveals previously undetectable populations of antiviral CD8+ T cells." Eur J Immunol **34**(6): 1570-1577.

Belkaid, Y. and K. Tarbell (2009). "Regulatory T cells in the control of host-microorganism interactions (*)." Annu Rev Immunol **27**: 551-589.

Betts, M. R., J. M. Brenchley, D. A. Price, S. C. De Rosa, D. C. Douek, M. Roederer and R. A. Koup (2003). "Sensitive and viable identification of antigen-specific CD8+ T cells by a flow cytometric assay for degranulation." J Immunol Methods **281**(1-2): 65-78.

Betts, M. R., D. A. Price, J. M. Brenchley, K. Lore, F. J. Guenaga, A. Smed-Sorensen, D. R. Ambrozak, S. A. Migueles, M. Connors, M. Roederer, D. C. Douek and R. A. Koup (2004). "The functional profile of primary human antiviral CD8+ T cell effector activity is dictated by cognate peptide concentration." J Immunol **172**(10): 6407-6417.

Bondanza, A., L. Hambach, Z. Aghai, B. Nijmeijer, S. Kaneko, S. Mastaglio, M. Radrizzani, K. Fleischhauer, F. Ciceri, C. Bordignon, C. Bonini and E. Goulmy (2011). "IL-7 receptor expression identifies suicide gene-modified allospecific CD8+ T cells capable of self-renewal and differentiation into antileukemia effectors." Blood **117**(24): 6469-6478.

Bornhauser, M., C. Thiede, U. Platzbecker, A. Kiani, U. Oelschlaegel, J. Babatz, D. Lehmann, K. Holig, J. Radke, S. Tuve, M. Wermke, R. Wehner, H. Jahnisch, M. P. Bachmann, E. P. Rieber, J. Schetelig, G. Ehninger and M. Schmitz (2011). "Prophylactic transfer of BCR-ABL-, PR1-, and WT1-reactive donor T cells after T cell-depleted allogeneic hematopoietic cell transplantation in patients with chronic myeloid leukemia." Blood **117**(26): 7174-7184.

Bourgeois, C., H. Veiga-Fernandes, A. M. Joret, B. Rocha and C. Tanchot (2002). "CD8 lethargy in the absence of CD4 help." Eur J Immunol **32**(8): 2199-2207.

Boyer, S. N., D. E. Wazer and V. Band (1996). "E7 protein of human papilloma virus-16 induces degradation of retinoblastoma protein through the ubiquitin-proteasome pathway." Cancer Res **56**(20): 4620-4624.

Brenchley, J. M., N. J. Karandikar, M. R. Betts, D. R. Ambrozak, B. J. Hill, L. E. Crotty, J. P. Casazza, J. Kuruppu, S. A. Migueles, M. Connors, M. Roederer, D. C. Douek and R. A. Koup (2003). "Expression of CD57 defines replicative senescence and antigen-induced apoptotic death of CD8+ T cells." Blood **101**(7): 2711-2720.

Chapuis, A. G., G. B. Ragnarsson, H. N. Nguyen, C. N. Chaney, J. S. Pufnock, T. M. Schmitt, N. Duerkopp, I. M. Roberts, G. L. Pogosov, W. Y. Ho, S. Ochsenreither, M. Wolfl, M. Bar, J. P. Radich, C. Yee and P. D. Greenberg (2013). "Transferred WT1-reactive CD8+ T cells can mediate antileukemic activity and persist in post-transplant patients." Sci Transl Med **5**(174): 174ra127.

Chattopadhyay, P. K., J. Yu and M. Roederer (2005). "A live-cell assay to detect antigen-specific CD4+ T cells with diverse cytokine profiles." Nat Med **11**(10): 1113-1117.

Chaturvedi, A. K., E. A. Engels, R. M. Pfeiffer, B. Y. Hernandez, W. Xiao, E. Kim, B. Jiang, M. T. Goodman, M. Sibug-Saber, W. Cozen, L. Liu, C. F. Lynch, N. Wentzensen, R. C. Jordan, S. Altekruse, W. F. Anderson, P. S. Rosenberg and M. L. Gillison (2011). "Human papillomavirus and rising oropharyngeal cancer incidence in the United States." J Clin Oncol **29**(32): 4294-4301.

Cheever, M. A., J. P. Allison, A. S. Ferris, O. J. Finn, B. M. Hastings, T. T. Hecht, I. Mellman, S. A. Prindiville, J. L. Viner, L. M. Weiner and L. M. Matrisian (2009). "The prioritization of cancer antigens: a national cancer institute pilot project for the acceleration of translational research." Clin Cancer Res **15**(17): 5323-5337.

Chu, H. H., J. J. Moon, K. Takada, M. Pepper, J. A. Molitor, T. W. Schacker, K. A. Hogquist, S. C. Jameson and M. K. Jenkins (2009). "Positive selection optimizes the number and function of MHCII-restricted CD4+ T cell clones in the naive polyclonal repertoire." Proc Natl Acad Sci U S A **106**(27): 11241-11245.

Cieri, N., B. Camisa, F. Cocchiarella, M. Forcato, G. Oliveira, E. Provasi, A. Bondanza, C. Bordignon, J. Peccatori, F. Ciceri, M. T. Lupo-Stanghellini, F. Mavilio, A. Mondino, S. Bicciato, A. Recchia and C. Bonini (2013). "IL-7 and IL-15 instruct the generation of human memory stem T cells from naive precursors." Blood **121**(4): 573-584.

Clerici, M., M. Merola, E. Ferrario, D. Trabattoni, M. L. Villa, B. Stefanon, D. J. Venzon, G. M. Shearer, G. De Palo and E. Clerici (1997). "Cytokine production patterns in cervical intraepithelial neoplasia: association with human papillomavirus infection." J Natl Cancer Inst **89**(3): 245-250.

Clute, S. C., L. B. Watkin, M. Cornberg, Y. N. Naumov, J. L. Sullivan, K. Luzuriaga, R. M. Welsh and L. K. Selin (2005). "Cross-reactive influenza virus-specific CD8+ T cells contribute to lymphoproliferation in Epstein-Barr virus-associated infectious mononucleosis." J Clin Invest **115**(12): 3602-3612.

Corthay, A. (2009). "How do regulatory T cells work?" Scand J Immunol **70**(4): 326-336.

Corthay, A. (2014). "Does the immune system naturally protect against cancer?" Front Immunol **5**: 197.

Corthay, A., D. K. Skovseth, K. U. Lundin, E. Rosjo, H. Omholt, P. O. Hofgaard, G. Haraldsen and B. Bogen (2005). "Primary antitumor immune response mediated by CD4+ T cells." Immunity **22**(3): 371-383.

Cunningham, A. C., J. G. Zhang, J. V. Moy, S. Ali and J. A. Kirby (1997). "A comparison of the antigen-presenting capabilities of class II MHC-expressing human lung epithelial and endothelial cells." Immunology **91**(3): 458-463.

Daayana, S., E. Elkord, U. Winters, M. Pawlita, R. Roden, P. L. Stern and H. C. Kitchener (2010). "Phase II trial of imiquimod and HPV therapeutic vaccination in patients with vulval intraepithelial neoplasia." Br J Cancer **102**(7): 1129-1136.

de Jong, A., M. I. van Poelgeest, J. M. van der Hulst, J. W. Drijfhout, G. J. Fleuren, C. J. Melief, G. Kenter, R. Offringa and S. H. van der Burg (2004). "Human papillomavirus type 16-positive cervical cancer is associated with impaired CD4+ T-cell immunity against early antigens E2 and E6." Cancer Res **64**(15): 5449-5455.

de la Rosa, M., S. Rutz, H. Dorninger and A. Scheffold (2004). "Interleukin-2 is essential for CD4+CD25+ regulatory T cell function." Eur J Immunol **34**(9): 2480-2488.

de Saint Basile, G., G. Menasche and A. Fischer (2010). "Molecular mechanisms of biogenesis and exocytosis of cytotoxic granules." <u>Nat Rev Immunol</u> **10**(8): 568-579.

Debbabi, H., S. Ghosh, A. B. Kamath, J. Alt, D. E. Demello, S. Dunsmore and S. M. Behar (2005). "Primary type II alveolar epithelial cells present microbial antigens to antigen-specific CD4+ T cells." <u>Am J Physiol Lung Cell Mol Physiol</u> **289**(2): L274-279.

Dudley, M. E., C. A. Gross, R. P. Somerville, Y. Hong, N. P. Schaub, S. F. Rosati, D. E. White, D. Nathan, N. P. Restifo, S. M. Steinberg, J. R. Wunderlich, U. S. Kammula, R. M. Sherry, J. C. Yang, G. Q. Phan, M. S. Hughes, C. M. Laurencot and S. A. Rosenberg (2013). "Randomized selection design trial evaluating CD8+-enriched versus unselected tumor-infiltrating lymphocytes for adoptive cell therapy for patients with melanoma." <u>J Clin Oncol</u> **31**(17): 2152-2159.

Dudley, M. E., J. R. Wunderlich, T. E. Shelton, J. Even and S. A. Rosenberg (2003). "Generation of tumor-infiltrating lymphocyte cultures for use in adoptive transfer therapy for melanoma patients." <u>J Immunother</u> **26**(4): 332-342.

Enouz, S., L. Carrie, D. Merkler, M. J. Bevan and D. Zehn (2012). "Autoreactive T cells bypass negative selection and respond to self-antigen stimulation during infection." <u>J Exp Med</u> **209**(10): 1769-1779.

Fakhry, C., W. H. Westra, S. Li, A. Cmelak, J. A. Ridge, H. Pinto, A. Forastiere and M. L. Gillison (2008). "Improved survival of patients with human papillomavirus-positive head and neck squamous cell carcinoma in a prospective clinical trial." <u>J Natl Cancer Inst</u> **100**(4): 261-269.

Foster, A. E., G. Dotti, A. Lu, M. Khalil, M. K. Brenner, H. E. Heslop, C. M. Rooney and C. M. Bollard (2008). "Antitumor activity of EBV-specific T lymphocytes transduced with a dominant negative TGF-beta receptor." <u>J Immunother</u> **31**(5): 500-505.

Frentsch, M., O. Arbach, D. Kirchhoff, B. Moewes, M. Worm, M. Rothe, A. Scheffold and A. Thiel (2005). "Direct access to CD4+ T cells specific for defined antigens according to CD154 expression." <u>Nat Med</u> **11**(10): 1118-1124.

Frentsch, M., R. Stark, N. Matzmohr, S. Meier, S. Durlanik, A. R. Schulz, U. Stervbo, K. Jurchott, F. Gebhardt, G. Heine, M. A. Reuter, M. R. Betts, D. Busch and A. Thiel (2013). "CD40L expression permits CD8+ T cells to execute immunologic helper functions." <u>Blood</u> **122**(3): 405-412.

Gattinoni, L., E. Lugli, Y. Ji, Z. Pos, C. M. Paulos, M. F. Quigley, J. R. Almeida, E. Gostick, Z. Yu, C. Carpenito, E. Wang, D. C. Douek, D. A. Price, C. H. June, F. M. Marincola, M. Roederer and N. P. Restifo (2011). "A human memory T cell subset with stem cell-like properties." <u>Nat Med</u> **17**(10): 1290-1297.

Ghiringhelli, F., C. Menard, P. E. Puig, S. Ladoire, S. Roux, F. Martin, E. Solary, A. Le Cesne, L. Zitvogel and B. Chauffert (2007). "Metronomic cyclophosphamide regimen selectively depletes CD4+CD25+ regulatory T cells and restores T and NK effector functions in end stage cancer patients." <u>Cancer Immunol Immunother</u> **56**(5): 641-648.

Goldstein, M. J., B. Varghese, J. D. Brody, R. Rajapaksa, H. Kohrt, D. K. Czerwinski, S. Levy and R. Levy (2011). "A CpG-loaded tumor cell vaccine induces antitumor CD4+ T cells that are effective in adoptive therapy for large and established tumors." <u>Blood</u> **117**(1): 118-127.

Goodyear, O. C., G. Pratt, A. McLarnon, M. Cook, K. Piper and P. Moss (2008). "Differential pattern of CD4+ and CD8+ T-cell immunity to MAGE-A1/A2/A3 in patients with monoclonal

gammopathy of undetermined significance (MGUS) and multiple myeloma." Blood **112**(8): 3362-3372.

Gotter, J., B. Brors, M. Hergenhahn and B. Kyewski (2004). "Medullary epithelial cells of the human thymus express a highly diverse selection of tissue-specific genes colocalized in chromosomal clusters." J Exp Med **199**(2): 155-166.

Gros, A., P. F. Robbins, X. Yao, Y. F. Li, S. Turcotte, E. Tran, J. R. Wunderlich, A. Mixon, S. Farid, M. E. Dudley, K. Hanada, J. R. Almeida, S. Darko, D. C. Douek, J. C. Yang and S. A. Rosenberg (2014). "PD-1 identifies the patient-specific CD8(+) tumor-reactive repertoire infiltrating human tumors." J Clin Invest **124**(5): 2246-2259.

Haabeth, O. A., A. A. Tveita, M. Fauskanger, F. Schjesvold, K. B. Lorvik, P. O. Hofgaard, H. Omholt, L. A. Munthe, Z. Dembic, A. Corthay and B. Bogen (2014). "How Do CD4(+) T Cells Detect and Eliminate Tumor Cells That Either Lack or Express MHC Class II Molecules?" Front Immunol **5**: 174.

Haluszczak, C., A. D. Akue, S. E. Hamilton, L. D. Johnson, L. Pujanauski, L. Teodorovic, S. C. Jameson and R. M. Kedl (2009). "The antigen-specific CD8+ T cell repertoire in unimmunized mice includes memory phenotype cells bearing markers of homeostatic expansion." J Exp Med **206**(2): 435-448.

Heemskerk, B., P. Kvistborg and T. N. Schumacher (2013). "The cancer antigenome." EMBO J **32**(2): 194-203.

Heusinkveld, M., R. Goedemans, R. J. Briet, H. Gelderblom, J. W. Nortier, A. Gorter, V. T. Smit, A. P. Langeveld, J. C. Jansen and S. H. van der Burg (2012). "Systemic and local human papillomavirus 16-specific T-cell immunity in patients with head and neck cancer." Int J Cancer **131**(2): E74-85.

Heylmann, D., M. Bauer, H. Becker, S. van Gool, N. Bacher, K. Steinbrink and B. Kaina (2013). "Human CD4+CD25+ regulatory T cells are sensitive to low dose cyclophosphamide: implications for the immune response." PLoS One **8**(12): e83384.

Hinrichs, C. S., Z. A. Borman, L. Cassard, L. Gattinoni, R. Spolski, Z. Yu, L. Sanchez-Perez, P. Muranski, S. J. Kern, C. Logun, D. C. Palmer, Y. Ji, R. N. Reger, W. J. Leonard, R. L. Danner, S. A. Rosenberg and N. P. Restifo (2009). "Adoptively transferred effector cells derived from naive rather than central memory CD8+ T cells mediate superior antitumor immunity." Proc Natl Acad Sci U S A **106**(41): 17469-17474.

Hodi, F. S., S. J. O'Day, D. F. McDermott, R. W. Weber, J. A. Sosman, J. B. Haanen, R. Gonzalez, C. Robert, D. Schadendorf, J. C. Hassel, W. Akerley, A. J. van den Eertwegh, J. Lutzky, P. Lorigan, J. M. Vaubel, G. P. Linette, D. Hogg, C. H. Ottensmeier, C. Lebbe, C. Peschel, I. Quirt, J. I. Clark, J. D. Wolchok, J. S. Weber, J. Tian, M. J. Yellin, G. M. Nichol, A. Hoos and W. J. Urba (2010). "Improved survival with ipilimumab in patients with metastatic melanoma." N Engl J Med **363**(8): 711-723.

Hoffmann, T. K., C. Arsov, K. Schirlau, M. Bas, U. Friebe-Hoffmann, J. P. Klussmann, K. Scheckenbach, V. Balz, H. Bier and T. L. Whiteside (2006). "T cells specific for HPV16 E7 epitopes in patients with squamous cell carcinoma of the oropharynx." Int J Cancer **118**(8): 1984-1991.

Hong, J. J., S. A. Rosenberg, M. E. Dudley, J. C. Yang, D. E. White, J. A. Butman and R. M. Sherry (2010). "Successful treatment of melanoma brain metastases with adoptive cell therapy." Clin Cancer Res **16**(19): 4892-4898.

Hosen, N., Y. Sonoda, Y. Oji, T. Kimura, H. Minamiguchi, H. Tamaki, M. Kawakami, M. Asada, K. Kanato, M. Motomura, M. Murakami, T. Fujioka, T. Masuda, E. H. Kim, A. Tsuboi, Y. Oka, T. Soma, H. Ogawa and H. Sugiyama (2002). "Very low frequencies of human normal CD34+ haematopoietic progenitor cells express the Wilms' tumour gene WT1 at levels similar to those in leukaemia cells." Br J Haematol **116**(2): 409-420.

Hsieh, C. S., H. M. Lee and C. W. Lio (2012). "Selection of regulatory T cells in the thymus." Nat Rev Immunol **12**(3): 157-167.

Inozume, T., K. Hanada, Q. J. Wang, M. Ahmadzadeh, J. R. Wunderlich, S. A. Rosenberg and J. C. Yang (2010). "Selection of CD8+PD-1+ lymphocytes in fresh human melanomas enriches for tumor-reactive T cells." J Immunother **33**(9): 956-964.

Jayaprakash, V., M. Reid, E. Hatton, M. Merzianu, N. Rigual, J. Marshall, S. Gill, J. Frustino, G. Wilding, T. Loree, S. Popat and M. Sullivan (2011). "Human papillomavirus types 16 and 18 in epithelial dysplasia of oral cavity and oropharynx: a meta-analysis, 1985-2010." Oral Oncol **47**(11): 1048-1054.

Joffre, O. P., E. Segura, A. Savina and S. Amigorena (2012). "Cross-presentation by dendritic cells." Nat Rev Immunol **12**(8): 557-569.

Jung, A. C., S. Guihard, S. Krugell, S. Ledrappier, A. Brochot, V. Dalstein, S. Job, A. de Reynies, G. Noel, B. Wasylyk, C. Clavel and J. Abecassis (2013). "CD8-alpha T-cell infiltration in human papillomavirus-related oropharyngeal carcinoma correlates with improved patient prognosis." Int J Cancer **132**(2): E26-36.

Kang, T. H., J. Y. Chung, A. Monie, S. I. Pai, C. F. Hung and T. C. Wu (2010). "Enhancing DNA vaccine potency by co-administration of xenogenic MHC class-I DNA." Gene Ther **17**(4): 531-540.

Kapp, M., S. Stevanovic, K. Fick, S. M. Tan, J. Loeffler, A. Opitz, T. Tonn, G. Stuhler, H. Einsele and G. U. Grigoleit (2009). "CD8+ T-cell responses to tumor-associated antigens correlate with superior relapse-free survival after allo-SCT." Bone Marrow Transplant **43**(5): 399-410.

Keilholz, U., A. Letsch, A. Busse, A. M. Asemissen, S. Bauer, I. W. Blau, W. K. Hofmann, L. Uharek, E. Thiel and C. Scheibenbogen (2009). "A clinical and immunologic phase 2 trial of Wilms tumor gene product 1 (WT1) peptide vaccination in patients with AML and MDS." Blood **113**(26): 6541-6548.

Kenter, G. G., M. J. Welters, A. R. Valentijn, M. J. Lowik, D. M. Berends-van der Meer, A. P. Vloon, F. Essahsah, L. M. Fathers, R. Offringa, J. W. Drijfhout, A. R. Wafelman, J. Oostendorp, G. J. Fleuren, S. H. van der Burg and C. J. Melief (2009). "Vaccination against HPV-16 oncoproteins for vulvar intraepithelial neoplasia." N Engl J Med **361**(19): 1838-1847.

Kershaw, M. H., J. A. Westwood and P. K. Darcy (2013). "Gene-engineered T cells for cancer therapy." Nat Rev Cancer **13**(8): 525-541.

Kim, R., M. Emi and K. Tanabe (2007). "Cancer immunoediting from immune surveillance to immune escape." Immunology **121**(1): 1-14.

Kitawaki, T., N. Kadowaki, K. Fukunaga, Y. Kasai, T. Maekawa, K. Ohmori, T. Kondo, R. Maekawa, M. Takahara, M. Nieda, K. Kuzushima, T. Ishikawa and T. Uchiyama (2011). "A phase I/IIa clinical trial of immunotherapy for elderly patients with acute myeloid leukaemia using dendritic cells co-pulsed with WT1 peptide and zoledronate." Br J Haematol **153**(6): 796-799.

Klebanoff, C. A., S. E. Finkelstein, D. R. Surman, M. K. Lichtman, L. Gattinoni, M. R. Theoret, N. Grewal, P. J. Spiess, P. A. Antony, D. C. Palmer, Y. Tagaya, S. A. Rosenberg, T. A. Waldmann and N. P. Restifo (2004). "IL-15 enhances the in vivo antitumor activity of tumor-reactive CD8+ T cells." Proc Natl Acad Sci U S A **101**(7): 1969-1974.

Klebanoff, C. A., L. Gattinoni and N. P. Restifo (2012). "Sorting through subsets: which T-cell populations mediate highly effective adoptive immunotherapy?" J Immunother **35**(9): 651-660.

Klein, L., M. Klugmann, K. A. Nave, V. K. Tuohy and B. Kyewski (2000). "Shaping of the autoreactive T-cell repertoire by a splice variant of self protein expressed in thymic epithelial cells." Nat Med **6**(1): 56-61.

Klein, L., B. Kyewski, P. M. Allen and K. A. Hogquist (2014). "Positive and negative selection of the T cell repertoire: what thymocytes see (and don't see)." Nat Rev Immunol **14**(6): 377-391.

Klussmann, J. P., S. J. Weissenborn, U. Wieland, V. Dries, J. Kolligs, M. Jungehuelsing, H. E. Eckel, H. P. Dienes, H. J. Pfister and P. G. Fuchs (2001). "Prevalence, distribution, and viral load of human papillomavirus 16 DNA in tonsillar carcinomas." Cancer **92**(11): 2875-2884.

Kotturi, M. F., I. Scott, T. Wolfe, B. Peters, J. Sidney, H. Cheroutre, M. G. von Herrath, M. J. Buchmeier, H. Grey and A. Sette (2008). "Naive precursor frequencies and MHC binding rather than the degree of epitope diversity shape CD8+ T cell immunodominance." J Immunol **181**(3): 2124-2133.

Krishnadas, D. K., M. M. Stamer, K. Dunham, L. Bao and K. G. Lucas (2011). "Wilms' tumor 1-specific cytotoxic T lymphocytes can be expanded from adult donors and cord blood." Leuk Res **35**(11): 1520-1526.

Krug, L. M., T. Dao, A. B. Brown, P. Maslak, W. Travis, S. Bekele, T. Korontsvit, V. Zakhaleva, J. Wolchok, J. Yuan, H. Li, L. Tyson and D. A. Scheinberg (2010). "WT1 peptide vaccinations induce CD4 and CD8 T cell immune responses in patients with mesothelioma and non-small cell lung cancer." Cancer Immunol Immunother **59**(10): 1467-1479.

Kuball, J., K. de Boer, E. Wagner, M. Wattad, E. Antunes, R. D. Weeratna, A. P. Vicari, C. Lotz, S. van Dorp, S. Hol, P. D. Greenberg, W. Heit, H. L. Davis and M. Theobald (2011). "Pitfalls of vaccinations with WT1-, Proteinase3- and MUC1-derived peptides in combination with MontanideISA51 and CpG7909." Cancer Immunol Immunother **60**(2): 161-171.

Kwok, W. W., V. Tan, L. Gillette, C. T. Littell, M. A. Soltis, R. B. LaFond, J. Yang, E. A. James and J. H. DeLong (2012). "Frequency of epitope-specific naive CD4(+) T cells correlates with immunodominance in the human memory repertoire." J Immunol **188**(6): 2537-2544.

Lauwen, M. M., S. Zwaveling, L. de Quartel, S. C. Ferreira Mota, J. A. Grashorn, C. J. Melief, S. H. van der Burg and R. Offringa (2008). "Self-tolerance does not restrict the CD4+ T-helper response against the p53 tumor antigen." Cancer Res **68**(3): 893-900.

Lee, J. Y., S. E. Hamilton, A. D. Akue, K. A. Hogquist and S. C. Jameson (2013). "Virtual memory CD8 T cells display unique functional properties." Proc Natl Acad Sci U S A **110**(33): 13498-13503.

Lee, Y. K., H. Turner, C. L. Maynard, J. R. Oliver, D. Chen, C. O. Elson and C. T. Weaver (2009). "Late developmental plasticity in the T helper 17 lineage." Immunity **30**(1): 92-107.

Li, W., X. M. Deng, C. X. Wang, X. Zhang, G. X. Zheng, J. Zhang and J. B. Feng (2010). "Down-regulation of HLA class I antigen in human papillomavirus type 16 E7 expressing HaCaT cells: correlate with TAP-1 expression." Int J Gynecol Cancer **20**(2): 227-232.

Liu, W., A. L. Putnam, Z. Xu-Yu, G. L. Szot, M. R. Lee, S. Zhu, P. A. Gottlieb, P. Kapranov, T. R. Gingeras, B. Fazekas de St Groth, C. Clayberger, D. M. Soper, S. F. Ziegler and J. A. Bluestone (2006). "CD127 expression inversely correlates with FoxP3 and suppressive function of human CD4+ T reg cells." J Exp Med **203**(7): 1701-1711.

Lopez-Albaitero, A., J. V. Nayak, T. Ogino, A. Machandia, W. Gooding, A. B. DeLeo, S. Ferrone and R. L. Ferris (2006). "Role of antigen-processing machinery in the in vitro resistance of squamous cell carcinoma of the head and neck cells to recognition by CTL." J Immunol **176**(6): 3402-3409.

Luznik, L. and E. J. Fuchs (2002). "Donor lymphocyte infusions to treat hematologic malignancies in relapse after allogeneic blood or marrow transplantation." Cancer Control **9**(2): 123-137.

Lv, H., E. Havari, S. Pinto, R. V. Gottumukkala, L. Cornivelli, K. Raddassi, T. Matsui, A. Rosenzweig, R. T. Bronson, R. Smith, A. L. Fletcher, S. J. Turley, K. Wucherpfennig, B. Kyewski and M. A. Lipes (2011). "Impaired thymic tolerance to alpha-myosin directs autoimmunity to the heart in mice and humans." J Clin Invest **121**(4): 1561-1573.

Mackall, C. L., T. J. Fry and R. E. Gress (2011). "Harnessing the biology of IL-7 for therapeutic application." Nat Rev Immunol **11**(5): 330-342.

Maslak, P. G., T. Dao, L. M. Krug, S. Chanel, T. Korontsvit, V. Zakhaleva, R. Zhang, J. D. Wolchok, J. Yuan, J. Pinilla-Ibarz, E. Berman, M. Weiss, J. Jurcic, M. G. Frattini and D. A. Scheinberg (2010). "Vaccination with synthetic analog peptides derived from WT1 oncoprotein induces T-cell responses in patients with complete remission from acute myeloid leukemia." Blood **116**(2): 171-179.

Maurer, U., J. Brieger, E. Weidmann, P. S. Mitrou, D. Hoelzer and L. Bergmann (1997). "The Wilms' tumor gene is expressed in a subset of CD34+ progenitors and downregulated early in the course of differentiation in vitro." Exp Hematol **25**(9): 945-950.

Miltenyi, S., W. Muller, W. Weichel and A. Radbruch (1990). "High gradient magnetic cell separation with MACS." Cytometry **11**(2): 231-238.

Moon, J. J., H. H. Chu, M. Pepper, S. J. McSorley, S. C. Jameson, R. M. Kedl and M. K. Jenkins (2007). "Naive CD4(+) T cell frequency varies for different epitopes and predicts repertoire diversity and response magnitude." Immunity **27**(2): 203-213.

Morita, S., Y. Oka, A. Tsuboi, M. Kawakami, M. Maruno, S. Izumoto, T. Osaki, T. Taguchi, T. Ueda, A. Myoui, S. Nishida, T. Shirakata, S. Ohno, Y. Oji, K. Aozasa, J. Hatazawa, K. Udaka, H. Yoshikawa, T. Yoshimine, S. Noguchi, I. Kawase, S. Nakatsuka, H. Sugiyama and J. Sakamoto (2006). "A phase I/II trial of a WT1 (Wilms' tumor gene) peptide vaccine in patients with solid malignancy: safety assessment based on the phase I data." Jpn J Clin Oncol **36**(4): 231-236.

Munoz, N., F. X. Bosch, X. Castellsague, M. Diaz, S. de Sanjose, D. Hammouda, K. V. Shah and C. J. Meijer (2004). "Against which human papillomavirus types shall we vaccinate and screen? The international perspective." Int J Cancer **111**(2): 278-285.

Murphy, K. M. (2011). Immunobiology. United States, Garland Science.

Nasman, A., M. Romanitan, C. Nordfors, N. Grun, H. Johansson, L. Hammarstedt, L. Marklund, E. Munck-Wikland, T. Dalianis and T. Ramqvist (2012). "Tumor infiltrating CD8+ and Foxp3+ lymphocytes correlate to clinical outcome and human papillomavirus (HPV) status in tonsillar cancer." PLoS One **7**(6): e38711.

Neefjes, J., M. L. Jongsma, P. Paul and O. Bakke (2011). "Towards a systems understanding of MHC class I and MHC class II antigen presentation." Nat Rev Immunol **11**(12): 823-836.

Obar, J. J., K. M. Khanna and L. Lefrancois (2008). "Endogenous naive CD8+ T cell precursor frequency regulates primary and memory responses to infection." Immunity **28**(6): 859-869.

Oka, Y., A. Tsuboi, M. Murakami, M. Hirai, N. Tominaga, H. Nakajima, O. A. Elisseeva, T. Masuda, A. Nakano, M. Kawakami, Y. Oji, K. Ikegame, N. Hosen, K. Udaka, M. Yasukawa, H. Ogawa, I. Kawase and H. Sugiyama (2003). "Wilms tumor gene peptide-based immunotherapy for patients with overt leukemia from myelodysplastic syndrome (MDS) or MDS with myelofibrosis." Int J Hematol **78**(1): 56-61.

Oka, Y., A. Tsuboi, T. Taguchi, T. Osaki, T. Kyo, H. Nakajima, O. A. Elisseeva, Y. Oji, M. Kawakami, K. Ikegame, N. Hosen, S. Yoshihara, F. Wu, F. Fujiki, M. Murakami, T. Masuda, S. Nishida, T. Shirakata, S. Nakatsuka, A. Sasaki, K. Udaka, H. Dohy, K. Aozasa, S. Noguchi, I. Kawase and H. Sugiyama (2004). "Induction of WT1 (Wilms' tumor gene)-specific cytotoxic T lymphocytes by WT1 peptide vaccine and the resultant cancer regression." Proc Natl Acad Sci U S A **101**(38): 13885-13890.

Onizuka, S., I. Tawara, J. Shimizu, S. Sakaguchi, T. Fujita and E. Nakayama (1999). "Tumor rejection by in vivo administration of anti-CD25 (interleukin-2 receptor alpha) monoclonal antibody." Cancer Res **59**(13): 3128-3133.

Ott, P. A., F. S. Hodi and C. Robert (2013). "CTLA-4 and PD-1/PD-L1 blockade: new immunotherapeutic modalities with durable clinical benefit in melanoma patients." Clin Cancer Res **19**(19): 5300-5309.

Pala, P., A. Verhoef, J. R. Lamb and P. J. Openshaw (2000). "Single cell analysis of cytokine expression kinetics by human CD4+ T-cell clones during activation or tolerance induction." Immunology **100**(2): 209-216.

Paludan, C., K. Bickham, S. Nikiforow, M. L. Tsang, K. Goodman, W. A. Hanekom, J. F. Fonteneau, S. Stevanovic and C. Munz (2002). "Epstein-Barr nuclear antigen 1-specific CD4(+) Th1 cells kill Burkitt's lymphoma cells." J Immunol **169**(3): 1593-1603.

Pedersen, S. R., M. R. Sorensen, S. Buus, J. P. Christensen and A. R. Thomsen (2013). "Comparison of vaccine-induced effector CD8 T cell responses directed against self- and non-self-tumor antigens: implications for cancer immunotherapy." J Immunol **191**(7): 3955-3967.

Perez-Diez, A., N. T. Joncker, K. Choi, W. F. Chan, C. C. Anderson, O. Lantz and P. Matzinger (2007). "CD4 cells can be more efficient at tumor rejection than CD8 cells." Blood **109**(12): 5346-5354.

Piersma, S. J., E. S. Jordanova, M. I. van Poelgeest, K. M. Kwappenberg, J. M. van der Hulst, J. W. Drijfhout, C. J. Melief, G. G. Kenter, G. J. Fleuren, R. Offringa and S. H. van der Burg (2007). "High number of intraepithelial CD8+ tumor-infiltrating lymphocytes is associated with the absence of lymph node metastases in patients with large early-stage cervical cancer." Cancer Res **67**(1): 354-361.

Pinto, S., D. Sommermeyer, C. Michel, S. Wilde, D. Schendel, W. Uckert, T. Blankenstein and B. Kyewski (2014). "Mis-initiation of intrathymic MART-1 transcription and biased TCR usage explain the high frequency of MART-1-specific T cells." Eur J Immunol.

Pittet, M. J., D. Valmori, P. R. Dunbar, D. E. Speiser, D. Lienard, F. Lejeune, K. Fleischhauer, V. Cerundolo, J. C. Cerottini and P. Romero (1999). "High frequencies of naive Melan-A/MART-1-specific CD8(+) T cells in a large proportion of human histocompatibility leukocyte antigen (HLA)-A2 individuals." J Exp Med **190**(5): 705-715.

Pollok, K. E., Y. J. Kim, Z. Zhou, J. Hurtado, K. K. Kim, R. T. Pickard and B. S. Kwon (1993). "Inducible T cell antigen 4-1BB. Analysis of expression and function." J Immunol **150**(3): 771-781.

Porras, C., C. Bennett, M. Safaeian, S. Coseo, A. C. Rodriguez, P. Gonzalez, M. Hutchinson, S. Jimenez, M. E. Sherman, S. Wacholder, D. Solomon, L. J. van Doorn, C. Bougelet, W. Quint, M. Schiffman, R. Herrero, A. Hildesheim and H. P. V. V. T. G. Costa Rica (2010). "Determinants of seropositivity among HPV-16/18 DNA positive young women." BMC Infect Dis **10**: 238.

Porter, D. L., B. L. Levine, M. Kalos, A. Bagg and C. H. June (2011). "Chimeric antigen receptor-modified T cells in chronic lymphoid leukemia." N Engl J Med **365**(8): 725-733.

Powell, D. J., Jr., M. E. Dudley, P. F. Robbins and S. A. Rosenberg (2005). "Transition of late-stage effector T cells to CD27+ CD28+ tumor-reactive effector memory T cells in humans after adoptive cell transfer therapy." Blood **105**(1): 241-250.

Preuss, S. F., A. Weinell, M. Molitor, M. Stenner, R. Semrau, U. Drebber, S. J. Weissenborn, E. J. Speel, C. Wittekindt, O. Guntinas-Lichius, T. K. Hoffmann, G. D. Eslick and J. P. Klussmann (2008). "Nuclear survivin expression is associated with HPV-independent carcinogenesis and is an indicator of poor prognosis in oropharyngeal cancer." Br J Cancer **98**(3): 627-632.

Prince, M. E., R. Sivanandan, A. Kaczorowski, G. T. Wolf, M. J. Kaplan, P. Dalerba, I. L. Weissman, M. F. Clarke and L. E. Ailles (2007). "Identification of a subpopulation of cells with cancer stem cell properties in head and neck squamous cell carcinoma." Proc Natl Acad Sci U S A **104**(3): 973-978.

Quezada, S. A., T. R. Simpson, K. S. Peggs, T. Merghoub, J. Vider, X. Fan, R. Blasberg, H. Yagita, P. Muranski, P. A. Antony, N. P. Restifo and J. P. Allison (2010). "Tumor-reactive CD4(+) T cells develop cytotoxic activity and eradicate large established melanoma after transfer into lymphopenic hosts." J Exp Med **207**(3): 637-650.

Ramos, C. A., N. Narala, G. M. Vyas, A. M. Leen, U. Gerdemann, E. M. Sturgis, M. L. Anderson, B. Savoldo, H. E. Heslop, M. K. Brenner and C. M. Rooney (2013). "Human papillomavirus type 16 E6/E7-specific cytotoxic T lymphocytes for adoptive immunotherapy of HPV-associated malignancies." J Immunother **36**(1): 66-76.

Ramqvist, T. and T. Dalianis (2010). "Oropharyngeal cancer epidemic and human papillomavirus." Emerg Infect Dis **16**(11): 1671-1677.

Rech, A. J., R. Mick, S. Martin, A. Recio, N. A. Aqui, D. J. Powell, Jr., T. A. Colligon, J. A. Trosko, L. I. Leinbach, C. H. Pletcher, C. K. Tweed, A. DeMichele, K. R. Fox, S. M. Domchek, J. L. Riley and R. H. Vonderheide (2012). "CD25 blockade depletes and selectively reprograms regulatory T cells in concert with immunotherapy in cancer patients." Sci Transl Med **4**(134): 134ra162.

Rezvani, K., J. M. Brenchley, D. A. Price, Y. Kilical, E. Gostick, A. K. Sewell, J. Li, S. Mielke, D. C. Douek and A. J. Barrett (2005). "T-cell responses directed against multiple HLA-A*0201-restricted epitopes derived from Wilms' tumor 1 protein in patients with leukemia and healthy donors: identification, quantification, and characterization." <u>Clin Cancer Res</u> **11**(24 Pt 1): 8799-8807.

Rezvani, K., M. Grube, J. M. Brenchley, G. Sconocchia, H. Fujiwara, D. A. Price, E. Gostick, K. Yamada, J. Melenhorst, R. Childs, N. Hensel, D. C. Douek and A. J. Barrett (2003). "Functional leukemia-associated antigen-specific memory CD8+ T cells exist in healthy individuals and in patients with chronic myelogenous leukemia before and after stem cell transplantation." <u>Blood</u> **102**(8): 2892-2900.

Rezvani, K., A. S. Yong, S. Mielke, B. Jafarpour, B. N. Savani, R. Q. Le, R. Eniafe, L. Musse, C. Boss, R. Kurlander and A. J. Barrett (2011). "Repeated PR1 and WT1 peptide vaccination in Montanide-adjuvant fails to induce sustained high-avidity, epitope-specific CD8+ T cells in myeloid malignancies." <u>Haematologica</u> **96**(3): 432-440.

Rezvani, K., A. S. Yong, B. N. Savani, S. Mielke, K. Keyvanfar, E. Gostick, D. A. Price, D. C. Douek and A. J. Barrett (2007). "Graft-versus-leukemia effects associated with detectable Wilms tumor-1 specific T lymphocytes after allogeneic stem-cell transplantation for acute lymphoblastic leukemia." <u>Blood</u> **110**(6): 1924-1932.

Riddell, S. R. (2007). "Engineering antitumor immunity by T-cell adoptive immunotherapy." <u>Hematology Am Soc Hematol Educ Program</u>: 250-256.

Robins, H. S., S. K. Srivastava, P. V. Campregher, C. J. Turtle, J. Andriesen, S. R. Riddell, C. S. Carlson and E. H. Warren (2010). "Overlap and effective size of the human CD8+ T cell receptor repertoire." <u>Sci Transl Med</u> **2**(47): 47ra64.

Rosenberg, S. A., J. R. Yannelli, J. C. Yang, S. L. Topalian, D. J. Schwartzentruber, J. S. Weber, D. R. Parkinson, C. A. Seipp, J. H. Einhorn and D. E. White (1994). "Treatment of patients with metastatic melanoma with autologous tumor-infiltrating lymphocytes and interleukin 2." <u>J Natl Cancer Inst</u> **86**(15): 1159-1166.

Russell, S., T. Angell, M. Lechner, D. Liebertz, A. Correa, U. Sinha, N. Kokot and A. Epstein (2013). "Immune cell infiltration patterns and survival in head and neck squamous cell carcinoma." <u>Head Neck Oncol</u> **5**(3): 24.

Sabbagh, L., L. M. Snell and T. H. Watts (2007). "TNF family ligands define niches for T cell memory." <u>Trends Immunol</u> **28**(8): 333-339.

Sallusto, F., J. Geginat and A. Lanzavecchia (2004). "Central memory and effector memory T cell subsets: function, generation, and maintenance." <u>Annu Rev Immunol</u> **22**: 745-763.

Sampson, J. H., R. J. Schmittling, G. E. Archer, K. L. Congdon, S. K. Nair, E. A. Reap, A. Desjardins, A. H. Friedman, H. S. Friedman, J. E. Herndon, 2nd, A. Coan, R. E. McLendon, D. A. Reardon, J. J. Vredenburgh, D. D. Bigner and D. A. Mitchell (2012). "A pilot study of IL-2Ralpha blockade during lymphopenia depletes regulatory T-cells and correlates with enhanced immunity in patients with glioblastoma." <u>PLoS One</u> **7**(2): e31046.

Santegoets, S. J., A. W. Turksma, M. M. Suhoski, A. G. Stam, S. M. Albelda, E. Hooijberg, R. J. Scheper, A. J. van den Eertwegh, W. R. Gerritsen, D. J. Powell, Jr., C. H. June and T. D. de Gruijl (2013). "IL-21 promotes the expansion of CD27+ CD28+ tumor infiltrating lymphocytes with high cytotoxic potential and low collateral expansion of regulatory T cells." <u>J Transl Med</u> **11**: 37.

Scally, S. W., J. Petersen, S. C. Law, N. L. Dudek, H. J. Nel, K. L. Loh, L. C. Wijeyewickrema, S. B. Eckle, J. van Heemst, R. N. Pike, J. McCluskey, R. E. Toes, N. L. La Gruta, A. W. Purcell, H. H. Reid, R. Thomas and J. Rossjohn (2013). "A molecular basis for the association of the HLA-DRB1 locus, citrullination, and rheumatoid arthritis." J Exp Med **210**(12): 2569-2582.

Scheffner, M., B. A. Werness, J. M. Huibregtse, A. J. Levine and P. M. Howley (1990). "The E6 oncoprotein encoded by human papillomavirus types 16 and 18 promotes the degradation of p53." Cell **63**(6): 1129-1136.

Schiffman, M., P. E. Castle, J. Jeronimo, A. C. Rodriguez and S. Wacholder (2007). "Human papillomavirus and cervical cancer." Lancet **370**(9590): 890-907.

Schmittel, A., U. Keilholz and C. Scheibenbogen (1997). "Evaluation of the interferon-gamma ELISPOT-assay for quantification of peptide specific T lymphocytes from peripheral blood." J Immunol Methods **210**(2): 167-174.

Schoenbrunn, A., M. Frentsch, S. Kohler, J. Keye, H. Dooms, B. Moewes, J. Dong, C. Loddenkemper, J. Sieper, P. Wu, C. Romagnani, N. Matzmohr and A. Thiel (2012). "A converse 4-1BB and CD40 ligand expression pattern delineates activated regulatory T cells (Treg) and conventional T cells enabling direct isolation of alloantigen-reactive natural Foxp3+ Treg." J Immunol **189**(12): 5985-5994.

Seddiki, N., B. Santner-Nanan, J. Martinson, J. Zaunders, S. Sasson, A. Landay, M. Solomon, W. Selby, S. I. Alexander, R. Nanan, A. Kelleher and B. Fazekas de St Groth (2006). "Expression of interleukin (IL)-2 and IL-7 receptors discriminates between human regulatory and activated T cells." J Exp Med **203**(7): 1693-1700.

Seder, R. A., P. A. Darrah and M. Roederer (2008). "T-cell quality in memory and protection: implications for vaccine design." Nat Rev Immunol **8**(4): 247-258.

Sharma, A., M. Rajappa, A. Saxena and M. Sharma (2007). "Cytokine profile in Indian women with cervical intraepithelial neoplasia and cancer cervix." Int J Gynecol Cancer **17**(4): 879-885.

Shedlock, D. J. and H. Shen (2003). "Requirement for CD4 T cell help in generating functional CD8 T cell memory." Science **300**(5617): 337-339.

Sloand, E. M., J. J. Melenhorst, Z. C. Tucker, L. Pfannes, J. M. Brenchley, A. Yong, V. Visconte, C. Wu, E. Gostick, P. Scheinberg, M. J. Olnes, D. C. Douek, D. A. Price, A. J. Barrett and N. S. Young (2011). "T-cell immune responses to Wilms tumor 1 protein in myelodysplasia responsive to immunosuppressive therapy." Blood **117**(9): 2691-2699.

Starr, T. K., S. C. Jameson and K. A. Hogquist (2003). "Positive and negative selection of T cells." Annu Rev Immunol **21**: 139-176.

Su, L. F., B. A. Kidd, A. Han, J. J. Kotzin and M. M. Davis (2013). "Virus-specific CD4(+) memory-phenotype T cells are abundant in unexposed adults." Immunity **38**(2): 373-383.

Sun, J. C. and M. J. Bevan (2003). "Defective CD8 T cell memory following acute infection without CD4 T cell help." Science **300**(5617): 339-342.

Sylwester, A. W., B. L. Mitchell, J. B. Edgar, C. Taormina, C. Pelte, F. Ruchti, P. R. Sleath, K. H. Grabstein, N. A. Hosken, F. Kern, J. A. Nelson and L. J. Picker (2005). "Broadly targeted human cytomegalovirus-specific CD4+ and CD8+ T cells dominate the memory compartments of exposed subjects." J Exp Med **202**(5): 673-685.

Teague, R. M., B. D. Sather, J. A. Sacks, M. Z. Huang, M. L. Dossett, J. Morimoto, X. Tan, S. E. Sutton, M. P. Cooke, C. Ohlen and P. D. Greenberg (2006). "Interleukin-15 rescues tolerant CD8+ T cells for use in adoptive immunotherapy of established tumors." Nat Med **12**(3): 335-341.

Tjin, E. P., G. Krebbers, K. J. Meijlink, W. van de Kasteele, E. H. Rosenberg, J. Sanders, P. M. Nederlof, B. A. van de Wiel, J. B. Haanen, C. J. Melief, F. A. Vyth-Dreese and R. M. Luiten (2014). "Immune-escape markers in relation to clinical outcome of advanced melanoma patients following immunotherapy." Cancer Immunol Res **2**(6): 538-546.

Tran, E., S. Turcotte, A. Gros, P. F. Robbins, Y. C. Lu, M. E. Dudley, J. R. Wunderlich, R. P. Somerville, K. Hogan, C. S. Hinrichs, M. R. Parkhurst, J. C. Yang and S. A. Rosenberg (2014). "Cancer immunotherapy based on mutation-specific CD4+ T cells in a patient with epithelial cancer." Science **344**(6184): 641-645.

Tyler, E. M., A. A. Jungbluth, R. J. O'Reilly and G. Koehne (2013). "WT1-specific T-cell responses in high-risk multiple myeloma patients undergoing allogeneic T cell-depleted hematopoietic stem cell transplantation and donor lymphocyte infusions." Blood **121**(2): 308-317.

Tyler, E. M. and G. Koehne (2013). "The emergence of WT1-specific T-cell responses following allogeneic T cell-depleted hematopoietic stem cell transplantation and low-dose donor lymphocyte infusions is associated with a graft-vs.- myeloma effect." Oncoimmunology **2**(7): e24963.

Uttenthal, B., I. Martinez-Davila, A. Ivey, C. Craddock, F. Chen, A. Virchis, P. Kottaridis, D. Grimwade, A. Khwaja, H. Stauss and E. C. Morris (2014). "Wilms' Tumour 1 (WT1) peptide vaccination in patients with acute myeloid leukaemia induces short-lived WT1-specific immune responses." Br J Haematol **164**(3): 366-375.

Van der Sluis T.C., V. D. S., Huppelschoten S, Jordanova E.S., Sloots A., Boon L., Smit V.T.H.B.M., Welters M.J.P., Ossendorp F., Van der Water B., Arens R., Van der Burg S., Melief C. (2014). Vaccine-induced cytokine-producing T cells synergize with cisplatin to cause massive infiltration of tumoricidal leukocytes. CIMT Mainz. **2014:** 73.

Van Driessche, A., Z. N. Berneman and V. F. Van Tendeloo (2012). "Active specific immunotherapy targeting the Wilms' tumor protein 1 (WT1) for patients with hematological malignancies and solid tumors: lessons from early clinical trials." Oncologist **17**(2): 250-259.

Van Lummel, M., G. Duinkerken, P. A. Van Veelen, A. De Ru, R. Cordfunke, A. Zaldumbide, I. Gomez-Tourino, S. Arif, M. Peakman, J. W. Drijfhout and B. O. Roep (2014). "Posttranslational modification of HLA-DQ binding islet autoantigens in type 1 diabetes." Diabetes **63**(1): 237-247.

Van Rooij, N., M. M. Van Buuren, D. Philips, A. Velds, M. Toebes, B. Heemskerk, L. J. Van Dijk, S. Behjati, H. Hilkmann, D. El Atmioui, M. Nieuwland, M. R. Stratton, R. M. Kerkhoven, C. Kesmir, J. B. Haanen, P. Kvistborg and T. N. Schumacher (2013). "Tumor exome analysis reveals neoantigen-specific T-cell reactivity in an ipilimumab-responsive melanoma." J Clin Oncol **31**(32): e439-442.

Van Tendeloo, V. F., A. Van de Velde, A. Van Driessche, N. Cools, S. Anguille, K. Ladell, E. Gostick, K. Vermeulen, K. Pieters, G. Nijs, B. Stein, E. L. Smits, W. A. Schroyens, A. P. Gadisseur, I. Vrelust, P. G. Jorens, H. Goossens, I. J. de Vries, D. A. Price, Y. Oji, Y. Oka, H. Sugiyama and Z. N. Berneman (2010). "Induction of complete and molecular remissions in acute myeloid leukemia by Wilms' tumor 1 antigen-targeted dendritic cell vaccination." Proc Natl Acad Sci U S A **107**(31): 13824-13829.

Walter, S., T. Weinschenk, A. Stenzl, R. Zdrojowy, A. Pluzanska, C. Szczylik, M. Staehler, W. Brugger, P. Y. Dietrich, R. Mendrzyk, N. Hilf, O. Schoor, J. Fritsche, A. Mahr, D. Maurer, V. Vass, C. Trautwein, P. Lewandrowski, C. Flohr, H. Pohla, J. J. Stanczak, V. Bronte, S. Mandruzzato, T. Biedermann, G. Pawelec, E. Derhovanessian, H. Yamagishi, T. Miki, F. Hongo, N. Takaha, K. Hirakawa, H. Tanaka, S. Stevanovic, J. Frisch, A. Mayer-Mokler, A. Kirner, H. G. Rammensee, C. Reinhardt and H. Singh-Jasuja (2012). "Multipeptide immune response to cancer vaccine IMA901 after single-dose cyclophosphamide associates with longer patient survival." Nat Med **18**(8): 1254-1261.

Wan, Y. Y. and R. A. Flavell (2009). "How diverse--CD4 effector T cells and their functions." J Mol Cell Biol **1**(1): 20-36.

Wang, J., A. Ioan-Facsinay, E. I. van der Voort, T. W. Huizinga and R. E. Toes (2007). "Transient expression of FOXP3 in human activated nonregulatory CD4+ T cells." Eur J Immunol **37**(1): 129-138.

Watanabe, Y., F. Katou, H. Ohtani, T. Nakayama, O. Yoshie and K. Hashimoto (2010). "Tumor-infiltrating lymphocytes, particularly the balance between CD8(+) T cells and CCR4(+) regulatory T cells, affect the survival of patients with oral squamous cell carcinoma." Oral Surg Oral Med Oral Pathol Oral Radiol Endod **109**(5): 744-752.

Weber, G., U. Gerdemann, I. Caruana, B. Savoldo, N. F. Hensel, K. R. Rabin, E. J. Shpall, J. J. Melenhorst, A. M. Leen, A. J. Barrett and C. M. Bollard (2013). "Generation of multi-leukemia antigen-specific T cells to enhance the graft-versus-leukemia effect after allogeneic stem cell transplant." Leukemia **27**(7): 1538-1547.

Weber, G., J. Karbach, S. Kuci, H. Kreyenberg, A. Willasch, E. Koscielniak, T. Tonn, T. Klingebiel, W. S. Wels, E. Jager and P. Bader (2009). "WT1 peptide-specific T cells generated from peripheral blood of healthy donors: possible implications for adoptive immunotherapy after allogeneic stem cell transplantation." Leukemia **23**(9): 1634-1642.

Wedemeyer, H., E. Mizukoshi, A. R. Davis, J. R. Bennink and B. Rehermann (2001). "Cross-reactivity between hepatitis C virus and Influenza A virus determinant-specific cytotoxic T cells." J Virol **75**(23): 11392-11400.

Wehler, T. C., M. Karg, E. Distler, A. Konur, M. Nonn, R. G. Meyer, C. Huber, U. F. Hartwig and W. Herr (2008). "Rapid identification and sorting of viable virus-reactive CD4(+) and CD8(+) T cells based on antigen-triggered CD137 expression." J Immunol Methods **339**(1): 23-37.

Wei, G., L. Wei, J. Zhu, C. Zang, J. Hu-Li, Z. Yao, K. Cui, Y. Kanno, T. Y. Roh, W. T. Watford, D. E. Schones, W. Peng, H. W. Sun, W. E. Paul, J. J. O'Shea and K. Zhao (2009). "Global mapping of H3K4me3 and H3K27me3 reveals specificity and plasticity in lineage fate determination of differentiating CD4+ T cells." Immunity **30**(1): 155-167.

Welsh, R. M., J. W. Che, M. A. Brehm and L. K. Selin (2010). "Heterologous immunity between viruses." Immunol Rev **235**(1): 244-266.

Wiegers, G. J., M. Kaufmann, D. Tischner and A. Villunger (2011). "Shaping the T-cell repertoire: a matter of life and death." Immunol Cell Biol **89**(1): 33-39.

Wilson, D. B., D. H. Wilson, K. Schroder, C. Pinilla, S. Blondelle, R. A. Houghten and K. C. Garcia (2004). "Specificity and degeneracy of T cells." Mol Immunol **40**(14-15): 1047-1055.

Wirth, T. C., H. H. Xue, D. Rai, J. T. Sabel, T. Bair, J. T. Harty and V. P. Badovinac (2010). "Repetitive antigen stimulation induces stepwise transcriptome diversification but preserves a core signature of memory CD8(+) T cell differentiation." Immunity **33**(1): 128-140.

Wolfl, M., J. Kuball, M. Eyrich, P. G. Schlegel and P. D. Greenberg (2008). "Use of CD137 to study the full repertoire of CD8+ T cells without the need to know epitope specificities." Cytometry A **73**(11): 1043-1049.

Wolfl, M., J. Kuball, W. Y. Ho, H. Nguyen, T. J. Manley, M. Bleakley and P. D. Greenberg (2007). "Activation-induced expression of CD137 permits detection, isolation, and expansion of the full repertoire of CD8+ T cells responding to antigen without requiring knowledge of epitope specificities." Blood **110**(1): 201-210.

Wolfl, M., K. Merker, H. Morbach, S. W. Van Gool, M. Eyrich, P. D. Greenberg and P. G. Schlegel (2011). "Primed tumor-reactive multifunctional CD62L+ human CD8+ T cells for immunotherapy." Cancer Immunol Immunother **60**(2): 173-186.

Wong, S. B., R. Bos and L. A. Sherman (2008). "Tumor-specific CD4+ T cells render the tumor environment permissive for infiltration by low-avidity CD8+ T cells." J Immunol **180**(5): 3122-3131.

Xie, Y., A. Akpinarli, C. Maris, E. L. Hipkiss, M. Lane, E. K. Kwon, P. Muranski, N. P. Restifo and P. A. Antony (2010). "Naive tumor-specific CD4(+) T cells differentiated in vivo eradicate established melanoma." J Exp Med **207**(3): 651-667.

Xu, Y., M. Zhang, C. A. Ramos, A. Durett, E. Liu, O. Dakhova, H. Liu, C. J. Creighton, A. P. Gee, H. E. Heslop, C. M. Rooney, B. Savoldo and G. Dotti (2014). "Closely related T-memory stem cells correlate with in vivo expansion of CAR.CD19-T cells and are preserved by IL-7 and IL-15." Blood **123**(24): 3750-3759.

Yasukawa, M., H. Fujiwara, T. Ochi, K. Suemori, H. Narumi, T. Azuma and K. Kuzushima (2009). "Clinical efficacy of WT1 peptide vaccination in patients with acute myelogenous leukemia and myelodysplastic syndrome." Am J Hematol **84**(5): 314-315.

Ye, Q., D. G. Song, M. Poussin, T. Yamamoto, A. Best, C. Li, G. Coukos and D. J. Powell, Jr. (2014). "CD137 accurately identifies and enriches for naturally occurring tumor-reactive T cells in tumor." Clin Cancer Res **20**(1): 44-55.

Zhang, Y., G. Joe, E. Hexner, J. Zhu and S. G. Emerson (2005). "Host-reactive CD8+ memory stem cells in graft-versus-host disease." Nat Med **11**(12): 1299-1305.

Zippelius, A., M. J. Pittet, P. Batard, N. Rufer, M. de Smedt, P. Guillaume, K. Ellefsen, D. Valmori, D. Lienard, J. Plum, H. R. MacDonald, D. E. Speiser, J. C. Cerottini and P. Romero (2002). "Thymic selection generates a large T cell pool recognizing a self-peptide in humans." J Exp Med **195**(4): 485-494.

6   Publications

Schmied S., Gostick E., Price D., Abken H., Assenmacher M., Richter A. Analysis of the functional WT1-specific T cell repertoire in healthy donors reveals a discrepancy between CD4$^+$ and CD8$^+$ memory formation. Submitted to *Immunology*.

Schmied S., Assenmacher M., Richter A. Functional HPV16-reactive T cells in periphery and tumor tissue of HPV16^{pos} HNSCC patients. Submitted to *The International Journal of Cancer*.

Abstracts

Schmied S., Richter A., Assenmacher M. Generation and characterization of WT1-specific T cells for clinical research towards adoptive tumor therapy. 11th Annual Cancer Immunotherapy (CIMT) Meeting 2013, Mainz, Germany

Schmied S., Richter A., Assenmacher M. Generating and characterizing WT1-specific T cells – research towards adoptive tumor therapy. 43rd Annual meeting of the German Society of Immunology (DGfI) 2013, Mainz, Germany

Schmied S., Richter A., Assenmacher M. WT1-specific T cells exhibiting a non-exhausted, functional phenotype can be generated from the natural repertoire of healthy donors for clinical use 55th Annual Meeting of the American Society of Hematology (ASH), 2013, New Orleans, USA

Schmied S., Richter A., Assenmacher M. Functional WT1-reactive T cells are present in the natural naive and memory repertoire of healthy donors. 12th Annual Cancer Immunotherapy (CIMT) Meeting 2014, Mainz, Germany

Schmied S., Richter A., Assenmacher M. Functional HPV16-directed CD4$^+$ T cell immunity detected in blood represents HPV16-directed immunity in tumor tissue of HPV16^{pos} HNSCC patients. 44th Annual meeting of the German Society of Immunology (DGfI) 2014, Bonn, Germany

7   Curriculum Vitae

Sabine Schmied, MSc. Biol.

Date of Birth March 17th 1982
Nationality German

01/2011 – 09/2014	**PhD Thesis** **Miltenyi Biotec GmbH**, Bergisch Gladbach R&D, Division of cell biology, Mario Assenmacher, Anne Richter Supervision: Prof. Dr. Hinrich Abken and Prof. Dr. Thomas Wunderlich, University of Cologne Title: "Characterization of tumor-antigen-specific T cells – insights into WT1- and HPV16-specific T cell repertoires"
04/2010 – 08/2010	**Internship** **University Hospital "Rechts der Isar"**, Munich Department of Immunology, Angela Krackhardt
12/2007 – 09/2008	**Master Thesis** **Max-Planck Institute of Biochemistry**, Martinsried Department of Molecular Cell Biology, Stefan Jentsch Supervision: Prof. Dr. Stefan Jentsch, Prof. Dr. Martin Scheffner Title: *"Rad51: New Mutants and Ess1 as a Putative New Regulator of Homologous Recombination"*
06/2006 – 08/2006	**Internship** **GATC Biotech AG**, Konstanz
02/2006 – 03/2006	**Bachelor Thesis** **German Cancer Research Center**, Heidelberg Department of Radiopharmaceutical Chemistry Supervision: Prof. Dr. Alexander Bürkle Title: *"Untersuchungen zur Bioverfügbarkeit von partikelgebundenem 3-NBA in der Lunge"*
10/2003 – 09/2008	**University of Konstanz** Biological Sciences (MSc) Focus: Cellular & Molecular Biology Degree in "Master of Science" (GPA: outstanding)
10/2002 – 08/2003	**Leuphana University Lüneburg**, Environmental Sciences (Diplom)
09/2001 – 08/2002	**Voluntary Year of Environmental Service**
08/1992 – 06/2001	**Abitur** **Klettgau Gymnasium Waldshut-Tiengen**

Köln, 05th March 2015